INFORMATION TO USERS

This manuscript has been reproduced from the microfilm master. UMI films the text directly from the original or copy submitted. Thus, some thesis and dissertation copies are in typewriter face, while others may be from any type of computer printer.

The quality of this reproduction is dependent upon the quality of the copy submitted. Broken or indistinct print, colored or poor quality illustrations and photographs, print bleedthrough, substandard margins, and improper alignment can adversely affect reproduction.

In the unlikely event that the author did not send UMI a complete manuscript and there are missing pages, these will be noted. Also, if unauthorized copyright material had to be removed, a note will indicate the deletion.

Oversize materials (e.g., maps, drawings, charts) are reproduced by sectioning the original, beginning at the upper left-hand corner and continuing from left to right in equal sections with small overlaps.

ProQuest Information and Learning
300 North Zeeb Road, Ann Arbor, MI 48106-1346 USA
800-521-0600

UMI®

University of Alberta

Ultraviolet Fluorescence of Peptides and Proteins on Microchip

by

Kowlasar Misir ©

A thesis submitted to the Faculty of Graduate Studies and Research in partial fulfillment of the requirements for the degree of Master of Science.

Department of Chemistry
Edmonton, Alberta
Spring 2005

Thought without learning is labour lost, learning without thought is perilous.

-Source unknown

For my family

THESIS ABSTRACT

The wide applicability of Micro Total Analysis Systems, μTAS, in the area of protein analysis has been extensively demonstrated, gauging from publication output in this area. This work focuses on the development of a detection method for peptides and proteins that is independent of labelling chemistries. Initial work was centred on the development of a tryptophan based fluorescence detector that could subsequently be used for the detection of peptides and proteins. The construction of a native fluorescence detector is described and the optimisation procedure detailed. The limit of detection (LOD) under optimised conditions was calculated to be ~ 230 nM (S/N = 3). This corresponds to a mass detection limit of ~ 5.5 amole. Approaches towards the improvement of the LOD were investigated: the effect of the system electronics, background electrolyte, light scattering and quartz chip luminescence on the limit of detection was interrogated. The most probable limiting factor was identified to be luminescence arising from the chip substrate. The detector was then applied to the detection of model peptides and proteins after separation by microchip capillary electrophoresis. Separation efficiencies of 1.6 million plates/m were observed. Cytochrome C was digested off chip and the digest separated on-chip to demonstrate the capability of the assay.

ACKNOWLEDGEMENTS

As I contemplated and anticipated finishing this undertaking that I so boldly rushed into, I could not help but being excited about writing this section. Firstly, because it signals that the end is imminent, and secondly, it is here that I will be afforded the opportunity to express my heartfelt thanks and sincere gratitude to all those extraordinary people who have contributed to shaping my life and work over the past three years. I know that this section will be long, and I do beg your indulgence. I would posit that my graduate experience differed from that of most of my peers in that I was embarking on my first research experience. Unlike almost everyone else, I had no inkling about how begin such an endeavour. Nevertheless, it was an amazing journey, one of monumental learning, both about the exciting and sometimes depressing nature of research, and what excites me as an individual. That being said, this work presented here would not have been possible without the help of some amazing people. I do apologise in advance for any unintentional omissions I know I may make in my quest to enumerate those who have contributed.

Foremost on this list is my research supervisor, Dr. Jed Harrison. I wish to thank him for being understanding, and not giving up on me when the going got tough. The boss afforded me the opportunity to make this project work, and provided timely guidance. I wish to thank him for both his patience and impatience and for all the amazing opportunities that he provides for his graduate students. We are indeed some of the most fortunate and privileged in the division. It was a pleasure working for him and I wish to express my sincere thanks for his guidance and introduction into the field of microfluidics.

I would like to thank James Bao for his initial assistance in answering my numerous questions and the useful directions that he gave me during my baby steps as a researcher. It took some convincing, but eventually, I managed to secure his help during this initial time. He continued to answer my numerous questions, and for that I am thankful.

During my initial puppy eyed days in the laboratory, I wondered at the indifferent demeanour of Justine Taylor. I later learnt that we all become somewhat jaded sometime in our graduate career. However, I could not help but admire her perspicacity and her

amazing analytical abilities. On numerous occasions, she demonstrated her objectivity and was quite helpful in her latter years. She was an inspiration.

Guifeng Jiang joined me in what I termed the black-hole. It was such a pleasure having her as a bench partner, both for the excellent company and for the times when I needed some advice.

On my arrival in the great Canadian north, I was fortunate to meet some amazing people. Arlene Figley was one such individual. It signalled the beginning of great friendship, one which had provided me with many happy memories. I wish to record my sincere thanks and gratitude to Arlene for being such a wonderful person. I was also fortunate to become great friends with Jelena, a thoughtful and kind individual who always had comforting words and caring advice.

Dolores Martinez can be a character at times; irregardless of her mood, I was able to get her advice on many occasions. Thanks D-Lo for all the helpful discussions and interesting power plant conversations.

The members of the Harrison group contributed to making my stay an interesting and enjoyable one. I should thank Jing, Jane, and Yong, for the useful discussions, Josh and Sara for their good company and dinners, and Eric for dealing with the computer issues. Steve Dempster provided me with a wonderful drawing of my microscope and I wish to say thank you. I would also like to express my gratitude to the staff of the electronic and machine shop for all their help during the course of my research.

Coming to a new country is never an easy thing because differences in culture and climate pose additional hurdles that one needs to overcome. During my time I met some unique individuals: Karen, Hui Shin, Timon, Awet, Christie, Alberto, Nilay and Sheela – thanks for all the wonderful times. You have all made my adjustment and life in Edmonton fun and interesting. I would also like to acknowledge Shar, Nirala, Surya, Ryan, Kishan, and Philo for bringing me a touch of home in Edmonton and for the wonderful food and company. We indeed had some happy times.

A sincere thank you is extended to Dr. Renee Polziehn for providing a listening ear and the wonderful outreach opportunities. It afforded me an invaluable occasion to do wonderful things in the Edmonton community.

Finally, to my family, thank you.

TABLE OF CONTENTS

CHAPTER 1: LITERATURE REVIEW

1.1 Introduction....1
1.2 Micrototal Analysis Systems, μTAS....2
1.3 Application: Protein Separation and Detection in Microfluidic systems...4
1.3.1 Mass Spectrometry....4
1.3.2 Laser Induced Fluorescence....6
1.3.3 Electrochemical Detection....10
1.3.4 UV Absorption....11
1.4 Spectral Properties of the Aromatic Amino Acids, Peptides, and Proteins....11
1.4.1 Amino Acids....11
1.4.2 Peptides and Proteins....13
1.5 Laser Induced Native Fluorescence Detection....15
1.6 Capillary Electrophoresis....17
1.6.1 Historical Perspectives and Fundamentals of CE....17
1.6.2 Separation efficiency....20
1.7 Scope of this Thesis....21
1.8 References....23

CHAPTER 2: NATIVE FLUORESCENCE DETECTION ON CHIP

2.1 Introduction....27
2.2 Experimental Section....28
2.2.1 Solutions and Reagents....28
2.2.2 Glass fluorescence Measurements....29
2.2.3 Devices....29
2.2.3.1 Device Fabrication....31
2.2.3.2 Device Description and Operation....31
2.2.4 Instrumentation....32
2.2.5 Procedure....34
2.3 Results and Discussion....36
2.3.1 Device Fabrication....36
2.3.2 Spectrofluorometric Measurements....38
2.3.3 Detector Performance....39
2.3.3.1 Limit of detection Studies....39
2.3.4 Limiting Noise Analysis....43
2.3.4.1 Electronics: Amplifier and Detector....43
2.3.4.2 Background Signal....44

2.4 Conclusion....51
2.5 References....53

CHAPTER 3: SEPARATION OF PEPTIDES AND PROTEINS WITH NATIVE FLUORESCENCE DETECTION

3.1 Introduction....54
3.2 Experimental....54
3.2.1 Solutions and Reagents....54
3.2.2 Devices and Chip Operation; Procedure....55
3.2.3 Protein Digestion....56
3.3 Results and Discussion....56
3.3.1 Peptides....56
3.3.1.1 Separation and Detection....56
3.3.1.2 Limit of detection Studies....60
3.3.1.3 Off Chip Digestion and on Chip Separation and Detection....62
3.3.2 Proteins....64
3.3.2.1 Separation and detection....64
3.3.2.2 Effect of pH on Separation....67
3.3.2.3 Limit of Detection Studies....69
3.4 Evaluating the Detection Method....70
3.4.1 Overview/Discussion....70
3.4.2 Summary/Conclusion....73
3.5 Conclusion....74
3.6 References....75

CHAPTER 4: SUMMMARY

4.1 Conclusion and Suggestions for Future Research....77
4.2 References....79

LIST OF TABLES AND FIGURES

TABLES

Table 2-1 Noise study....45
Table 2-2 PMT Dark noise measurements....46
Table 2-3 Spectral Characteristics of Filters Used....48
Table 2-4 Background signal and noise with different filter Combinations....50

Table 3-1A Limit of detection comparison....72
Table 3-1B Limit of detection comparison....73

FIGURES

Figure 1-1 Miniaturization....2
Figure 1-2 Integrated microfluidic chip....6
Figure 1-3 Fractionator chip....7
Figure 1-4 Aromatic amino acids....12
Figure 1-5 Conventional CE system....19
Figure 1-6 Electrophoresis and electroosmosis....19

Figure 2-1 Schematic of Pocre Chip Device....31
Figure 2-2 Confocal epiluminiscent apparatus....32
Figure 2-3 Focusing application of reflecting microscope objective....34
Figure 2-4 Pictorial illustration of instrumental set-up....36
Figure 2-5 Image of etch quality obtained with Precision Quartz....37
Figure 2-6 Images of etch quality obtained with Hoya Quartz....38
Figure 2-7 Emission spectra for the aromatic amino acids as a function of excitation wavelength....39
Figure 2-8 Figure illustrating peak reproducibility for multiple injections....40
Figure 2-9 Figure illustrating reproducibility in retention time....41
Figure 2-10 Plot of S/N ratio as a function of tryptophan concentration....41
Figure 2-11 Peak area calibration Plot for tryptophan....42
Figure 2-12 Three separate electropherograms of 1 μM tryptophan....42
Figure 2-13 Plot of S/N ratio as a function of tryptophan concentration with a 36x reflecting objective....43
Figure 2-14 Effect of buffer concentration on background signal....46
Figure 2-15 Emission spectra for pristine quartz upon excitation at 266 nm...47
Figure 2-16 Emission spectra for quartz exposed to 266 laser light....48
Figure 2-17 Change in noise of the background as a function of tryptophan concentration for different filter combinations....49
Figure2-18 Signal intensity as a function of filter set combination at various concentrations of tryptophan....50
Figure 2-19 Plot of S/N ratio as a function of tryptophan concentration....51

Figure 3-1 Electropherogram for the separation of tryptophan and peptide A....57
Figure 3-2 Electropherogram for the separation of peptides C and D....57
Figure 3-3 Electropherogram for the separation of tryptophan and peptides A and B....58
Figure 3-4 Electropherogram for the separation for peptides A, B, C, and D....60
Figure 3-5 Electropherogram for the separation for peptides A, B, C, and D....60
Figure 3-6 Plot of S/N ratio as a function of Peptide A concentration....61
Figure 3-7 Plot of S/N ratio as a function of Peptide C concentration....61
Figure 3-8 Electropherogram for CE separation of horse heart cyt C digest....63
Figure 3-9 Electropherogram for the separation of horse heart cyt C on Chip....63
Figure 3-10 Electropherogram for the separation of four model proteins: carbonic anhydrase I and II, β-lactoglobulin B, and α-lactalbumin....64
Figure 3-11 Electropherogram for the separation of carbonic anhydrase I and II, β-lactoglobulin B, and α-lactalbumin, under various applied electric fields....64
Figure 3-12 Figure showing six consecutive analysis of a four protein mixture....65
Figure 3-13 Effect of applied field strength on plate number, N....66
Figure 3-14 Electrophoretic separation carbonic anhydrase I and II, β-lactoglobulin A and B, and α-lactalbumin....66
Figure 3-15 Electrophoretic separation of carbonic anhydrase I and II, β-lactoglobulin A and B, and α-lactalbumin at a higher field strength....67
Figure 3-16 Electrophoretic separation of carbonic anhydrase I and II, β-lactoglobulin B, and α-lactalbumin at various pH values....68
Figure 3-17 Plot of S/N as a functions of α-lactalbumin concentration....69

ABBREVIATIONS

1D	One Dimensional
2D	Two Dimensional
μ-CE	Microchip Capillary Electrophoresis
μ TAS	Micro Total Analysis Systems
BSA	Bovine Serum Albumin
CE	Capillary Electrophoresis
Cyt C	Cytochrome C
CZE	Capillary Zone Electrophoresis
DNA	Deoxyribose Nucleic Acid
EOF	Electroosmotic Flow
EPM	Electrophoretic Mobility
ID	Internal Diameter
IEF	Isoelectric Focusing
LIF	Laser Induced Fluorescence
LINF	Laser Induced Native Fluorescence
LOD	Limit of Detection
MEKC	Micellar Electrokinetic Chromatography
MS	Mass Spectrometry
N.A.	Numerical Aperture
Nd:YAG	Neodynium Yttrium Aluminium Garnet
NDA	Naphthalene-2,3-dicarboxaldehyde
OD	Ordinary Diameter
Peptide A	α_1-mating factor fragment
Peptide B	Bombesin
Peptide C	Luteinizing hormone releasing hormone
Peptide D	α_1-mating factor
pI	Isoelectric Point
PMMA	Poly(methyl methacrylate)
PMT	Photomultiplier Tube
RI	Refractive Index
S/N	Signal to Noise
SDS	Sodium Dodecyl Sulphate
TAS	Total Analysis Systems
UV	Ultra Violet

CHAPTER 1: LITERATURE REVIEW

1.1 INTRODUCTION

As time progresses, greater demands are placed on techniques and methodologies being employed in clinical diagnostics and control measurements. This stems from the need to be able to make diagnosis in shorter times and identifying potential threat agents almost immediately. Competitive diagnosis and identification times will allow for the prescription of appropriate measures accordingly. Such capabilities require measurement systems that are rapid, sensitive, and portable. Research towards miniaturization of chemical analysis systems can be seen as one approach towards the development of highly sensitive and versatile technologies. The cartoon representation in Figure 1-1 is a simple illustration that presents the view of one author of what can be envisioned [3].

The attractiveness of miniaturization is as follows: the entire sequence of analytical procedures such as sample extraction and derivatization, separation and detection can all be integrated on one platform. Reduction in size yields such advantages as rapid separations, and small sample volume, which in turn correlates to low reagent consumption and waste production, multiplicity, portability, integration and ultimately automation. Automation will allow for more precise and reproducible operations, thus producing higher quality data. In addition, synergistic capabilities which are not otherwise available may be attained from the ability to integrate multiple processes on a single platform. Further, as concern for environmental responsibility, monitoring and protection grows, this technology is uniquely poised to be of great value. Waste production is minimised, and it offers the ability for sophisticated rapid testing, and for the establishment of control systems. Thus, it can be envisioned that integrated systems will be developed to replace conventional discrete techniques, though the application will not see the miniaturization of everything, but rather the miniaturizing of specific components.

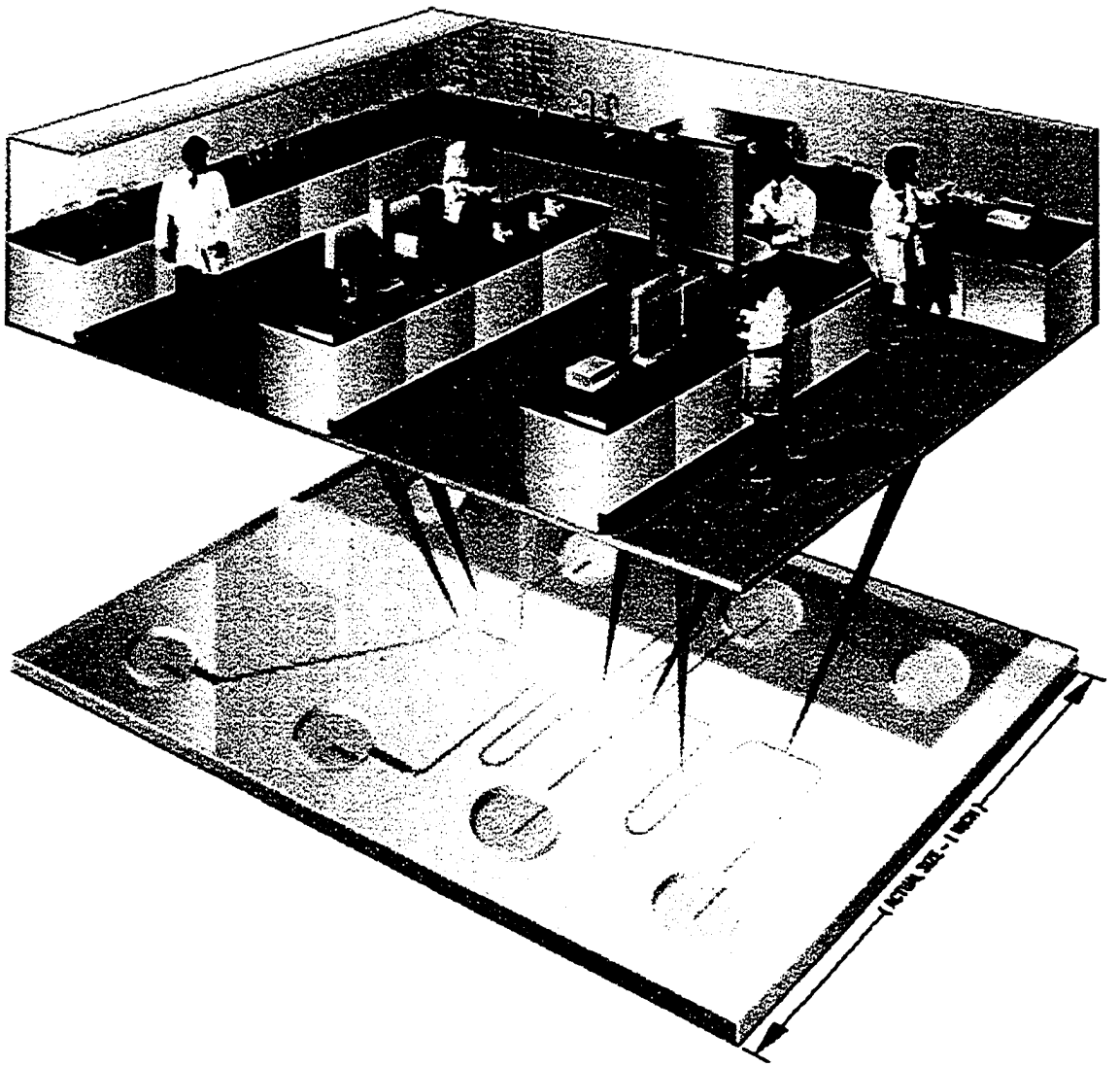

Figure 1-1: Pictorial illustration of what is envisioned as the revolutionary potential of the concept of miniaturization for future applications in the laboratory. Observe the miniaturization and integration of conventional bench-top systems onto a microfluidic device. Figure adapted from Chow [3]

1.2 MICRO TOTAL ANALYSIS SYSTEMS, μTAS

The concept of Total Analysis Systems (TAS) preceded the development of Micro Total Analysis Systems (μTAS). This evolved due to the need to develop portable systems to be used in environmental and waste monitoring systems, and the measurement of species concentration, particularly in the fields of biotechnology, process control, and medical sciences [4]. In a typical analytical operation, the following steps are identified as

being critical: sampling, sample transport and pre-treatment, separation of sample from an interfering matrix, measurement of species of interest, and data collection and quantification. These steps are extremely involved, labour intensive and costly. The idea of having an integrated and automated system is attractive, as it offers a significant reduction in cost and labour. From this need the concept of TAS was realised by the late Michael Widmer and co-workers. A logical extension to the TAS concept was miniaturization of these systems, as this would lead to a reduction in reagent cost, waste generation and analysis times [5]. The concept of miniaturization was by no means new; for example, Jorgensen and Lucas [6] showed the advantages to be accrued by going small when they performed open tubular capillary electrophoresis (CE) featuring small internal diameters to allow high voltages. This exemplified an area of instrumental development that led towards greater resolution, improvement of detection sensitivity and even method automation [7]. However, the modern microfluidic [8] concept that exploited miniaturization can be traced back to the development of a silicon based gas chromatograph at Stanford University [9] and the ink-jet printer nozzles at IBM [10, 11]. The report published in IEEE Transactions on Electron Devices by Stephen Terry and co-workers from Stanford Electronic Laboratories, Stanford University is regarded as the first example of a microfabricated device for chemical analysis. They described the design, fabrication and testing of a gas chromatograph integrated on a planar silicon wafer [9]. Though these now legendary devices were quite remarkable for their time, follow-up research was modest in the least. It was not until the pioneering work of Manz [12] and co-workers in the 1990s that the development of integrated microfluidic devices as they are known today began.

In 1992 Harrison and co-workers [13, 14] demonstrated CE experiments on a chip like structure. These early reports explored the feasibility of miniaturizing a chemical analysis system on a planar substrate. They demonstrated the use of electroosomotic pumping for flow control in a fluidic network. Since that time, the field has blossomed and branched off into many different areas [8]. The literature on miniaturized microfluidic device applications and development is so extensive that an exhaustive review is beyond the scope of this chapter. Some of the more recent research will be reviewed briefly to aid in setting this thesis into context. Excellent general reviews categorised by subject areas are available; for biological and chemical analysis [15-17], clinical and forensic analysis [18],

point of care testing [19], molecular diagnostics [20, 21] and medical diagnostics [22]. Other comprehensive reviews that deal with theory, history and more recent developments can be found contained in the manuscripts prepared by Andreas Manz and his colleagues [23-25]. The reader is directed to these for further information, if required.

1.3 APPLICATION: PROTEIN SEPARATION AND DETECTION IN MICROFLUIDIC SYSTEMS

This section will briefly review the developments of detectors in the area of proteomics and microfluidics; it is not intended to be exhaustive. The emphasis will be on the methods employed with respect to protein identification, and more importantly detection. Examples in the literature describing the major detection methodologies developed for protein detection within a microfluidic framework will be discussed.

Some of the major detection methods for microfluidics include mass spectrometry (MS) [2, 26-31], and laser induced fluorescence (LIF) [14, 32-37], both of which dominate the field. However, rapid developments in microfabrication technology have resulted in the ability to tailor detectors to suit particular needs. Electrochemical detectors (EC), which can be fabricated on chip have thus been given great attention [38-45]. Application of UV absorbance detectors for microfluidic applications has also been explored [46, 47]. Other detection methods reported for microfluidic applications includes Raman spectroscopy [48], chemiluminescence [49-51], refractive index (RI) detection [52], electrochemiluminiscence [53-55], optical emission spectroscopy [56], and Shaw convolution Fourier Transform detection[57].

1.3.1 MASS SPECTROMETRY

One of the major focuses of biological and analytical chemists for many years has been the separation and identification of all proteins present within cells, tissues and biofluids. This was and still remains an intriguing and demanding analytical problem [58]. Whilst academic interest is a major driving force in the direction of understanding the proteome, the pharmaceutical necessity in a typical proteomics based drug discovery effort is for more protein samples to be prepared and analysed more efficiently. The conventional approach involves the analysis of cell lysates by two- dimensional (2D) gel

electrophoresis which yields the familiar array of spots, each ideally corresponding to a single protein. The spots are then compared to a control and proteins of interest are manually excised, digested and identified by MS [59]. The rate limiting steps in this approach are the 1D and 2D electrophoretic steps, in addition to manual excision followed by digestion. The advent of microfluidic chip technology over the last decade has seen approaches in the direction of integrating several processes on a chip platform aimed at speeding up and addressing some of these issues. Scaling down may result in a superior ability to integrate and automate processes, which ultimately should result in a reduction of analysis time.

Since protein profiling relies almost exclusively on MS to identify proteins, a major focus of the research being conducted is aimed at speeding up and integrating the pre-MS steps. In addition, many successful efforts have been aimed at coupling microfluidic devices to the MS [2, 26, 29, 30, 60]. Integrated sample processing, enrichment, cleanup and/or fractionation prior to detection, and automated sample delivery leads to enhanced analysis efficiency [61]. In our laboratory, Wang [2] et al. described a microfluidic chip that integrated an electrospray interface to a mass spectrometer with a capillary electrophoresis channel, an injector and a protein digestion bed on a monolithic substrate (Figure 1-2). They demonstrated the rapid separation and identification of melittin within five seconds, and cytochrome C and bovine serum albumin within three to six minutes at room temperature. At the time of publication, this elegant work was one of the most integrated efforts presented so far. Following the success of this early work, efforts continued in our laboratory to integrate multiple pre-MS processes on chip. Taylor explored the development of the "fractionator" chip which integrated isoelectric focusing in a capillary, on-chip protein digestion and peptide preconcentration, followed by MS identification. The device was designed to process twenty incoming protein samples, thus yielding high throughput and multiplexed capabilities (Figure 1-3) [1]. This project is still being explored at present.

Another novel approach to protein processing was presented by Jin et al. [62] in which electroosomotic flow (EOF) was used to electrokinetically drive proteins through a proteolytic system packed with immobilised trypsin beads. Digestion of the protein was carried out in the proteolytic system and the tryptic digests analysed independently using

CE and MS, thus demonstrating another example of the integration of pre-MS steps onto a microfluidic platform. Application of microfluidic devices for the rapid analysis of trace level tryptic digests was also demonstrated. A modular microsystem consisting of an autosampler, a microfabricated device containing a large channel packed with C_{18} beads and an array of separation channels that could be interfaced to a mass spectrometer was described. With this system, the authors demonstrated the sequential injection, preconcentration and separation of peptide standards and tryptic digests with a throughput of ~ 12 samples/h and a concentration detection limit of ~5 nM [63].

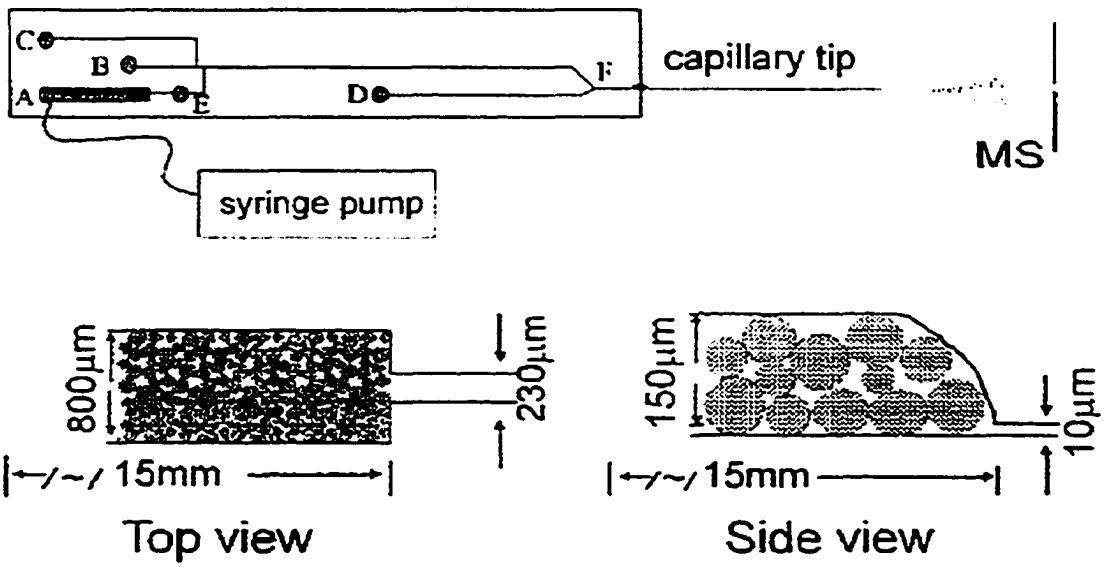

Figure 1-2: Schematic representation of the microfluidic platform with an integrated enzyme reaction bed and capillary electrophoresis chip coupled to a mass spectrometer. The features labelled top and side views are blow ups of the packed trypsin beads bed. Diagram adapted from Wang et al. [2]

1.3.2 LASER INDUCED FLUORESCENCE

In addition to efforts at integrating pre-MS steps and finding ways to alleviate the labour intensive methods conventionally used in proteomic analysis, microchip capillary electrophoresis (µ–CE) has also been receiving a lot of attention. It offers the much vaunted advantages of miniaturization such as short analysis times, small amounts of reagents, and the capability of constructing high-throughput screening systems.

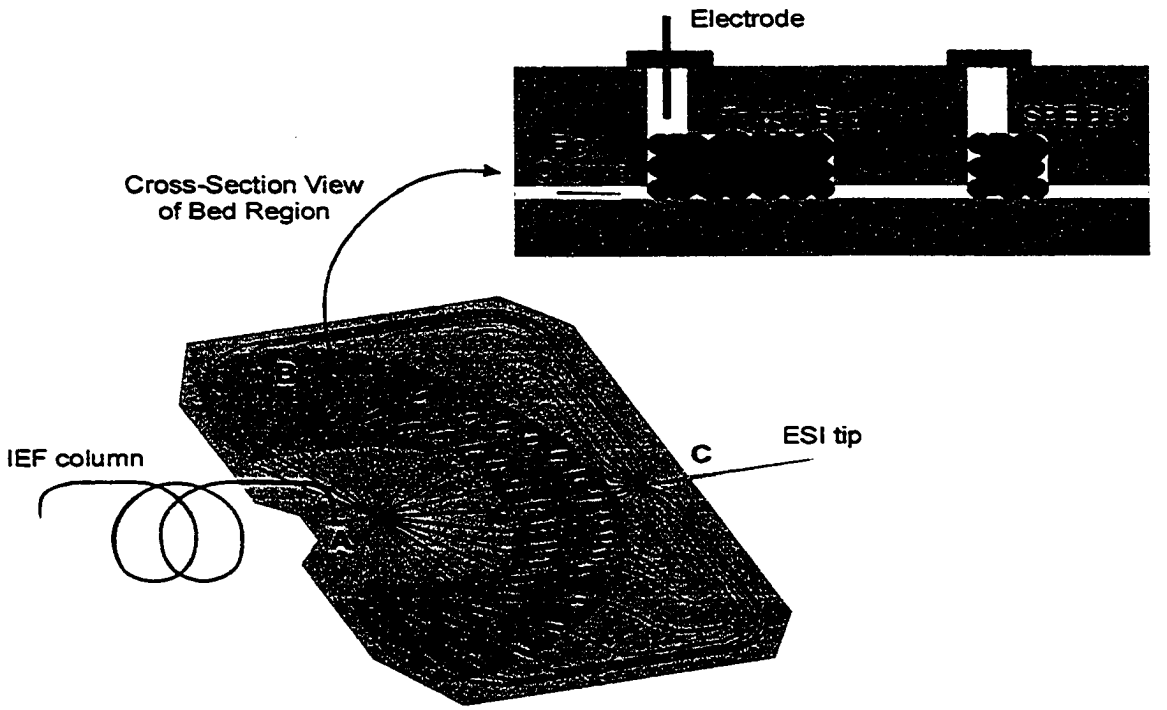

Figure 1-3: Device (fractionator) designed to accomplish multiplex protein sample processing. It couples an isoelectric focusing (IEF) column connected to chip at A, protein digestion and concentration beds (region B) and an electrospray tip (C) on a single microfluidic platform. Cartoon adapted from Taylor [1]

Coupled with the very sensitive laser induced fluorescence (LIF) detection scheme, μ–CE presents an alternative detection method for proteins that is sensitive and less labour intensive, as compared with conventional approaches. Liu and co-workers [64] demonstrated the separation of a mixture of five labelled proteins by μ–CE. In this work, the proteins were first labelled with tetramethylrhodamine isothiocynate (TRITC) off chip by mixing 70 μM protein solutions with 7 mM TRITC solution. The resulting TRITC labelled proteins were then diluted to a finial concentration of 3.5 μM prior to injection and detection on chip with LIF. The authors did not evaluate limits of detection (LOD). They did indicate that the small channel dimensions allowed for the use of high ionic strength buffers, thus minimizing protein adsorption on the walls of the channels. Other researchers also investigated various labelling schemes on chip, either before separation or after separation [33-37, 65]. Gottschlich et al. [65] developed a microchip that integrated enzymatic reactions, electrophoretic separation of the reactants from the

products, in addition to post separation labelling of proteins and peptides prior to detection. In this work, insulin B chain was digested in 15 min under stop flow conditions in a heated channel followed by separation, which was completed within one minute. The separated reaction products were then labelled with naphthalene-2,3-dicarboxyaldehyde (NDA) and detected by LIF. The authors also demonstrated the reduction of disulphide bridges using insulin as a model protein, performing the reaction at elevated temperatures. Proteins were also separated by μ–CE and subsequently labelled on chip by post column addition of a fluorogenic dye. NanoOrange is a dye that binds noncovalently with the hydrophobic regions of the proteins to form highly fluorescent complexes and this was utilised in the labelling of the bovine serum proteins, α-lactalbumin, β-lactoglobulin A and β-lactoblobulin B after separation, prior to LIF detection [37]. The authors reported the following molar detection limits (S/N = 3) for the model proteins: α-lactalbumin, 85 nM; β lactoglobulin A, 70 nM; and β-lactoglobulin B, 70 nM.

Another approach has been in the development of protocols analogous to those used for double stranded DNA analysis, in which intercalating dyes were added to the separation media. Jin et al. [66] demonstrated a dynamic labelling mechanism that allows for the exploitation of the sensitive LIF detection scheme, but circumvents the tedious labelling steps that are typically required. In their manuscript, they described the use of NanoOrange as an intercalating dye in the separation buffer, which interacts hydrophobically with the proteins-SDS complexes. This approach demands that the dye fluoresces significantly when bound to the protein-SDS complex as opposed to the scenario when it is bound to SDS micelles. The researchers acknowledged that the LOD was an important parameter to be used in evaluating the value of their method, but stated that at this time, the work was a proof of concept and thus evaluating LOD would be premature. They have since published another report detailing the development of a refined buffer system which is more amenable to dynamic labelling with a commercially available dye. The new publication reported the LOD (S/N = 3) for bovine serum albumin (BSA) to be 1 μg/mL [67].

A microfabricated analytical device that illustrated the integration of multiple operations on-chip was developed by Bousse and co-workers [68] at Caliper Technologies Corporation. They described the development of a glass microchip that performs a

protein sizing assay by integrating separation, staining, virtual destaining, and detection steps. In their approach, denatured SDS-protein complexes bind a fluorescent dye as the separation begins within the microchip. An intersection, situated at the end of the separation channel, serves to dilute the SDS present to below its critical micelle concentration, prior to detection, thus significantly reducing the background due to uncomplexed dye, which fluoresces when adsorbed in micelles. This publication reported an LOD (S/N = 3) of 30 nM for carbonic anhydrase. The authors also contrasted this detection limit to that obtained with SDS-PAGE (Coomassie brilliant blue) which was determined to be 140 nM.

An interesting construct published by Tabuchi et al. [69] described a novel pressurization technique to enhance the separation performance of μ–CE. Traditionally, μ–CE relies almost exclusively on electrokinetic injections [14, 32, 33, 70-75], followed by electrophoretic separation. The new construct presented by these authors used a pressurization technique prior to electrophoresis, which resulted in the achievement of dramatic reduction in migration time without compromising resolution. Using this technique, the authors demonstrated the separation of twelve samples of a protein mixture extracted from human lymphoblastic cell line within 15 s in a single run, using a twelve micro-channel array. In addition, they also demonstrated the pressurization technique using a standard mixture of model proteins and contrasted the effect of voltage and pressure injection on separation.

As is illustrated with the foregoing discussion, the analysis of protein samples by μ–CE is highly dependent on the use of labels. While this is necessary at times, perhaps to lower detection limits, it is also fraught with problems. In light of this, the use of the intrinsic fluorescence of species of interest can serve as an alternative for the need for labels. The issues hindering labelling will be discussed in Section 1.5 and will be preceded by a discussion on the spectral characteristics of the natively fluorescent amino acid moieties, peptides and proteins. The exploitation of native fluorescence of the aromatic amino acids residues present in proteins offers an attractive alternative to labelling for the detection of peptides and proteins. In addition to native fluorescence, EC detection also offers an alternative to labelling.

1.3.3 ELECTROCHEMICAL DETECTION

While LIF provides exquisite sensitivity with detection limits approaching the single molecule level [76-78] the detection system is much larger than the microfabricated devices, and thus, does not lend itself to developing totally miniaturized systems [38]. The development of alternative detectors that can be microfabricated on chip has attracted a lot of attention. EC detection, because of its ease of operation, low cost, selectivity and sensitivity has been generating great interest as an alternative detection mode for microfluidics [38-42].The principle of electrochemical detection is based upon the occurrence of redox reactions at the surface of the electrode, but it is not exclusive to this. Conductivity detection is considered as an EC technique, and has the ability to detect any analyte regardless if it contains an electroactive species or not.

Galloway et al. [38] developed an on-column contact conductivity detector on a poly(methyl methacrylate) (PMMA) chip for the detection of various mono- and polyanionic compounds after separation by electrophoresis. The researchers demonstrated the detection of amino acids, peptides, proteins and oligonucleotides and reported a concentration detection limit (S/N = 3) of 8 nM for alanine based on measurements made in the concentration range of ~15 – 100 nM. Free solution zone electrophoresis was also conducted for the separation of a ~0.23 μM solution containing nine peptides. A nine protein mixture (1.7 μM) was separated using micellar electrokinetic chromatography (MEKC) with conductivity detection on the PMMA chip. This is particularly attractive as an external fluorophore is not required, and the material is maintained in an analysable form for further processing, such as digestion followed by mass spectral fingerprinting for identification. Similar studies were carried out by Zuborova and co-workers [39] where they demonstrated the separation and detection of a mixture of five test proteins (100 μg/ml) on a PMMA chip with integrated conductivity detection. Studies were conducted on a series of chips to evaluate agreements in migration data, with the aim of generating good reproducibility towards a disposable device.

1.3.4 UV ABSORPTION

UV absorbance detectors are prevalent in many applications of conventional capillary electrophoretic and chromatographic devices. This has not been the case in chip based systems because of its poor sensitivity. However, there have been explorations in the development of UV detectors [46, 47, 79-81] for chip applications. Mao and Pawliszyn [81] demonstrated the feasibility of performing isoelectric focusing (IEF) on chip with absorption imaging detection. They achieved a detection limit of 30 μg/mL for myoglobin using a 10 μm optical path length. Vegvari and co-worker [80] explored the separation of peptides in carrier-free zone and gel electrophoresis in a hybrid microdevice. They observed that the separation in the gel medium gave better resolution, as compared with the free buffer experiment. No mention of the detection sensitivity was made.

1.4 SPECTRAL PROPERTIES OF THE AROMATIC AMINO ACIDS, PEPTIDES, AND PROTEINS

1.4.1 AMINO ACIDS

The structures of the three aromatic amino acids are presented in Figure 1-4. Teale and Weber [82] published a detailed report characterising the fluorescence of tryptophan, tyrosine and phenylalanine at neutral pH in aqueous media. They concluded that the fluorescence spectra of tryptophan, tyrosine and phenylalanine are "shown to consist of single bands in the ultraviolet region with maxima at 348, 303 and 282 nm respectively." Investigations to establish the quantum efficiency (+/- 1%) in neutral water yielded the following: phenylalanine had the smallest quantum efficiency (4%) followed by tryptophan and tyrosine, which had approximately the same quantum efficiency (20%). Finally, they discussed the "probability of energy transfer occurring among the aromatic amino acids in proteins and to the haem groups in haemoproteins", concluding that it is highly likely that these energy transfers do occur. Teale and Weber also postulated that energy transfers between the aromatic amino acids were feasible, from phenylalanine and tyrosine to tryptophan, in that order. Experimental evidence to support this was reported by Vladimirov. He noted that the emission from crystals of phenylalanine minimally contaminated with tryptophan was tryptophan-like in nature [83].

Chernitskii and Konev [84] also investigated the fluorescence of tryptophan in various media. They found that in 4% NaOH solution, the fluorescence maximum of tryptophan was shifted to 420 nm as compared with a maximum of 348 in neutral water.

Cowgill [85] investigated the effect of substituents on the fluorescence quantum yield of tryptophan and tyrosyl residues. He found that fluorescence loss was in "the order of increasing electronegativity of the substituents" on the phenol ring of the tyrosyl residue. In addition, he noted that factors other than electronegativity influence the fluorescence of tyrosine in peptides. Similar observations were made for tryptophan. Investigations on the effect of pH on the fluorescence of tryptophan and tyrosine showed that the quantum efficiency for both species is constant between the pH range 4 – 8. At lower pH (< 4), it was found that the quantum efficiency decreased for both amino acids and at higher pH (>9), the quantum efficiency for tryptophan rises while that for tyrosine falls. It was noted that beyond pH 11, tryptophan also loses fluorescence.

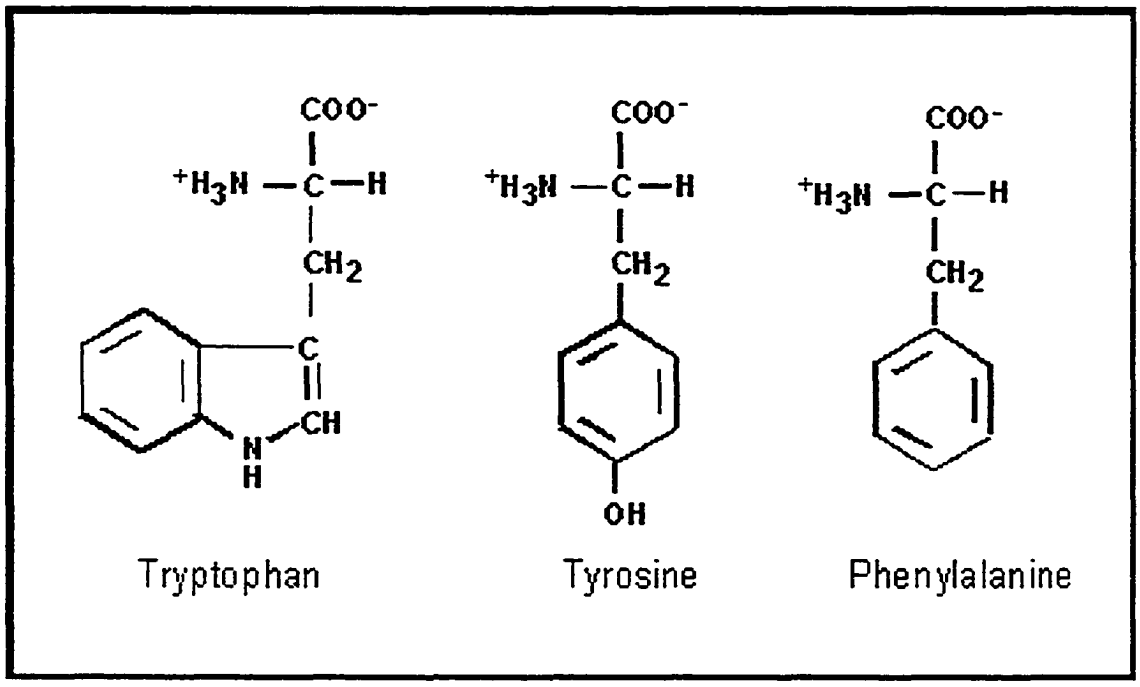

Figure 1-4: The three aromatic amino acids, tryptophan, W, tyrosine, Y, and phenylalanine, F that are responsible for the intrinsic fluorescence of proteins upon excitation with UV light.
Figure taken from http://www.biotek.com/products/tech_res_detail.php?id=130

1.4.2 PEPTIDES AND PROTEINS

According to Longworth [83], Konev was the first investigator to study the fluorescence of proteins. In his work, Konev showed that the fluorescence spectrum of a protein is a unique property of that protein. Further, he noted that protein fluorescence was not a combination of fluorescence emissions from the individual aromatic amino acids contained in it. In his investigations, Konev also demonstrated that proteins lacking the aromatic amino acids did not fluoresce, and those which lack tryptophan, though still containing tyrosine residues, emitted a spectrum characteristic of tyrosine. Shore and Pardee [86] also investigated the native fluorescence of proteins and related compounds. Their conclusions were summarised by Longworth: "proteins fluoresced in the UV under ambient conditions; the quantum yield of protein fluorescence was dependent on pH; proteins with similar aromatic amino acids composition showed differing fluorescence quantum yield; and fluorescence efficiency of proteins was comparable to fluorescence efficiency of the free amino acids"[83].

Teale [87] published a comprehensive report, building on his initial publication, in which he presented the fluorescence spectra of the aromatic amino acids. In this subsequent publication he described the fluorescence of the aromatic amino acids when they are contained in the poly peptide chains of globular proteins. In his study, fluorescence emission of over fifteen different proteins in water, 8 M urea and propane-1:2-diol was investigated. Studies were also carried out to interrogate what influence the viscosity and dielectric constant of the medium had on the quantum yields of tryptophan and glycotryptophan in solution. At the time, this very elegant work represented one of the most thorough analysis of the native fluorescence of proteins. Of all the proteins investigated, none showed a fluorescence emission spectrum that was characteristic of phenylalanine (emission maximum near 280 nm). Species that contained only phenylalanine as the aromatic residue, displayed fluorescence similar to the free amino acid in solution; however, the quantum efficiency was lower. In addition, proteins devoid of tryptophan, but possessing tyrosine residues exhibited tyrosine fluorescence, albeit, in low yield, or were not fluorescent. On the other hand, tryptophan-containing proteins exhibited a fluorescence spectrum characteristic of the free aromatic amino acid residue in solution. This was the case even when tyrosine was predominantly responsible for the

absorption at the excitation wavelength. The tyrosyl-carboxylate bond was deemed to be causing tyrosine fluorescence quenching, explaining the absence of tyrosine fluorescence in many of the proteins. In addition, it was found that as the viscosity increases, the fluorescence quantum yield of tryptophan increases, until it reaches a plateau. Finally, when the proteins were present in 8 M urea, there were large changes in the fluorescence quantum yield of tryptophan. This was attributed to the structural modification of the proteins that resulted from its presence in urea. It was also noted some of the observed changes in tryptophan fluorescence were reversible. For most of the proteins studied, propane-2 diol resulted in increased fluorescence quantum yield, with the serum albumins and lysozyme, being the exceptions.

Konev [84] notes that "the quantum yield of tryptophan in proteins is dependant on the macrostructural organisation and has lower values than free tryptophan in aqueous solution." He added, "tryptophan can exist in a hydrophobic microenvironment inside the protein globule or in a hydrophilic microenvironment on the surface of the protein, with the hydrophobic residues having a higher quantum yield. In addition, the peptide bond also has a quenching effect on fluorescence." Cowgill [88] also noted that peptide bonds decrease fluorescence. In his study, he measured the quantum efficiency of a series of peptides, and the effect of aromatic side chains, and pH on fluorescence. It was observed that the presence of a neighbouring aromatic ring had little effect on fluorescence of the species under investigation. For a peptide containing tyrosine and tryptophan, it was noted that all the fluorescence seemed to come from the tryptophan, as was observed previously by Teale [87]. Further, a peptide containing two tryptophan residues was shown to have a lower quantum yield, as compared to one containing a tryptophan and a tyrosine residue. The author also noted that the fluorescence of a peptide containing tryptophan and tyrosine is affected by the ionization of the phenolic ring of tyrosine. As a result, they concluded that some interaction must be occurring between the two groups, which imply that tyrosine does have an effect on the fluorescence.

To sum up, it can be concluded that the fluorescence emission of proteins and peptides will be dominated by tryptophan fluorescence, where present; fluorescence is dependent on pH, different tryptophan residues at different positions in the protein

structure will have differing fluorescent properties, and the fluorescence maxima is dependent on the nature of the media.

1.5 LASER INDUCED NATIVE FLUORESCENCE DETECTION

The above discussion lays the foundation upon which this section is built. The fact that the aromatic amino acids can fluoresce in the UV, thus implying that peptides and proteins containing these will possess similar characteristics is well known. However, not much was done in terms of exploiting this knowledge towards the development of detection schemes for peptides and proteins until the 1990s. The pioneering work of Jorgensen and Lucas [6] which demonstrated that amino acids and proteins could be separated by CE led to the development of CE as a separation tool. The subsequent application of lasers for detection in CE by Zare and Burton [89, 90] heralded a new revolution that resulted in CE becoming an unparalleled separation method. Due to the availability of fluorophores at common laser wavelengths, labelling schemes were developed for most applications for CE-LIF of species such as peptides and proteins [91-95]

LIF coupled with capillary electrophoresis provides a separation method that offers unparalleled efficiency and sensitivity [96, 97]. However, as noted, the utility of LIF applications hinges on the labelling of the sample of interest. This is not particularly useful in many applications, as labelling suffers from a wide variety of ailments. While labelling of amino acids and small peptides is relatively straightforward, labelling of proteins is often problematic. The issue is further compounded at low analyte concentrations, where labelling is non-quantitative, not very sensitive, suffers from slow reaction kinetics, the formation of multiply labelled products, and often, by-products of the labelling reaction lead to low yield of the labelled analyte and large fluorescent backgrounds [97, 98]. The formation of multiply labelled products is of particular concern with regard to proteins, due to the fact that many proteins contain free amine groups on their lysine side chains. As a consequence, the subtle charge differences that arises from differences in the number of labelled moieties results in broader peak profiles during the electrophoretic process. This particular problem can be addressed using a post column scheme, as was demonstrated by Jorgenson and Nickerson [94]. However, the other issues outlined above still remain.

A particularly attractive protein detection method would use a scheme that does not rely on labelling. Indirect LIF has been explored, where the running buffer is doped with a fluorescent species and the detection occurs through a reduction in background fluorescence [99]. This method typically has fairly high detection limits due to background fluorescence. Another interesting option is the use of lasers in the low UV region, which induce native fluorescence (Laser Induced Native Fluorescence, LINF) of the analyte molecules. Almost all proteins have some aromatic amino acids which naturally fluoresce, so the development of a native detection scheme for a microfluidic platform is a convenient approach to the development of a complete integrated system for protein analysis.

Not much work has been done that exploits the intrinsic fluorescence as a means of detecting peptides and proteins in CE. The first introduction to the use of native fluorescence detection in capillary electrophoresis was by Swaile and Sepaniak [100]. They reported a detection limit of 14 nM for conalbumin using a frequency doubled argon laser operating at 257 nm. This concentration detection limit was observed for a 50 μm ID capillary. The use of a smaller capillary (ID = 25 μm) resulted in an increase in the minimum detectable concentration to 25 nM. Lee and Yeung [101] reported improved detection limits for conalbumin and tryptophan. They were able to get a detection limit (S/N = 2) of 0.1 nM for conalbumin and 3 nM for tryptophan using the 275.4 nm line of an argon ion laser, with a 50 μm ID, 150 μm OD capillary. A pulsed native fluorescence system operating at 248 nm, with a 75 μm ID capillary was described by Chan et al. and they reported a detection limit (S/N = 2) of 3.3 nM for tryptophan, and 1.3 and 4 nM for conalbumin and bovine serum albumin respectively [102]. The authors contend that the the limit of detection (LOD) was at least two orders of magnitude more sensitive when compared to UV absorption at 214 nm. Using the same laser as Chan and co-workers, Chang and Yeung improved the LOD for tryptophan to 0.7 nM (S/N = 2) under low pH conditions [103]. Applying a laser that is similar to the one described in this work to a CE set-up, Chan [96] and co workers reported a detection limit of 2 nM for tryptophan using a 50 μm ID capillary. Timperman and co-workers [98] employed a frequency doubled Kr-ion laser operating at 284 nm with a sheath flow cell for CE (50 μm ID, 82 cm long) separations of peptides containing tryptophan and tyrosine. They reported an LOD (S/N=

3) of 0.2 nM for tryptophan and 20 nM for tyrosine. Tseng and Chang [104] performed on-line concentration and separation of proteins by capillary electrophoresis using polymer solutions and native fluorescence detection. They used an uncoated 75 μm ID capillary and a buffer solution containing ethidium bromide for the protein separations and reported LOD in the range of 13 – 79 nM for a series of model proteins. With preconcentration, the authors reported sub-nanomolar LOD.

To our knowledge, LINF detection has only been applied to CE and never to μ–CE. The microfluidic applications relied exclusively on the use of labelling agents, which as stated above, may not always be the favoured approach. Thus, the exploration of μ–CE and LIF that does not rely upon labelling was deemed to be a beneficial area of research.

1.6 CAPILLARY ELECTROPHORESIS

A brief historical review of CE will be presented here as this was the separation technology employed in the microfluidic applications investigated in this thesis. In Chapter 3, we applied the label free detector developed in the preceding chapter for the detection of peptides and proteins after CE separation. To bring into focus the theoretical underpinnings and as an introduction to the discussion in Chapter 3, some basic concepts of the separation process are presented, followed by a brief introduction to the characterization of the efficacy of the separation process. These are presented in the sections that follow.

1.6.1 HISTORICAL PERSPECTIVE AND FUNDAMANTALS OF CE

The concept of capillary zone electrophoresis (CZE) was first introduced by Hjerten in 1967 when he demonstrated the separation of a diverse range of analytes, from small species, such as inorganic ions to macromolecular species like proteins [105]. The use of a narrow 3 mm internal diameter (ID) glass tube allowed for charge based separations. In contrast to the 3 mm tube used by Hjerten, Virtanen demonstrated that the use of smaller ID glass tube (0.2 mm) would eliminate the issues arising from heat convection [106]. However, the potential of this significant development was not fully realised and

exploited until the pioneering work of Jorgenson and Lucas, which demonstrated the exemplary resolving power of CZE [6, 107, 108].

Conventionally, CE is performed in buffer filled capillaries and is driven by a combination of electroosomotic flow (EOF) and the inherent electrophoretic mobility (EPM) of the analyte species. A diagrammatic representation of the instrumental set-up is illustrated in Figure 1-5. The basis of the separation is the differences in the EPM of the individual analyte species in the sample [6, 108-110]. The EPM of a particular moiety is given by the following equation [111]:

$$\mu_{ep} = \frac{q}{6\pi\eta r} \qquad 1\text{-}1$$

where μ_{ep} is the electrophoretic mobility, q is the charge on the analyte species, r is the Stokes radius and η is the solution viscosity. The EPM of a molecule is dependent on the charge/size ratio of the sample at a given pH. Upon application of an external electric field, each ion will move towards the electrode of opposite charge and under steady state conditions, will reach a constant value. This is what is referred to as EPM.

Due to the presence of the exposed silanol groups, the surface of the fused silica capillaries and glass channels are inherently negatively charged. As a result, the positive charges from the bulk solution will aggregate along the channel walls. On application of an applied electric field, the presence of these excess positive charges induces migration towards the negative electrode. The result is the dragging of the entire bulk of the solution towards the negative terminal, a process referred to as electroosomotic flow and is given by Equation 1-2 [112]:

$$\mu_{eo} = \frac{\varepsilon\zeta}{4\pi\eta} \qquad 1\text{-}2$$

where ε is the dielectric constant of the solution, ζ is the zeta potential and η is the viscosity. The electroosomotic force results in a plug flow profile, as opposed to hydrodynamically driven flow which is parabolic in nature. This flat flow profile results in a narrow analyte zone and minimizes band broadening, one of the many advantages of this separation technique.

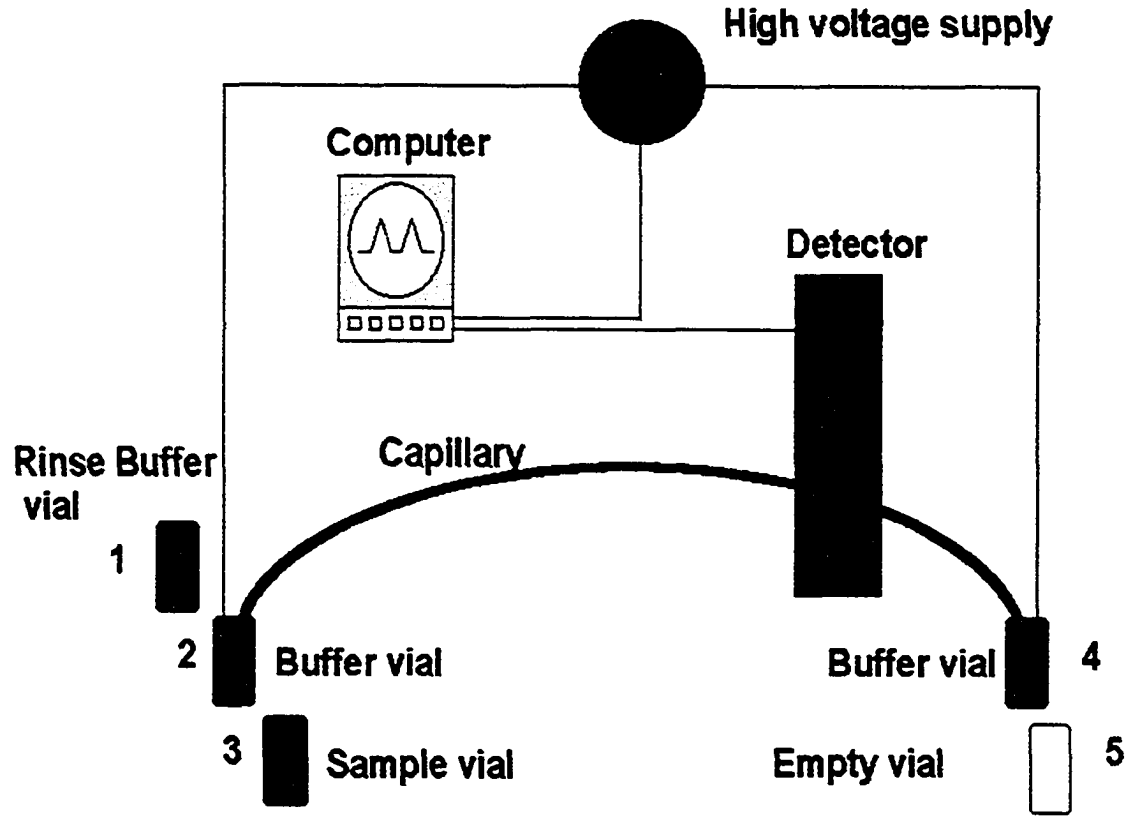

Figure 1-5: Schematic illustration of a conventional capillary electrophoresis system. Figure was adapted from the following website: *http://www.ceandcec.com/ce_theory.htm*

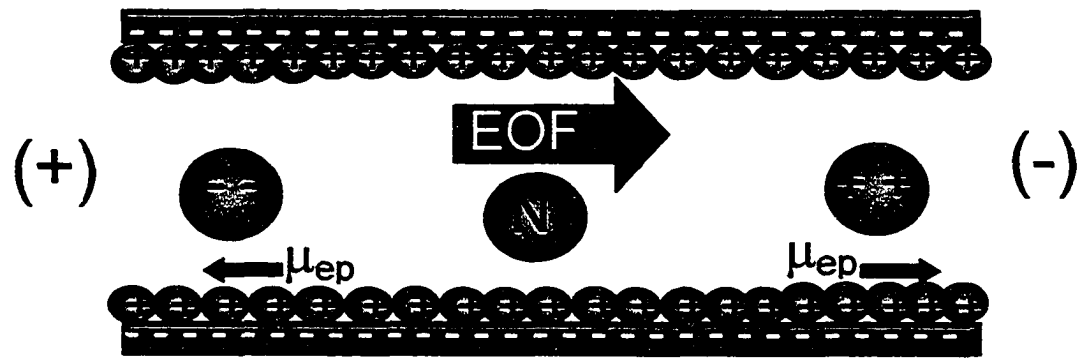

Figure 1-6: Schematic illustration of electroosmosis (EOF) and electrophoresis (μ_{ep}). Diagram shows the differential migration of the ions under the presence of an applied electric field.

The combination of EOF and EPM is what results in the separation of the analyte species in the sample. Figure 1-6 shows the result of these two phenomena in a separation process. The detail presented here to describe the process of CZE is by no means complete, but rather a simplification to contextualise the thesis. For a more in-depth analysis the reader is directed to the Handbook of Capillary Electrophoresis [111].

1.6.2 SEPARATION EFFICIENCY

The efficacy of a chromatographic separation is dependent on the degree of disengagement between the zone centres of the species in the sample, and the degree of band broadening that a particular column tends to produce, which is also referred to as the efficiency, N of the column. The same concepts can be applied to the electrokinetic separation in capillaries to describe its efficiency and effectiveness. A measure of the number of theoretical plates, or efficiency, described by N can be computed using the formula in Equation 1-3:

$$N = \frac{L_d^2}{\sigma_{tot}^2} \qquad 1\text{-}3$$

where L_d is the distance from the injector to the detector, and σ^2_{tot} is the total variance associated with a Gaussian peak. Equation 1-3 can be restated in terms of baseline bandwidth. The baseline width of a Gaussian peak is related to the total standard deviation by the following equation:

$$W_b = 4\sigma_{tot} \qquad 1\text{-}4$$

Thus, Equation 1-3 now becomes:

$$N = 16\frac{L_d^2}{W^2{}_b} \qquad 1\text{-}5$$

Alternatively, for a normal Gaussian distribution, the width of the peak at half maximum corresponds to 2.354 σ, thus $W_{1/2}$ = 2.354 σ and Equation 1-3 can be rewritten as Equation 1-6, with $W_{1/2}$ measured in units of length:

$$N = 5.54\frac{L_d^2}{W_{1/2}^2} \qquad 1\text{-}6$$

The above equation can also be expressed in units of time:

$$N = 5.54\frac{t_r^2}{W_{1/2}^2} \qquad 1\text{-}7$$

where t_r is the retention time.

The most common definition of peak or band separation is resolution, R_S, and this can also be used in characterising CE separations. R_S expresses the separation between the peak centres (Gaussian peaks) in terms of the average baseline width of the peaks and is given by the following equation:

$$R_S \equiv \frac{t_{r2} - t_{r1}}{\frac{1}{2}(w_1 + w_2)} \qquad 1\text{-}8$$

where t_{r1} and t_{r2} are the retention times, and w_1 and w_2 are the baseline bandwidths of the two analyte peaks expressed in units of time, respectively. As is observed in Equation 1-8, R_S is unitless; it can be rewritten in a similar fashion as was done with the efficiency equation, as long as both measured components are in the same units.

1.7 SCOPE OF THIS THESIS

Microfluidics has demonstrated exemplary potential to revolutionize the way laboratory analysis is done. Of particular interest is the fact that most conventional CE applications are quite suited for miniaturization due to the unmistakeable improvements in separation performance at these dimensions. Thus the overall aim of the work that resulted in this thesis was to develop a detection scheme for peptides and proteins that exploited μ-CE and LIF, but did not rely on extrinsic fluorophores.

Chapter 2 presents the mechanics that went into the fabrication of the microfluidic chip and the development of the LINF detector. The intrinsic fluorescence of tryptophan upon excitation with a 266 nm laser was explored and the system was optimised to utilise the fluorescence originating from this aromatic amino acid. The LOD determined and the efforts made to reduce this are presented, along with an analysis of the limiting factors that inhibit the dynamic range of the system.

In Chapter 3, the detection scheme was applied for the detection of peptides and proteins after μ-CE separation. Model peptides and proteins were separated and detected

upon excitation with the 266 nm UV laser, based on their intrinsic fluorescence. The quality of protein separation was investigated at differing pHs. A model protein was digested off-chip and the protein fragments separated on-chip to demonstrate the ability of the system to handle real digests.

Finally, Chapter 4 provides a brief summary of the achievements in the preceding chapters, in addition to a brief outlook for future investigations.

1.8 REFERENCES

(1) Taylor, J., University of Alberta, Edmonton, Alberta, Canada, 2003.
(2) Wang, C.; Oleschuk, R.; Ouchen, F.; Li, J.; Thibault, P.; Harrison, D. J. *Rapid Communications in Mass Spectrometry* **2000**, *14*, 1377-1383.
(3) Chow, A. W. *AIChE Journal* **2002**, *48*, 1590-1595.
(4) Manz, A.; Effenhauser, C. S. In *American Laboratory*, 1994, pp 15-18.
(5) Manz, A.; Harrison, D. J.; Verpoorte, E.; Widmer, H. M. In *Advances in Chromatography*; Brown, P. R., Grushka, E., Eds.; Marcel Dekker, Inc.: New York, 1993; Vol. 33, pp 1-66.
(6) Jorgenson, J. W.; Lucas, K. D. *Anal. Chem.* **1981**, *53*, 1298-1302.
(7) Novotny, M. V.; Cobb, K. A.; Liu, J. *Electrophoresis* **1990**, *11*, 735-749.
(8) Erickson, D.; Li, D. *Analytica Chimica Acta* **2004**, *507*, 11-26.
(9) Terry, S. C.; Jerman, J. H.; Angell, J. B. *IEEE Trans. Electron Devices* **1979**, *ED - 26*, 1880-1886.
(10) Bassous, E.; Taub, H. H.; Kuhn, L. *Appl. Phys. Lett.* **1977**, *31*, 135-137.
(11) Petersen, K. E. *IEEE Trans. Electron Devices* **1979**, *ED -26*, 1918-1920.
(12) Manz, A.; Grabber, N.; Widmer, H. M. *Sensors and Actuators B* **1990**, *1*, 244-248.
(13) Manz, A.; Harrison, D. J.; Verpoorte, E.; Fettinger, J. C.; Paulus, A.; Ludi, H.; Widmer, H. M. *Journal of Chromatography* **1992**, *593*, 253-258.
(14) Harrison, D. J.; Manz, A.; Fan, Z. H.; Ludi, H.; Widmer, H. M. *Anal. Chem.* **1992**, *64*, 1926-1932.
(15) Jakeway, S. C.; de Mello, A.; Russel, E. L. *Fresenius J Anal. Chem.* **2000**, *366*, 525-539.
(16) Chovan, T.; Guttman, A. *Trends in Biotechnology* **2002**, *20*, 116-122.
(17) Beebe, D. J.; Mensing, G. A.; Walkker, G. M. *Annu. Rev. Biomed. Eng.* **2002**, *4*, 261-286.
(18) Verpoorte, E. *Electrophoresis* **2002**, *23*, 677-712.
(19) Tudos, A. J.; Besselink, G. A. J.; Schasfoort, R. B. M. *Lab on a Chip* **2001**, *1*, 83-95.
(20) Huang, Y.; Mather, E. L.; Bell, J. L.; Madou, M. *Anal. Bioanal. Chem.* **2002**, *372*, 49-65.
(21) Landers, J. P. *Anal. Chem.* **2003**, *75*, 2919-2927.
(22) Vo-Dinh, T.; Cullum, B. *Fresenius J. Anal. Chem.* **2000**, *366*, 540-551.
(23) Auroux, P.-A.; Iossifidis, D.; Reyes, D. R.; Manz, A. *Anal. Chem.* **2002**, *74*, 2637-2652.
(24) Reyes, D. R.; Iossifidis, D.; Auroux, P.-A.; Manz, A. *Anal. Chem.* **2002**, *74*, 2623-2636.
(25) Vilkner, T.; Janasek, D.; Manz, A. *Anal. Chem.* **2004**, *76*, 3373-3386.
(26) Xue, Q.; Foret, F.; Dunayevskiy, Y. M.; Zavracky, P. M.; McGruer, N. E.; Karger, B. L. *Anal. Chem.* **1997**, *69*, 426-430.
(27) Figeys, D.; Aebersold, R. *Anal. Chem.* **1998**, *70*, 3721-3727.
(28) Figeys, D.; Ning, Y.; Aebersold, R. *Anal. Chem.* **1997**, *69*, 3153-3160.
(29) Bings, N. H.; Wang, C.; Skinner, C. D.; Colyer, C. L.; Thibault, P.; Harrison, D. J. *Anal. Chem.* **1999**, *71*, 3292-3296.

(30) Wen, J.; Xiang, F.; Matson, D. W.; Udseth, H. R.; Smith, R. D. *Electrophoresis* **2000**, *21*, 191-197.
(31) Lazar, I. M.; Ramsey, R. S.; Ramsey, J. M. *Anal. Chem.* **2001**, *73*, 1733-1739.
(32) Harrison, D. J.; Fluri, K.; Seiler, K.; Fan, Z. H.; Effenhauser, C. S.; Manz, A. *Science* **1993**, *261*, 895-897.
(33) Jacobson, S. C.; Hergenroder, R.; Moore, A. W.; Ramsey, J. M. *Anal. Chem.* **1994**, *66*, 4127-4132.
(34) Jacobson, S. C.; Koutny, L. B.; Hergenroder, R.; Moore, A. W.; Ramsey, J. M. *Anal. Chem.* **1994**, *66*, 3472-3476.
(35) Colyer, C. L.; Mangru, S. D.; Harrison, D. J. *Journal of Chromatography A* **1997**, *781*, 271-276.
(36) Fluri, K.; Fitzpatrick, G.; Chiem, N.; Harrison, D. J. *Anal. Chem.* **1996**, *68*, 4285-4290.
(37) Liu, Y.; Foote, R. S.; Jacobson, S. C.; Ramsey, R. S.; Ramsey, J. M. *Anal. Chem.* **2000**, *72*, 4608-4613.
(38) Galloway , M.; Stryjewski, W.; Henry, A.; Ford, S. M.; Llopis, S.; McCarley, R. L.; Soper, S. A. *Anal. Chem.* **2002**, *74*, 2407-2415.
(39) Zuborova, M.; Demianova, Z.; Kaniansky, D.; M., M.; Stanislawski, B. *Journal of Chromatography A* **2003**, *990*, 179-188.
(40) Wang, J.; Pumera, M.; Chatrathi, M. P.; Escarpa, A.; Konrad, R.; Griebel, A.; Dorner, W.; Lowe, H. *Electrophoresis* **2002**, *23*, 596-601.
(41) Wang, J.; Polsky, R.; Tian, B.; Chatrathi, M. P. *Anal. Chem.* **2000**, *72*, 5285-5289.
(42) Zeng, Y.; Chen, H.; Pang, D.-W.; Wang, Z.-L.; Cheng, J.-K. *Anal. Chem.* **2002**, *74*, 2441-2445.
(43) Tantra, R.; Manz, A. *Anal. Chem.* **2000**, *72*, 2875-2878.
(44) Martin, R. S.; Gawron, A. J.; Lunte, S. M. *Anal. Chem.* **2000**, *72*, 3196-3202.
(45) Laugere, F.; Guijt, R. M.; Bastemeijier, J.; van der Steen, G.; Berthold, A.; Baltuseen, E.; DSarro, P.; van Dedem, G. W. K.; Vellekoop, M.; Bossche, A. *Anal. Chem.* **2003**, *75*, 306-312.
(46) Liang, Z.; Chiem, N.; Ocvirk, G.; Tang, T.; Fluri, K.; Harrison, D. J. *Anal. Chem.* **1996**, *68*, 1040-1046.
(47) Salimi-Moosavi, H.; Jiang, Y.; Lester, L.; McKinnon, G.; Harrison, D. J. *Electrophoresis* **2000**, *21*, 1291-1299.
(48) Walker, P. A.; Morris, M. D. *Anal. Chem.* **1998**, *70*, 3766-3769.
(49) Hashimoto, M. H.; Tsukagoshi, K.; Nakajima, K.; Kondo, K.; Arai, A. J. *Journal of Chromatography A* **2000**, *867*, 271-279.
(50) Mangru, S. D.; Harrison, D. J. *Electrophoresis* **1998**, *68*, 2301-2307.
(51) Liu, B.-F.; Ozaki, M.; Utsumi, Y.; Hattori, T.; Terabe, S. *Anal. Chem.* **2003**, *75*, 36-41.
(52) Burggraf, N.; Krattinger, B.; de Mello, A.; de Rooij, N. F.; Manz, A. *Analyst* **1998**, *123*, 1443-1447.
(53) Zan, W.; Alvarez, J.; Sun, L.; Crooks, R. M. *Anal. Chem.* **2003**, *75*, 1233-1238.
(54) Arora, A.; de Mello, A.; Manz, A. *Analytical Communications* **1997**, *34*, 393-395.
(55) Arora, A.; Eijkel, J. C. T.; Morf, W. E.; Manz, A. *Anal. Chem.* **2001**, *73*, 3282-3288.
(56) Eijkel, J. C. T.; Stoeri, H.; Manz, A. *Anal. Chem.* **2000**, *72*.

(57) Kwok, Y. C.; Manz, A. *Micro Total Analysis Systems 2000*, Enschede, The Netherlands 2000; Kluwer Academic Publishers; 603-606.
(58) Issaq, H. J.; Conrads, T. P.; Janini, G. M.; Veenstra, T. D. *Electrophoresis* **2002**, *23*, 3048-3061.
(59) Mouradian, S. *Current Opinion in Chemical Biology* **2001**, *6*, 51-56.
(60) Ramsey, R. S.; Ramsey, J. M. *Anal. Chem.* **1997**, *69*, 1174-1178.
(61) Lion, N.; Gobry, V.; Jensen, H.; Rossier, J. S.; Girault, H. H. *Electrophoresis* **2002**, *23*, 3583-3588.
(62) Jin, L. J.; Ferrance, J.; Sanders, J. C.; Landers, J. P. *Lab on a Chip* **2003**, *3*, 11-18.
(63) Li, J.; LeRiche, T.; Tremblay, T.-L.; Wang, C.; Bonneil, E.; Harrison, D. J.; Thibault, P. *Molecular and Cellular Proteomics* **2002**, 157-168.
(64) Liu, Y.; Foote, R. S.; Culbertson, C. T.; Jacobson, S. C.; Ramsey, J. S.; Ramsey, J. M. *Journal of Microcolumn Separations* **2000**, *12*, 407-411.
(65) Gottschlich, N.; Culbertson, C. T.; McKnight, T. E.; Jacobson, S. C.; Ramsey, J. M. *Journal of Chromatography B* **2000**, *745*, 243-249.
(66) Jin, L. J.; Giordano, B. C.; Landers, J. P. *Anal. Chem.* **2001**, *73*, 4994-4999.
(67) Giordano, B. C.; Jin, L. J.; Couch, A. J.; Ferrance, J. P.; Landers, J. P. *Anal. Chem.* **2004**, *76*, 4705-4714.
(68) Bousse, L.; Mouradian, S.; Minalla, A.; Yee, H.; Williams, K.; Dubrow, R. *Anal. Chem.* **2001**, *73*, 1207-1212.
(69) Tabuchi, M.; Kuramitsu, Y.; Nakamura, K.; Baba, Y. *Anal. Chem.* **2003**, *75*, 3799-3805.
(70) Griffiths, S. K.; Nilson, R. H. *Anal. Chem.* **2000**, *72*, 5473-5482.
(71) Kutter, J. P.; Jacobson, S. C.; Ramsey, J. M. *Anal. Chem.* **1997**, *69*, 5165-5171.
(72) Paegel, B. M.; Hutt, L. D.; Simpson, P. C.; Mathies, R. A. *Anal. Chem.* **2000**, *72*, 3030.3037.
(73) Ocvirk, G.; Munrow, M.; Tang, T.; Oleschuk, R.; Westra, K.; Harrison, D. J. *Electrophoresis* **2000**, *21*, 107-115.
(74) Effenhauser, C. S.; Manz, A.; Widmer, H. M. *Anal. Chem.* **1993**, *65*, 2637-2642.
(75) Seiler, K.; Harrison, D. J.; Manz, A. *Anal. Chem.* **1993**, *65*, 1481-1488.
(76) Effenhauser, C. S.; Bruin, G. J. M.; Paulus, A.; Ehrat, M. *Anal. Chem.* **1997**, *69*, 3451-3457.
(77) Haab, B. B.; Mathies, R. A. *Anal. Chem.* **1999**, *71*, 5137-5145.
(78) Fister, J. C. I.; Jacobson, S. C.; Davis, L. M.; Ramsey, J. M. *Anal. Chem.* **1998**, *70*, 431-437.
(79) Lu, H.; Schmidt, M. A.; Jensen, K. F. *Lab on a Chip* **2001**, *1*, 22-28.
(80) Vegvari, A.; Hjerten, S. *Electrophoresis* **2003**, *24*, 3815-3820.
(81) Mao, Q.; Pawliszyn, J. *Analyst* **1999**, *124*, 637-641.
(82) Teale, F. W. J.; Weber, G. *Biochemical Journal* **1957**, *65*, 476-482.
(83) Longworth, J. W. In *Excited States of Proteins and Nucleic Acids*; Steiner, F. R., Weinryb, I., Eds.; Plenum Press: New York, 1971, pp Chapters 5, 6.
(84) Konev, S. V. *Fluorescence and Phosphorescence of Proteins and Nucleic Acids*; Plenum Press: New York, 1967.
(85) Cowgill, R. W. *Archives of Biochemistry and Biophysics* **1963**, *100*, 36-44.
(86) Shore, V. G.; Pardee, A. B. *Archives of Biochemistry and Biophysics* **1956**, *60*, 100-107.

(87) Teale, F. W. J. *Biochemical Journal* **1960**, *76*, 381-388.
(88) Cowgill, R. W. *Biochim. Biophys. Acta* **1963**, *75*, 272-273.
(89) Burton, D. E.; Sepaniak, M. J.; Maskarinec, M. P. *Journal of Chromatographic Science* **1986**, *24*, 347-351.
(90) Gassmann, E.; Kuo, J. E.; Zare, R. N. *Science* **1985**, *230*, 813-814.
(91) Harvey, M. D.; Bablekis, V.; Banks, P. R.; Skinner, C. D. *Journal of Chromatography B* **2001**, *754*, 345-356.
(92) Ye, M.; Hu, S.; Quigley, W. C.; Dovichi, N. J. *Journal of Chromatography A* **2004**, *1022*, 201-206.
(93) Sepaniak, M. J.; Swaile, D. F.; Powell, A. C. *Journal of Chromatography* **1989**, *480*, 185-196.
(94) Nickerson, B.; Jacobson, J. W. *Journal of Chromatography* **1989**, *480*, 157-168.
(95) Jorgenson, J. W.; Rose, D. J. J. *Journal of Chromatography* **1988**, *447*, 117-131.
(96) Chan, K. C.; Muschik, G. M.; Issaq, H. J. *Electrophoresis* **2000**, *21*, 2062-2066.
(97) Zhang, X.; Sweedler, J. V. *Anal. Chem.* **2001**, *73*, 5620-5624.
(98) Timperman, A. T.; Oldenburg, K. T.; Sweedler, J. V. *Anal. Chem.* **1995**, *67*, 3421-3426.
(99) Kuhr, W. G.; Yeung, E. S. *Anal. Chem.* **1988**, *60*, 2642-2646.
(100) Swaile, D. F.; Sepaniak, M. J. *Journal of Liquid Chromatography* **1991**, *14*, 869-893.
(101) Lee, T. T.; Yeung, E. S. *Journal of Chromatography* **1992**, *595*, 319-325.
(102) Chan, K. C.; Janini, G. M.; Muschik, G. M.; Issaq, H. J. *Journal of Liquid Chromatography* **1993**, *16*, 1877-1890.
(103) Chang, H.-T.; Yeung, E. S. *Anal. Chem.* **1995**, *67*, 1079-1083.
(104) Tseng, W.-L.; Chang, H.-T. *Anal. Chem.* **2000**, *72*, 4805-4811.
(105) Hjerten, S. *Chromatogr. Rev.* **1967**, *9*, 122-124.
(106) Virtanen, R. *Acta. Polytechnica Scand.* **1974**, *123*, 1.
(107) Jorgenson, J. W.; Lucas, K. D. *Clinical Chemistry* **1981**, *27*, 1551-1553.
(108) Jorgenson, J. W.; Lucas, K. D. *Science* **1983**, *222*, 266-272.
(109) Gordon, M. J.; Huang, X.; Pentoney, S. L. J.; Zare, R. N. *Science* **1988**, *242*, 224-228.
(110) Grossman, P. D.; Colburn, J. C.; Lauer, H. H. *Anal. Chem.* **1989**, *61*, 1186-1194.
(111) Oda, R. P.; Landers, J. P. In *Handbook of Capillary Electrophoresis,* 2 nd ed.; Landers, J. P., Ed.; CRC Press Inc.: New York, 1996.
(112) Li, S. F. Y. *Capillary electrophoresis: principles, practice and applications*; Elsevier: Amsterdam, 1993.

CHAPTER 2: NATIVE FLUORESCENCE DETECTION ON CHIP

2.1 INTRODUCTION

Laser induced fluorescence is one of the most sensitive detection modes in capillary electrophoresis and has become the first choice for detection of microchip separations. In most of its applications, the species of interest has been fluorescently modified, which is successful due to the wide availability of fluorophores at the common laser wavelengths in the visible region. However, the exploitation of the intrinsic ultra-violet (UV) fluorescent properties of fluorophores is attractive, as it eliminates the labelling steps, which can be problematic. This is particularly so in protein analysis, where multiply labelled peaks results in broad peak profiles and reduction in separation efficiency and UV chromophores are usually present.

Protein fluorescence was not used as a capillary electrophoresis (CE) detection method for peptides and proteins until the early 1990s, when Swaile and Sepaniak [1] employed native fluorescence for the detection of conalbumin. This detection scheme was not widely adopted due to the high cost of high powered, gas phase lasers available in the deep UV at that time. Swaile and Sepaniak [1] utilised the frequency doubled output of the 514 nm line from a high power argon ion laser, which did not provide an excellent match between the excitation wavelengths and excitation maxima for the fluorophores in question. Subsequent work in this area saw the utilization of the 275.4 nm line of the argon ion laser [2] and of a frequency doubled krypton laser [3]. All of these are expensive gas phase, water-cooled lasers that require significant maintenance. The need for specialised skills, coupled with the high cost and size of these lasers, saw very little interest develop in the area of native fluorescence detection.

The availability of relatively inexpensive, small and rugged, UV solid state lasers has renewed exploitation of intrinsic UV fluorophores for detection applications [4, 5]. For example, using a 266 nm diode based laser, Issaq and co-workers [5] reported a LOD for tryptophan on the order of 2 nM (S/N = 2), when applied to fused silica capillaries with a 50 μm internal diameter. The authors used a Nd:YAG (Neodynium:Yttrium Aluminium Garnet) solid state laser, which is optically pumped. The basic wavelength of this laser is 1.064 μm, and this wavelength has often been doubled to 530 nm or quadrupled to 266 nm. Frequency multiplexing is often achieved by using a birefringent material which has

a crystal structure that lacks symmetry. Such lasers, available at 266 nm are pulsed. Because these lasers are now more available and less costly, we foresee an increased interest in their application as a detection tool, especially in the area of protein analysis, as it alleviates the problematic and cumbersome labelling steps that are typically involved.

In this chapter, we explore the use of confocal epifluorescence microscopy to develop a label free optical method capable of detecting proteins and peptides within a microfluidic platform. This microscope setup was previously described by Ocvirk and co-workers for use as a visible wavelength detection system for labelled species. They reported a detection limit of 300 fM for fluorescein on microchip [6]. In this work, we rely on the intrinsic fluorescence of the aromatic amino acid tryptophan. The LOD obtained when using a 266 nm pulsed excitation source is reported, as well as investigations carried out in order to further probe and reduce the LOD.

2.2 EXPERIMENTAL

2.2.1 SOLUTIONS AND REAGENTS

All solutions were prepared with doubly distilled, deionised water (Millipore Canada) which was degassed by boiling. For on-chip studies, a 9.55 mM tryptophan (Sigma, USA) stock solution was prepared in filtered (0.2 μM pore size, Chromatographic Specialities Inc.) water and was diluted to the desired concentrations in the running buffer. All limits of detection (LOD) studies were performed in 25 mM boric acid (BDH Inc.) buffer, pH 9.0. The pH of the buffer was adjusted by titration with 1M NaOH (BDH Inc.) to the required value. Buffer solutions were filtered using a Nylon syringe filter (0.2 μM pore size, Chromatographic Specialities Inc.) prior to introduction into the microchip. The final sample solutions were not filtered.

Solutions of tryptophan, tyrosine, and phenylalanine (0.1 mM) were prepared in water for use in the determination of the emission spectra for the aromatic amino acids, when excited at various wavelengths (RF 5301 Spectrofluorometer).

2.2.2 GLASS FLUORESCENCE MEASUREMENT

The fluorescence from the quartz glass substrate used in the fabrication of microfluidic devices was measured using the RF 5301 Spectrofluorometer. The substrate was diced to the dimension of ~1.2 cm x 4.5 cm to fit the curvet holder in the instrument and was held in position with the aid of adhesive tape. It was then exposed to 266 nm light and the emission spectra recorded. The substrate was then blasted with a 266 UV Nd: YAG laser at various positions for several hours. Its fluorescence was subsequently re-measured.

2.2.3 DEVICES

2.2.3.1 Device Fabrication

Microfabrication of the devices was done at the University of Alberta Nanofab facility. Devices were fabricated in an ultra parallel (ultra parallel here describes the degree of "bow" that is characteristic of the particular substrate being used), round quartz substrate (Hoya, USA) that was approximately 100 mm x 100 mm in dimension and 0.525 mm thick. Fabrication followed standard photolithographic and wet chemical techniques, as published in the literature[7, 8], with some modifications, to produce channel structures in the fused silica wafer. The details of microfabrication are as follows: the substrates were sent to Micralyne (Edmonton, Alberta) for RF (radio frequency) cleaning and sputter metallization (500 Å Cr, 1500 Å Au). A layer of positive photoresist, HPR 504 (OCG Microelectronic Materials) was then spin coated on to the Cr-Au coated quartz substrate using a Solitec Photoresist Coater/Developer (500 rpm for 10 s, 4000 rpm for 40s). The substrate was subsequently baked at 115 °C for 30 min to strengthen the resist and then allowed to cool at room temperature for 15 min, before being patterned with the master mask to define the device characteristics, on the AB-M mask aligner. Exposure to UV light (λ = 365 nm) for 4 s served to transfer the mask pattern onto the substrate. The exposed resist was subsequently developed using a Microposit developer - 354 (25 s, Shipley Co., L.L.C, Massachusetts). The exposed Au and Cr were removed using gold (~18 s, KI: I_2 = 4:1 in H_2O) and chrome (~13 s, HNO_3, $(NH_4)_2Ce(NO_3)_6$, Arch Chemicals, Inc) etchants, respectively. The resulting mask pattern was etched into the quartz substrate by immersing it into a quartz etching solution (HF:HNO_3 = 20:14). The

depth of etching was controlled by monitoring etching time and by measuring the chip with a profilometer. A rate of 0.638 μm/min was observed. After the desired depth was attained, the unexposed photoresist was removed with acetone, followed by the removal of the Au and Cr using gold and chrome etchants, respectively.

Having completed the fabrication process, attention was then shifted to the production of a cover plate. After careful measurement, the positions of the channel terminals were marked on the cover plate, and the substrate mounted on a piece of scrap glass with the aid of Crystalbond™ (Aremco Products Inc.). A 4" x 4" 0211 glass (540 μm thick, square, Corning, NY, USA) plate was then mounted on top of the quartz substrate. The 0211 glass served to reduce fragmentation and break out as the drill contacts and passes through the quartz substrate, resulting in a more uniform finish. At this point, 2 mm access holes were then mechanically drilled (Drill bits from Lee Valley, Ontario) into the cover plate while immersing the sandwich containing the wafer in a water bath.

Quality bonding of the quartz substrates was not a trivial matter, as it required extra care; we followed the same steps as was used in Si – Si fusion bonding [8-11]. It was found that wafers needed to be of high parallelism (i.e. variation in surface roughness must be extremely small and very little "bow" should exist) and absolutely clean for cold bonding to occur. In addition, the face of the cover plate to be bonded onto the etched substrate needed to be the highly parallel side, as both sides of the wafer are not of the same ultra high parallel finish. The drilled cover plate was first sonicated in a water bath (Branson 1200, CT, USA) to get rid of any particulates created by drilling. The etched substrate and the cover plate were cleaned with hot piranha for 30 min, then rinsed with copious amounts of water. This was followed by scrubbing for approximately 1 min with soap solution (Sparkleen 1, Fisher Scientific) and extensive washing with water. The wafers were then dried and mounted in a wafer holder (Micro Automation Inc, Mounting Station Model 150). Each piece was then rinsed (5 cycles) and dried (10 cycles) in a high pressure cleaning station (Micro Automation 2066). The soap scrubbing and the high pressure washing/drying stages were repeated twice before one final high pressure washing and drying stage. At this time, the top and bottom wafers were then aligned and contacted gently together at one end to start the cold bonding process via electrostatic

interactions. In between washing, the wafers were always kept face down to prevent any particulates that might be in the air from contacting the surface. Thermal bonding of the etched wafer and cover plate was achieved by baking at 1000 ° C for approximately 9 hours (an upward ramp, room temperature to 800 °C @ 10 °C/min; 800 °C to 1000 °C @ 3 °C/min, hold 7h; a cooling ramp, 1000 °C to 800 °C @ 3 °C/min). The oven was then turned off and allowed to cool to room temperature before the device was removed. At this stage, the chip was ready for use. Reservoirs with a capacity of ~ 100 μL were made on top of the access holes with the use of pipette tips and sealed using epoxy glue.

2.2.3.2 Device Description and Operation

The design of the POCRE [8] chip device used for these experiments is shown in Figure 2-1. All channels were isotropically etched to a depth of approximately 10 μm, giving a width of approximately 30 μm for the narrow channels and 230 for the wide channels. The separation channel was 3.2 cm long and the injector to detector length was 3.1 cm. The injector design on these devices were of the double – T format which geometrically defines the sample plug volume [12, 13].

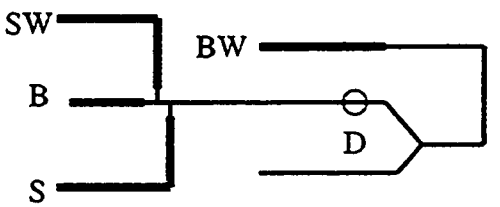

Figure 2-1: POCRE chip device. S= Sample, SW = Sample waste, B = Buffer, BW = Buffer waste, and D = Detector position. Injector to detector distance = 3.1 cm. See text for other details

Prior to use, the device was initially wet with water for about 20 min, conditioned with 0.1 M NaOH for 30 min (to deprotonate the channel surface) followed by the running buffer for 30 min (to equilibrate the channels with the running buffer). This regimen was followed religiously every day, or as needed before any experiments were conducted.

2.2.4 INSTRUMENTATION

Initial experiments were conducted to ascertain the fluorescent emission intensity of the aromatic amino acids at various excitation wavelengths: 229, 244, 257, 284, and 288 nm. The acquisitions were performed using an RF 5301 PC spectrofluorometer (Shimadzu) with a Xe lamp and R3788-02 and R212-14 photomultiplier tubes.

The optical set-up for on-chip experiments is illustrated in Figure 2-2. It is similar to that described by Ocvirk and co-workers [6], except that the microscope was positioned below the chip.

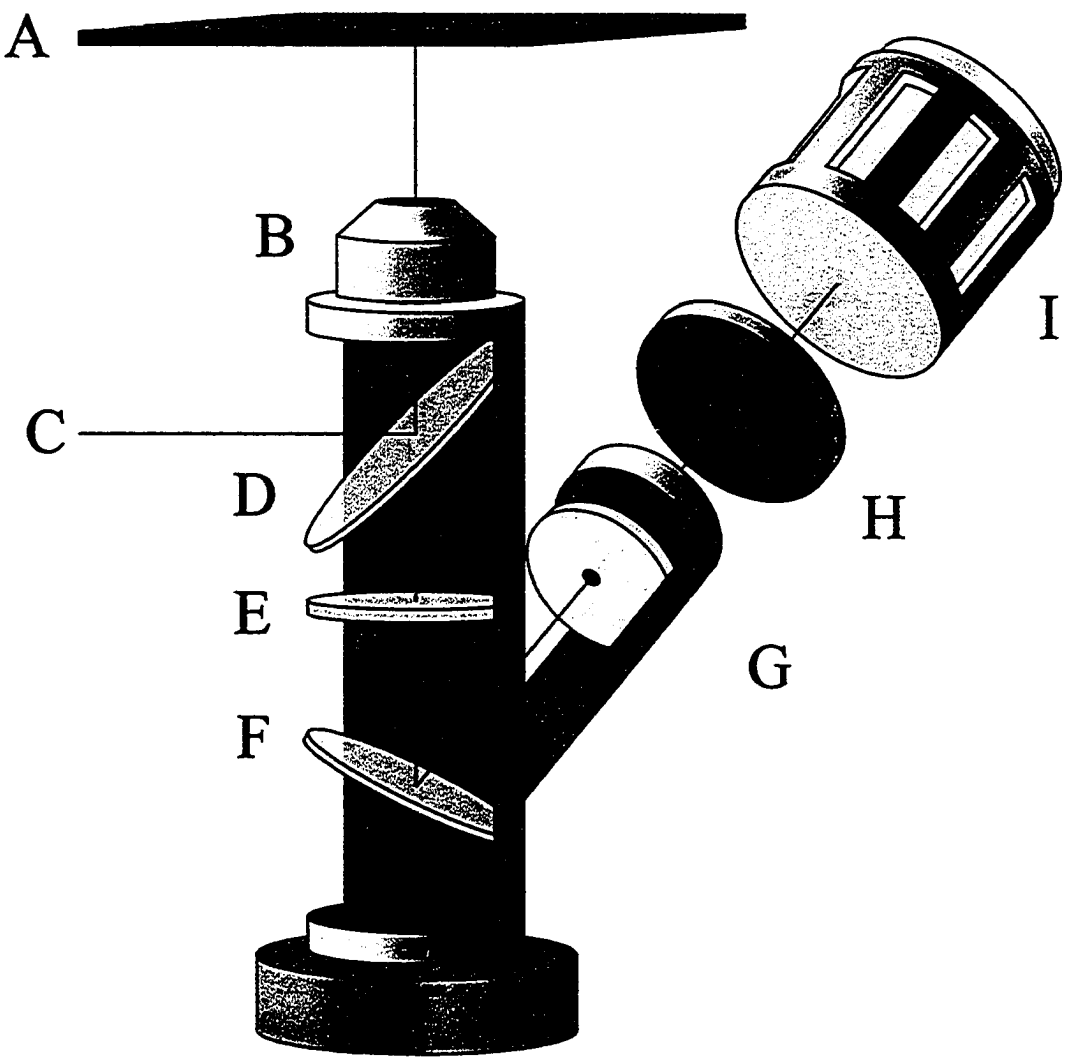

Figure 2-2: Confocal epiluminiscent set-up. A, chip; B, UV objective; C, 266 Nd:YAG laser beam; D, dichroic mirror; E, tube lens; F, quartz mirror; G, pinhole, 600 μm; H, band pass filter; I, PMT

It was comprised of a confocal microscope set-up equipped with a 266 UV laser as its excitation source. The excitation light from the 266 nm pulsed UV laser (JDS Uniphase, pulse width <600 psec., repetition rate = 6 – 10 kHz, power = 2 mW) was reflected by a dichroic mirror (XF 2000, Omega Optical, Brattleboro, VT) and focused in the microfluidic channel using a 13x UV microscope objective (NA = 0.13, focal length (f) = 11.53 mm, working distance = 6.82 mm, clear aperture = 3.00 mm, Newport, USA, U-13X). Fluorescence emission was collected by the microscope objective, passed through the dichroic mirror and was focused with a tube lens (Newport, SPX028AR.10, diameter = 25.4 mm, f = 200mm) and imaged through a pinhole (600 μm, Melles Griot, CA, USA) located at the focal point, onto the photomultiplier tube. An XF 3000 band pass filter (band pass = 100 nm, ~ 76% T, 290 – 380 nm, Omega Optical, Brattleboro, VT) was used for spectral filtering of the signal before it entered the photomultiplier tube (RF 1477, Hamamatsu, Tokyo, Japan; bias 600 V). The current generated by the impact of photons on the photocathode of the PMT was converted to voltage and amplified using a 10^6 gain trans-impedance amplifier (home built). It was then filtered using a 25 Hz low pass Bessel noise filter. Data acquisition and electronics control was accomplished with a Compaq PC via a Labview interface (National Instruments, Austin, TX.). The data collection rate was 2000 Hz with averaging of 100 points to give a data write rate of 20 Hz. The injection and separation processes were operated with a home built power rack connected to an IOtech relay system and controlled via the Lab-View program. The chip was mounted on a plexiglass platform, whose position could be controlled though the use of three translation stages (Newport, #423), above the confocal setup.

Experiments were also conducted with a 36x reflecting microscope objective (NA = 0.52, f = 5.4 mm, working distance = 10.4 mm, #1356, Thermo Oriel, Stratford, CT, USA). Figure 2-3 illustrates the focusing application of this objective lens. Collimated laser light, on reflection off the dichroic, passes through the aperture hole in the primary mirror onto the secondary mirror. From there it is reflected and diverged by the secondary mirror to fill the primary mirror. The primary mirror then focuses the spot in the fluidic channel. The mirror design employing a secondary mirror resulted in the creation of an 'obscuration zone". Since the laser spot size is 0.5 mm in diameter and the aperture diameter is 5.3 mm, it was necessary to expand the laser beam (x10) in order to

efficiently utilise this higher numerical aperture objective. A Keplerian type beam expansion system was constructed using two Plano-convex lenses. The positive lenses were positioned so that their focal points were nominally coincident. A short focal length lens (f = 12.7 mm, SPX010AR.10, Newport, USA) served to expand the beam, whilst a longer focal length lens (f= 150, SPX025AR.10, Newport) was used for collimation. This gave a magnification factor of 11.8. The remaining aspects of the instrumental set-up remained unchanged, as was described previously for the unexpanded beam set-up. A pictorial representation of the entire instrumental set-up is depicted in Figure 2-4

In addition to experimentation with the reflecting objective, different filters for optical filtering were also employed, in an effort to reduce any scattered or stray light entering the detector. A UG 11 (band pass = 250 – 390 nm, ~80%T, Melles Griot) and a UG 1(band pass = 300 - 400 nm, ~ 56%T, Melles Griot) were tested in various combinations with an XF 3000 filter (290 – 380 nm band pass) to investigate their effect on the observed signal and noise.

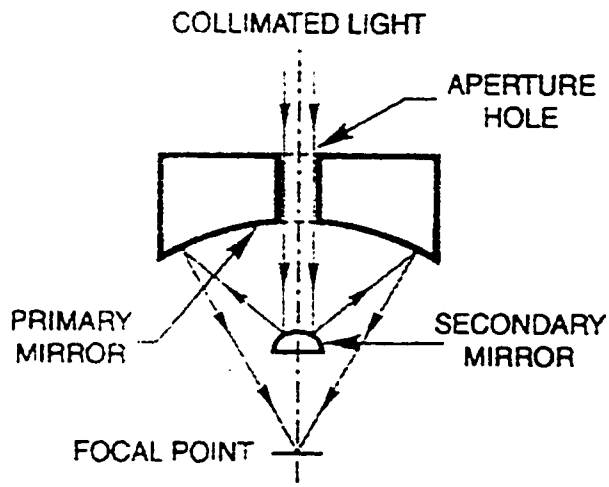

Figure 2.3: Focusing application of the reflecting microscope objective. Collimated laser light passes through the aperture hole in the primary mirror, to the secondary mirror. The secondary mirror reflects and diverges the laser beam to fill the primary mirror. The beam is then focused by the primary mirror.
Image taken from the microscope data sheet

2.2.5 PROCEDURE

The fact that we were working in the deep UV required the use of a fluorescent aid to align and direct the laser beam into our confocal microscope set-up. The laser was mounted on stands machined so that the laser beam roughly matched the height of the centre of the side aperture, through which it entered the microscope. Using a sticky label (White Multi-Purpose, Avery Dennison Canada, Inc.) pasted on a white paper background and mounted on a T-shaped metal stand, the position of the laser spot was marked as it exited the laser head. This was then engaged in placing the steering mirrors

(5108-A-UV, New Focus) at the appropriate positions to direct the laser path into the microscope. Care was taken to ensure that the laser light was parallel to the optical table (Newport) and that the integrity of its height was not compromised. The microscope objective was then mounted and the position of the pinhole aligned. This was done with the aid of the fluorescent light that was generated when the 266 nm laser contacted 0211 glass mounted on top of the chip holder. The pinhole was subsequently removed and replaced with a 10x Huygens eyepiece (Melles Griot) after which the chip was mounted and the separation channel brought into focus, with the laser off. After conditioning the channel described above, 10 μM tryptophan solution was electro-kinetically flushed from the buffer to the buffer waste reservoir. The eyepiece was replaced with the pinhole and PMT (containing the optical filter) and the optimal position ascertained by monitoring the fluorescence intensity with a Lab View program. The position of the pinhole was also re-optimised at this time.

Capillary zone electrophoresis was performed using tryptophan as the sample and 25 mM borate, pH 9.0 as the running buffer. The injection and separation events were electro-kinetically governed by a computer controlled high voltage power supply via a Lab View program, as was described previously [7, 14, 15]. For the LOD studies, an injection voltage of 3 kV was applied from sample to sample waste for 2 s followed by a separation voltage of 3 kV from buffer to separation waste. Sample and buffer solutions were alternated in order of increasing sample concentration to obtain calibration curves. In between samples, the reservoirs were rinsed three times, and channels flushed by pumping buffer though them for several minutes. No pinching or push back was used in these experiments, as it was expected that the injection volume was defined by the double-T injector. Data collected was analysed using Origin 7.0. In the S/N calculations for the electropherograms, the background corrected signal (peak height) was divided by the standard deviation of the background, determined from a portion of the electropherogram ($\Delta t \sim 8$ s) before the peak. These were used in the construction of S/N vs. concentration plots (hereafter referred to as calibration curves) and determination of the LOD for the chosen fluorophore with the optical detection method. The calibration curve was forced through the origin during fitting, and the limit of detection was established by extrapolation to S/N = 3.

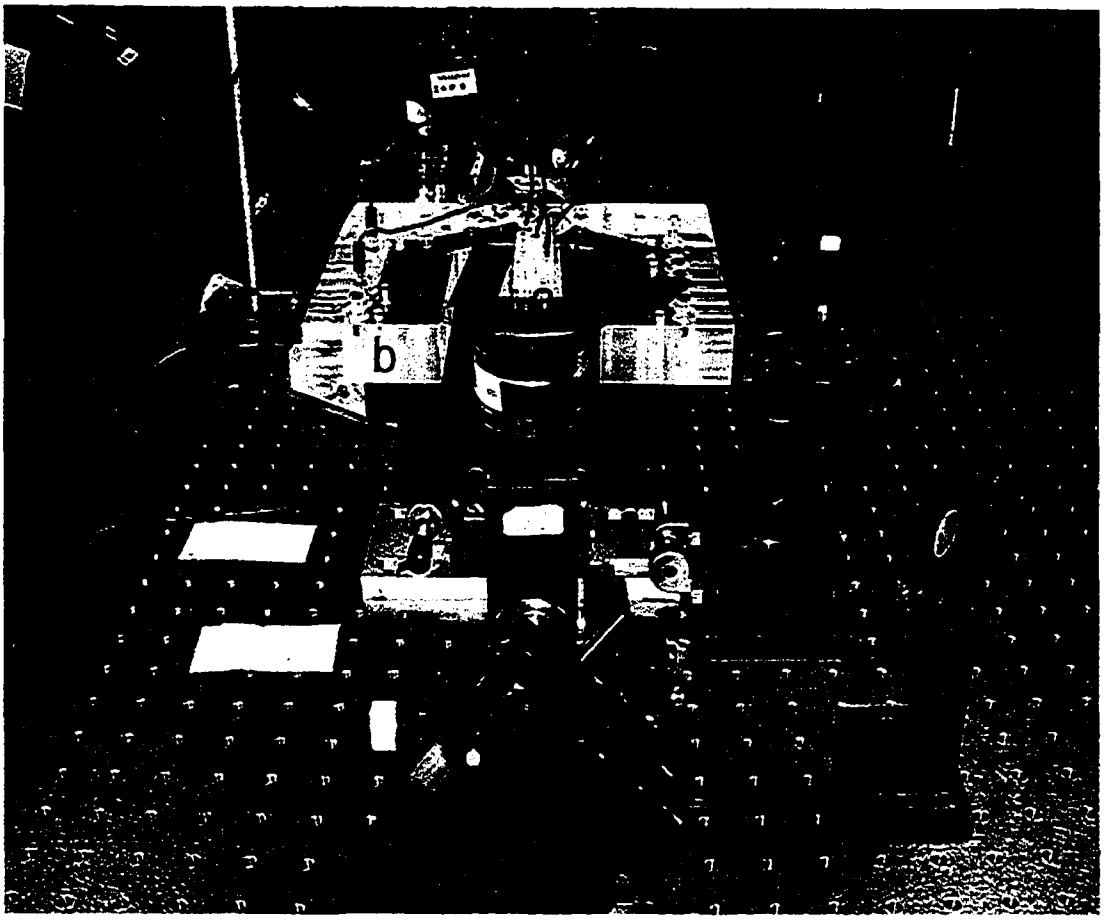

Figure 2-4: Pictorial representation of the instrumental set up utilized in these experiments. (a) Microchip; (b) Chip holder; (c) Reflecting microscope objective; (d) Confocal epiluminescent microscope; (e) PMT; (f) Lens used in construction of beam expander; (g) Steering mirrors for the laser beam.

2.3 RESULTS AND DISCUSSION

2.3.1 DEVICE FABRICATION

The type of glass and its pre-treatment is said to have significant effects on the quality of results obtained after etching. This has been reported before by Fan and Harrison [7], where they found that even within one glass type, the results can vary. In the current study, we found similar results with respect to quartz substrates. Substrates acquired from the University of Alberta Nanofab (Precision Glass), piranha cleaned, and processed yielded devices that were replete with pinholes, making them ill-suited for fluidic applications. It was thought that poor adhesion of the metal layers on the wafer led to these pinhole effects. To counter this, the substrates were sent to Micralyne for Radio

Frequency (RF) cleaning, and metallization. The RF is known to result in better adhesion. After processing, these substrates showed some improvement in appearance, but were still afflicted by pin-holing effects. Figure 2-5 shows one feature of the finished substrate. At this stage, it was decided that initial experiments could be conducted using these pieces until such time that smooth channels were obtained after etching. Hence, the substrate had to be coupled to the cover plate to produce the fluidic devices. However, the cold bonding of the substrate and cover plate [8] proved to be problematic. Very few areas of the substrate and cover plates were bonded. The wafers delaminated upon release of the contact force applied. A series of washing, drying, and scrubbing steps were employed, but to no avail. Quartz substrates were also acquired from Mark's Optics (Santa Anna, CA, USA). Again, bonding was not observed following the regular techniques used in glass bonding. Additional steps, such as immersion into KOH (1 M and 45 % for 10 and 2 min., respectively) prior to scrubbing, did not result in any improved performance, but rather seemed to have caused the surface to roughen, more so in the case of 45% KOH. Experimentation involving immersing both wafers in 0.5% HF prior to the cleaning technique was also not successful in producing cold bonding. Research into quartz bonding in the literature yielded other techniques, but these were more involved and would not have served our purposes [16-18].

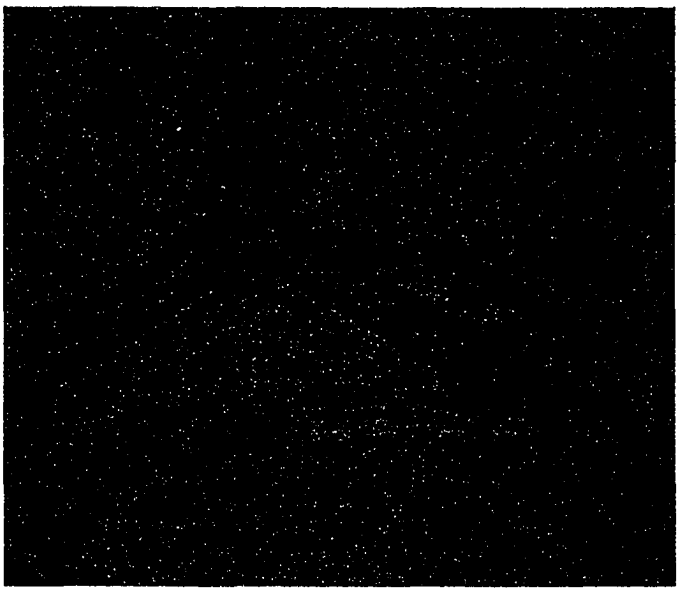

Figure 2.5: Image of finished device obtained; Channel width = 30 μm (Quartz substrates acquired from Precision Glass)

A wafer was then acquired from Micralyne (purchased from Hoya, USA), diced and taken through the cleaning process outlined in the first paragraph. The bonding with these pieces was exceptional when compared with the other pieces experimented with. Care was taken to ensure that the sides bonded were the sides recommended by the

manufacturer to be used in metallization and patterning. This and the fact that the manufacturer's claim that the side recommended for metallization is flat and homogenous may be credited for the success observed. Pieces were then taken through the cleaning and scrubbing steps, as elaborated upon in Section 2.3.2.1, and much improved bonding was achieved. The best results were obtained when there was minimal activity in the clean room around the bonding station. Hoya wafers (one RF cleaned and metallised) were procured from Micralyne and used in the fabrication of the quartz device. Figure 2-6 is representative of the quality of etching obtained after processing.

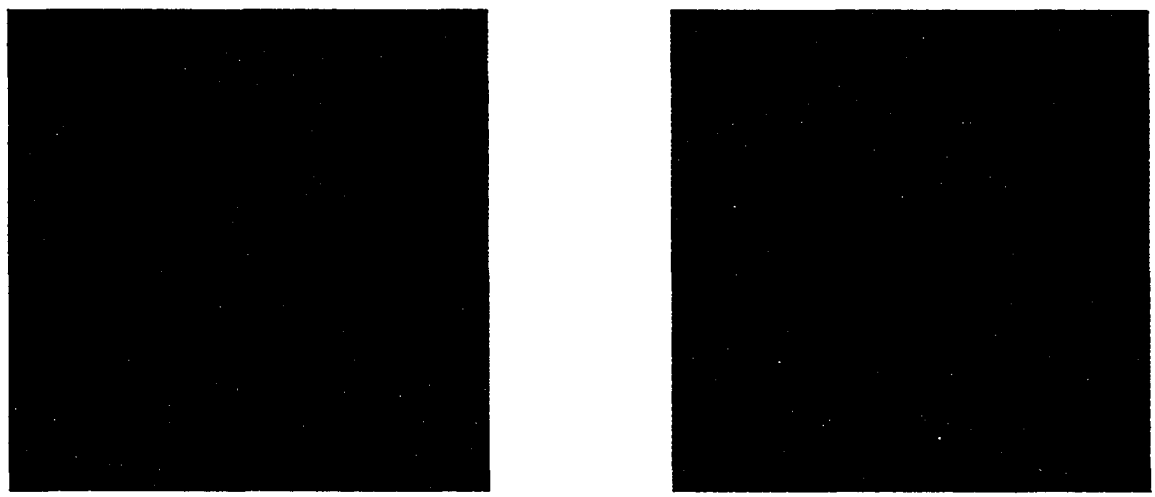

Figure 2-6: Images of the device obtained using Hoya quartz. Cleaning and metallization was done at Micralyne. Fabrication was done at the University of Alberta Nanofab facility.Channel size: narrow channels = 30 μm, wide channels = 230 μm

2.3.2 SPECTROFLUOREMETRIC MEASUREMENTS

Initial experiments were performed to ascertain the fluorescent emission intensity of the aromatic amino acids when excited at various wavelengths. The emission spectra obtained are presented in Figure 2-7. The maximum fluorescent emission for tryptophan occurred at excitation around 284-288 nm. In addition, tryptophan is the most fluorescent of the naturally occurring amino acids when excited at 266 nm, and is followed by tyrosine then phenylalanine. These results were expected, since tyrosine has a lower extinction coefficient and phenylalanine, a negligible extinction coefficient and a lower quantum efficiency as compared with tryptophan [5]. As a result, tryptophan was chosen to be the fluorophore for our optimisation studies.

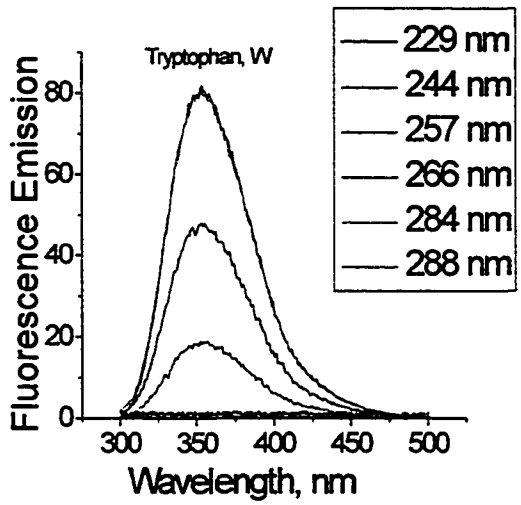

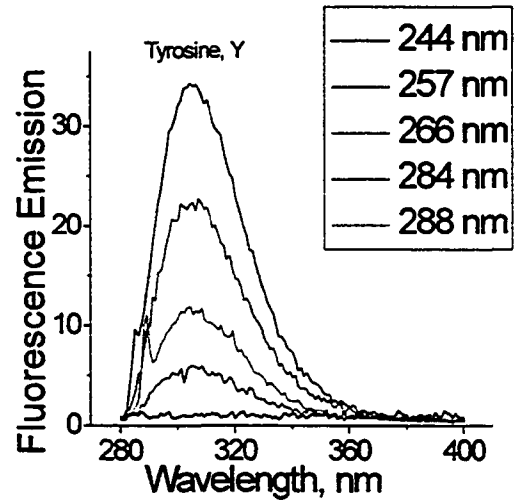

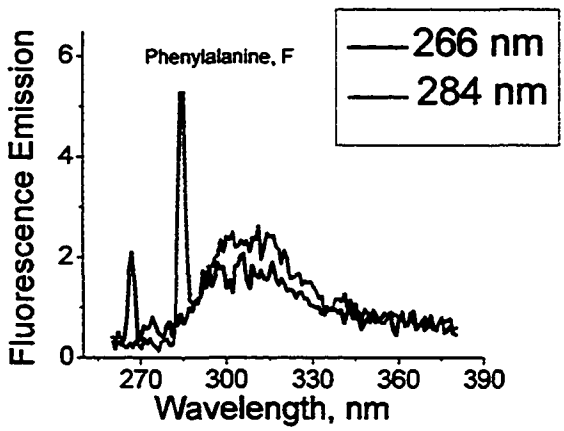

Figure 2-7: Emission spectra for the three aromatic amino acids, tryptophan, tyrosine and phenylalanine as a function of excitation wavelength. Spectra were obtained by interrogating 0.1 mM solutions of the samples using a RF 5301 PC Spectrofluorometer (Shimadzu). The intense band in the phenylalanine spectra is from scattered light from the excitation wavelength.

2.3.3 DETECTOR PERFORMANCE

The confocal epiluminiscent set-up benefits from high N.A. objective lenses that allow for small detection volumes and high light collection efficiencies. In addition, it permits the use of a pinhole at the image plane that serves to reduce collection of background reflections and scattered light from the walls of the chip, ultimately resulting in a lower LOD [6, 19].

2.3.3.1 Limit of Detection Studies

The double T injector design geometrically defines the injected plug length, which is normally independent of injection time, provided that sample leakage at channel intersections is absent [20]. As is illustrated in Figure 2-8, the electropherograms show quite

good reproducibility in peak intensity for multiple injections of 10 μM tryptophan. The relative standard deviation of the peak height reproducibility was 1.2%. Retention time for the peaks also show quite good reproducibility (RSD = 0.13 %), as is depicted in Figure 2-9. The LOD (S/N = 3) of the native fluorescence detection system was evaluated and under optimised conditions, was extrapolated to be ~ 230 nM based on measurements between 5-40 μM. The S/N calibration and peak area vs. concentration curves for the measurement is shown in Figures 2-10 and 2-11 respectively. The LOD was determined by extrapolation to S/N = 3. Figure 2-12 pictures the electropherogram resulting from several electro-kinetic injections and CE separations for 1 μM of tryptophan injected, for another series of experiments conducted. Included in the presentation, for comparison, is

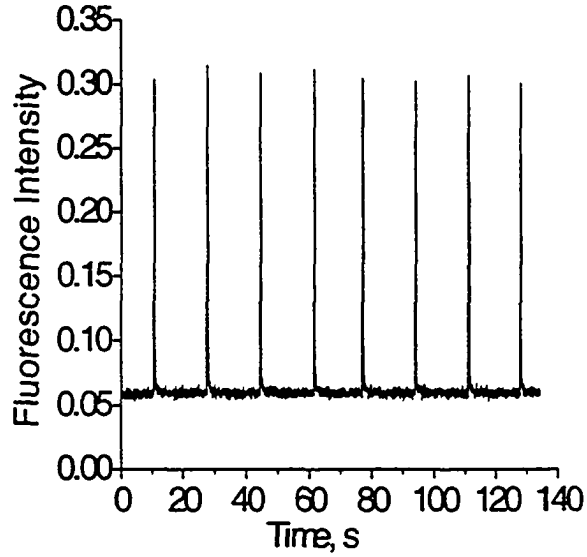

Figure 2-8: Figure illustrating the reproducibility in peak intensity for 8 injections: Injection time: 2 s at 3 kV; Separation voltage: 3 kV; PMT Voltage = 600 V; Sample = 10 μM W

the trace obtained for buffer being pumped electro-kinetically through the separation channel. Injections of buffer alone did not yield any peaks, confirming that the peak observed was from sample and not the buffer matrix. Using this single data point yielded S/N = 7.3 and a LOD of ~ 400 nM. As is evident, the noise level of the background signal is quite consequential.

Since collection efficiency scales as a function of N.A. [7], the use of a higher N.A. lens was employed in an effort to enhance the LO D. A mirror based UV lens with an N.A. of 0.52 (17 % obscuration), as compared with 0.13 N.A. with the original 13x UV objective, was used in this investigation. If light collection was the limiting factor in our measurements, we would expect a lens with a greater collection efficiency to collect more light and hence lead to an improvement in our detection capability. However, despite the

larger N.A. of the reflecting objective, no improvement of LOD was observed. Figure 2-13 shows a calibration curve constructed for the reflecting objective. The detection limit determined by extrapolation to S/N = 3 in this case was approximately the same, within experimental error, as was obtained previously with the smaller numerical aperture objective. Unfortunately, this is not a typical objective, in that the mirror design creates an obscuration factor. As a result, the collection of light could not be eliminated as one of the principal factors limiting detection.

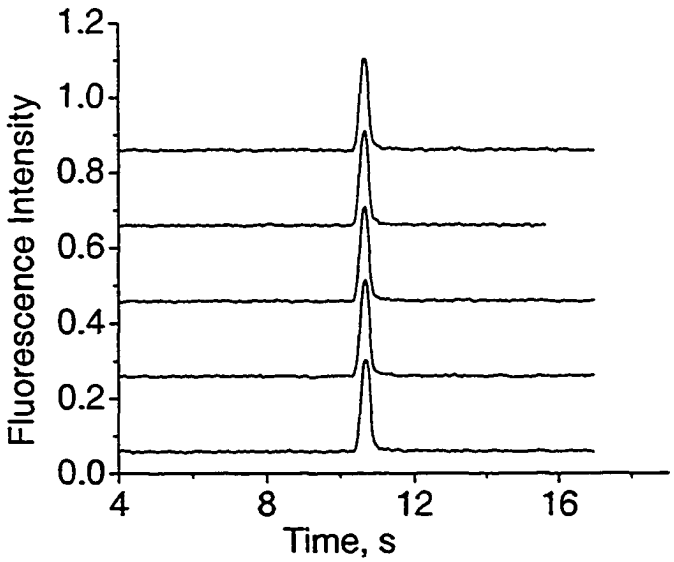

Figure 2-9: Five separate electropherograms of 10 μM W illustrating reproducibility in retention time: Injection time: 2 s at 3 kV; Separation voltage: 3 kV; PMT voltage = 600 V

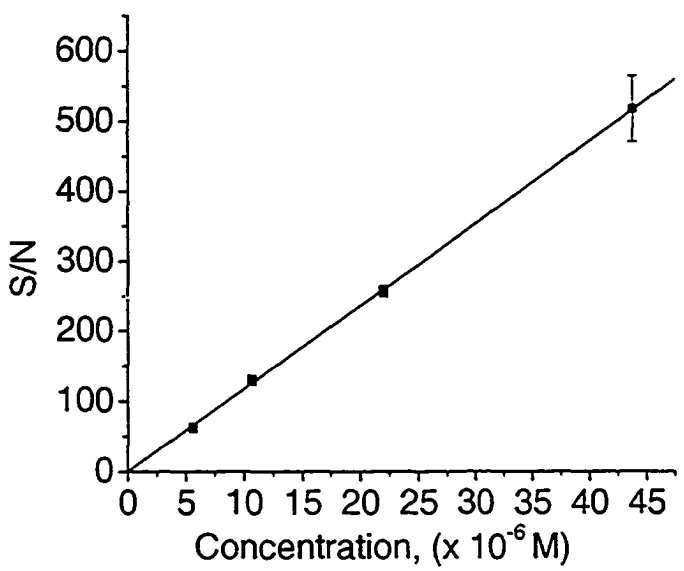

Figure 2-10: Plot of S/N ratio as a function of tryptophan concentration. Samples were electrokinetically injected for 2 s with a voltage of 3 kV. Separation voltage = 3 kV; PMT voltage = 600 V. Error bars are s. d. for 8 multiple injections. Data points fit with a linear function forced through the origin, R^2 = 0.9998. Error bars are s. d. for 6 multiple injections and where not shown, are smaller than the points

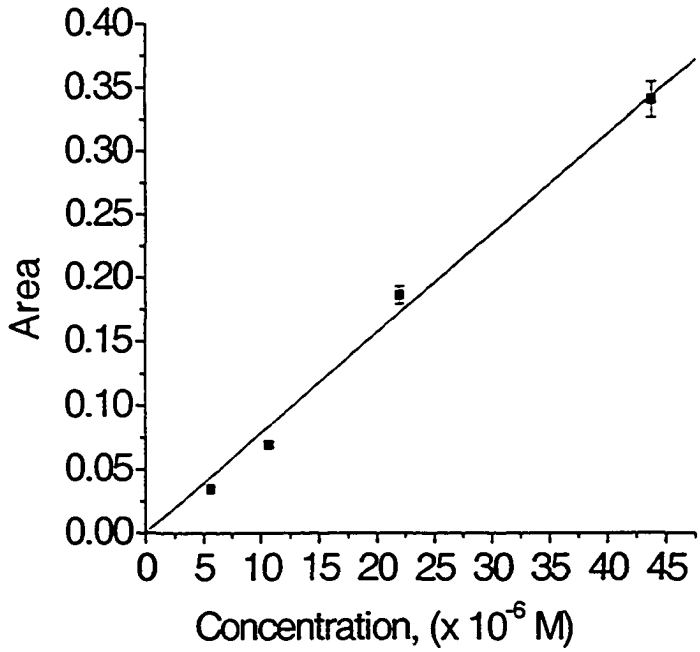

Figure 2-11: Peak area calibration plot for tryptophan. Data points were fit to a linear function and forced through the origin, R^2 = 0.9966 Error bars are s. d. for 6 multiple injections and where not shown, are smaller than the points

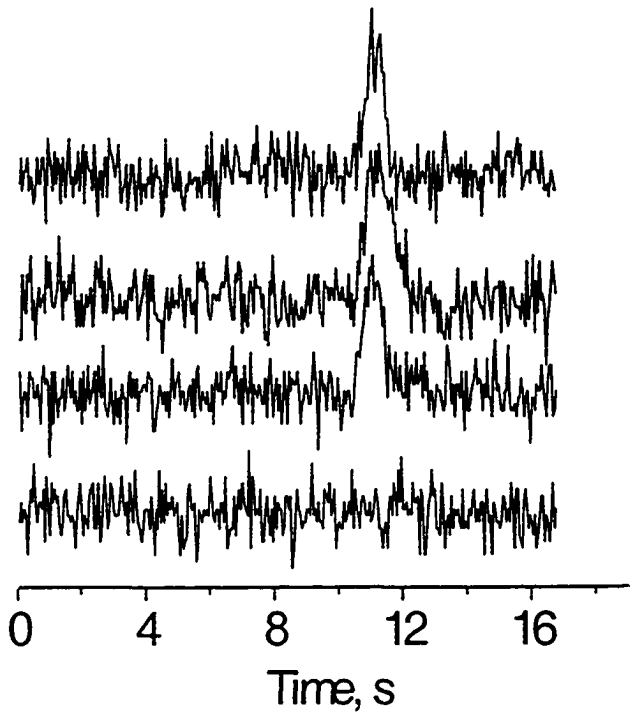

Figure 2-12: Graph comparing the signal level obtained for buffer being pumped through the separation channel and electropherograms obtained for the injection and separation of 1 μM W. Injection was done for 2 s at 3 kV; Separation voltage = 3 kV, PMT voltage = 600 V

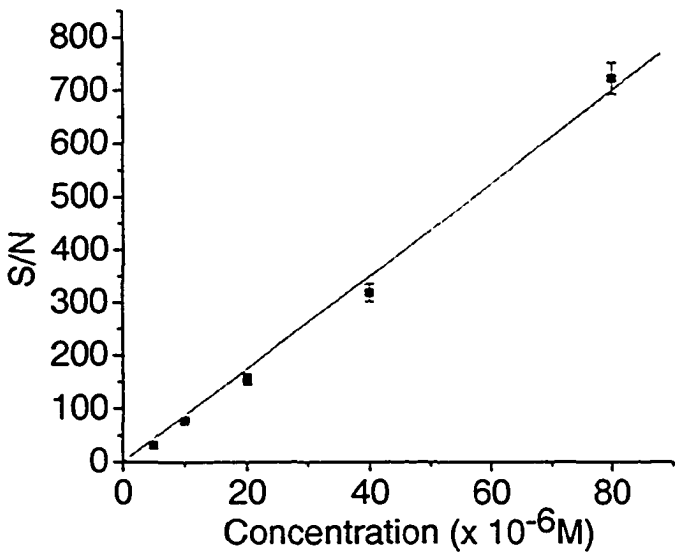

Figure 2-13: Plot of S/N ratio as a function of tryptophan concentration. In this case, the 36x reflecting microscope objective was used. Samples were electrokinetically injected for 2 s with a voltage of 3 kV. Separation voltage = 3 kV; PMT voltage = 600 V. Error bars are s. d. for 6 multiple injections and where not shown, are smaller than the points. Data points fit with a linear function forced through the origin, $R^2 = 0.9985$

2.3.4 LIMITING NOISE ANALYSIS

Signals vary in types: dark, background, and analytical. In each type of signal, there can be noise present. In order to fully exploit the experimental set-up for maximum sensitivity, knowledge of the dominant noise source(s) is essential. This allows for systematic optimization of the experimental variables and instrument set-up for improved S/N [21]. In our experiments, we observed a large background component and wanted to investigate whether a reduction could be achieved to improve the detection limits obtained. Since noise can be introduced from a variety of sources including the sample presentation system, buffers and reagents, the detector and signal processing system, we investigated whether these had any effect on the observed background signal.

2.3.4.1 Electronics: Amplifier and Detector

Using an oscilloscope (Tektronix 2430, Oregon, USA) as the detector read-out system, experiments were performed using different trans-impedance amplifiers, and PMT with 10 μM tryptophan being pumped electrokinetically though the separation channel. Simple measurements were made to determine if there was any major difference in S/N ratio when different combinations of PMT, filters and amplifiers were used. Table 2-1 shows raw and Bessel filtered signals using an R1477 PMT with various home built

amplifiers. Also shown is the effect of a higher PMT voltage on the S/N ratio. Our oldest style, home built amplifier, which has separate units for amplification and filtering, yielded only a fractional improvement in S/N ratio (S/N = 13.33 vs. 11.25), as compared with an amplifier with integrated amplification and filtering that was usually used in our experiments. We also experimented with grounding and floating the amplifiers and compared their performance. Grounding gave a S/N value of 11.65 as compared with 11.25 when the amplifier was floating. All of the systems tested gave similar performance. We note that the S/N values reported here are rough measurements made from visual inspection of the largest peak to peak excursion seen on the oscilloscope, but they provided evidence that none of the parameters varied was critical to changing the observed signal. This type of estimate using the outlying values usually gives an S/N estimate about 3.3x larger than the standard procedure.

Further, fluctuation in the laser power output was investigated and was eliminated as a contributing noise source. The difference in intensity from pulse to pulse was minimal.

2.3.4.2 Background Signal

Background noise is made up of two components: detector noise and background fluorescent noise. With respect to detector noise, the experiments discussed above indicate that we could not significantly change the detector noise with the amplifiers available. A study of the dark current noise from these different PMT's is shown in Table 2-2. The differences were not large and we concluded that the R1477 was not a major source of background noise. Background fluorescence noise can be attributed to two sources: there can be background fluorescence from the substrate, an independent parameter which cannot be easily controlled, and from the buffer matrix used in the experiment.

If our buffer matrix or water source is to be blamed, changing these will result in a change in background. Experiments with varying buffer concentrations and water sources were carried out to investigate this. The observed background signals are presented in Figure 2-14 for various buffer concentrations and two water sources

	LIGHT		DARK	
	Ch 1 (Filtered)	**Ch 2 (Raw)**	**Ch 1 (Filtered)**	**Ch 2 (Raw)**
R1477 and Standard Amplifier (Grey Box – amplifier and filter as one unit) – 10^6 Amp, 25 Hz Bessel filter; PMT: 600 V				
Average Signal	450 mV	450 mV	35 mV	35mV
P to P (Noise)	40 mV	200 mV	10-12 mV	40-60 mV
S/N	11.25	2.25	3.18	0.70
R1477 and Amplifier (Amplifier and filter discrete) – 10^6 Amp, 25 Hz Bessel filter: PMT 600 V				
Average Signal	500 mV	500 mV	50 mV	50 mV
P to P (Noise)	35-40 mV	150	10-14 mV	20-40 mV
S/N	13.33	3.33	4.17	1.67
R1477 and Amplifier (Amplifier and filter discrete) – 10^6 Amp, 25 Hz Bessel filter [common line on power for Amp connected to lab ground]; PMT 600 V				
Average Signal	350 mV*	400 mV	50 mV	50 mV
P to P (Noise)	30 mV*	~100-150 mV	6-10 mV	30-40 mV
S/N	11.67	3.20	6.25	1.43
R1477 and New Voltage (900 V) and Standard Amplifier				
Average Signal	5V	5 V	700 mV	700 mV
P to P (Noise)	500 mV	3-3.5 V	200 mV	1-1.25,V, occasionally 1.5V
S/N	10.00	1.54	3.50	0.62

Table 2-1: Noise Study: Simple measurements taken when the PMT output was connected to the oscilloscope. During the course of the measurement, 10 μM W was being pumped through the separation channel at 3 kV.

	RAW	FILTERED
Usual PMT; Voltage = 900		
Average Signal	700 mV	
P to P (Noise)	1.5 – 2 V	200 mV
S/N	0.67	3.5
Silver Box PMT; Voltage = 900		
Average Signal	1000 mV	
P to P (Noise)	1.5V	200 mV
S/N	0.78	5
R 3896 Sensitive PMT; Voltage 900		
Average Signal	3 V	
P to P (Noise)	2 - 2.5 V	0.7 - 1 V
S/N	1.3	3.5
R 3896 Sensitive PMT; Voltage 734		
Average Signal	1 V	
P to P (Noise)	1.25 V	200 mV
S/N	0.8	5

Table 2-2: PMT dark noise measurements

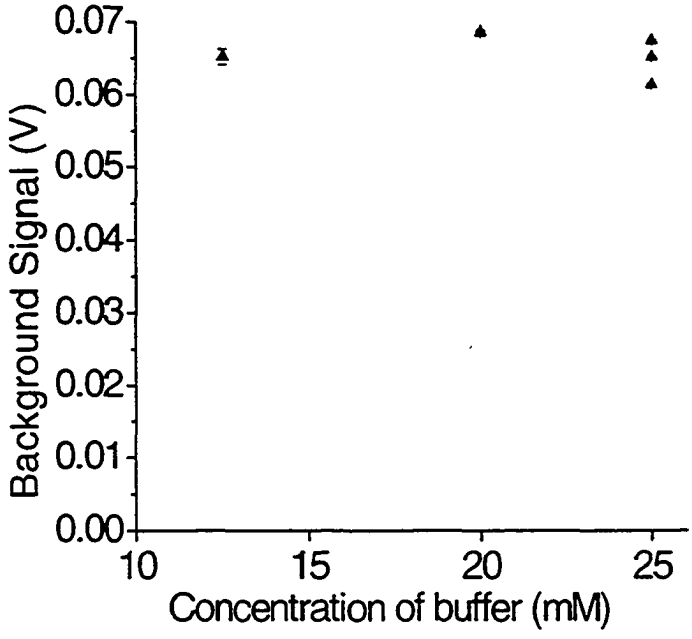

Figure 2-14: Graph showing the effect of buffer concentration, and water source (for 25 mM) on background signal, in addition to the variation of background signal on two different days for the same concentration of buffer (for 25 mM). Error bars are for 5 replicate measurements and are smaller than the point, where not visible.

The water used was Millipore purified water from our laboratory and Nanopure purified water from the Lucy's laboratory. As is evident from Figure 2-14, the differences in signal intensities are small and the variations from day to day are as large as between different concentrations. In addition, changing the source of water did not significantly alter the signal intensity observed, eliminating the source of water as being a contributing factor. As a result, it can be concluded that the noise contribution from our buffer system is not the key problem.

Yeung and Lee [2] reported luminescence from fused silica capillaries upon excitation at 275.4 nm. In our experiments, we observed that the quartz chip developed red luminescence after extended exposure to UV light. Background emission from pristine quartz was investigated and the spectrum is presented in Figure 2-15. As is observed from the spectra, the emission from pristine quartz clearly overlaps that of tryptophan, and will cause interference in tryptophan determination at low concentrations.

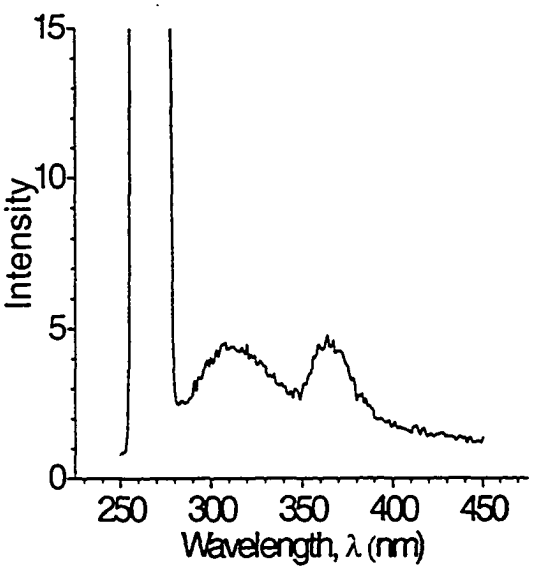

Figure 2-15: Emission spectra obtained for pristine quartz when exposed to 266 nm light. Experiment was conducted using a RF 5301 PC Spectrofluorometer (Shimadzu). Intense peak observed between 250 - 280 nm is from scattered light at the excitation wavelength

In our study, pristine quartz took 20 min to several hours to develop red luminescence, whilst the areas that were etched to form fluidic channels took ~ 1-20 min to reach a similar state. After months of use, the luminescence was observed instantaneously upon exposure to UV light. Pristine quartz was also exposed at various points to the 266 nm laser light used in the experiments and then the emission was remeasured using the 5301 PC Spectrofluorometer (Shimadzu). The spectrum obtained after illumination is shown in Figure 2-16. The intensity scales in Figures 2-15 and 2-16 are relative, as it was not possible to position the glass wafer reproducibly in the fluorescence spectrometer. It is clear that the emission at ~ 340 nm is increased relative to

that at ~ 310 nm and that the peak at ~ 310 nm has broadened after strong UV exposure. Further, if the widths and intensities of the 266 nm excitation lines in the figures are normalised, it appears that the UV exposed quartz emits much more than pristine quartz does. Nevertheless, the results clearly shows that colour centres develop in Hoya quartz with 266 nm exposure. This will cause a strong interference in the emission range of tryptophan that will be difficult to eliminate.

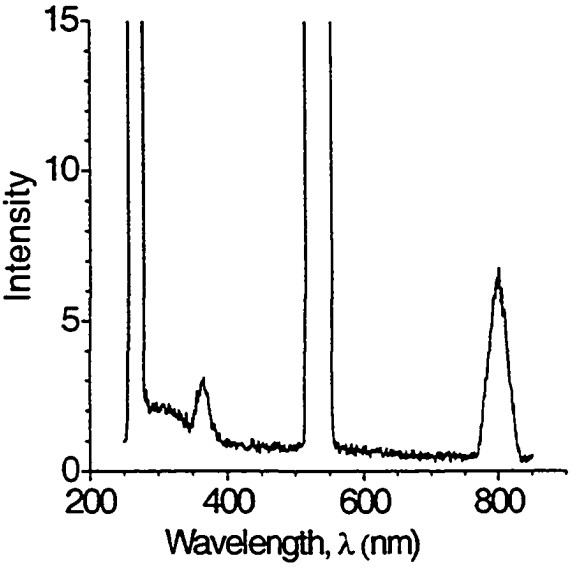

Figure 2-16: Emission spectra for quartz glass that was exposed to the 266 nm laser. Experiment was conducted using an RF 5301 PC Spectrofluorometer (Shimadzu). The intense peaks are from scattered light at the excitation wavelength and multiples of this wavelength. (A grating spectrometer effect.)

Background may also arise from elastic and inelastically scattered light. The spectrum in Figure 2-15 clearly shows that luminescence is present. In order to evaluate the contribution of elastic scattering to the signal observed, various filter combinations were tested. Table 2-3 identifies the filters used and presents their optical characteristics.

FILTER	BAND PASS (nm)	%T @350	% T @ 266
XF 3000	290-380	~ 76	~ 0
UG 11	250-390	~ 80	~ 10
UG 1	300-400	~ 56	~ 0

Table 2-3: Characteristics of the band pass filters employed for spectral filtering. In all cases, except where noted, the XF 3000 filter was used.

By cascading two filters that have the capacity to block 266 nm light by a factor of ~ 10^3, it is expected that scatter will consequently be reduced by ~ 10^6. Figures 2-17, 2-18 and 2-19 show the noise in the background, the signal for the sample, and the S/N ratio for a series of concentrations of tryptophan with different filter sets. As is observed in Figure 2-17, the noise in the background is independent of concentration. In some instances, there seems to be a trend towards a slight increase and this may be due to leakage of

tryptophan into the buffer channel [7, 20]. The noise decreased with increased filtering, but by a small amount compared to the 10^3 ratio expected for elastic scattering. Table 2-4 shows the background signal and background noise for the same data set analysed above in addition to data obtained on a different day. The background signal and noise from different days shows good agreement in terms of absolute signal intensity. In addition, it can be seen from the data presented in Table 2-4 and Figure 2-18 that the signal intensity decreases with increasing filtering. The decrease in signal is similar to the optical density in the band pass of the filter, when either the UG 11 (which transmits some 266 nm light) or the UG 1 (blocks 266 nm) is used in conjunction with the XF 3000 filter. This result indicates that the observed background is dominated by the quartz luminescence, not elastically scattered light, since an ~10^3 decrease would be expected for the UG 1 and XF 3000 combination. With the XF 3000 and UG 11 combination in place, the LOD was determined to be ~ 400 nM, while with the XF 3000 and UG 1, it was ~ 500 nM (refer to Figure 2-19). From these observations, it can be concluded that the S/N is not improved by the use of additional optical filters of similar band pass. This is consistent with the above interpretation.

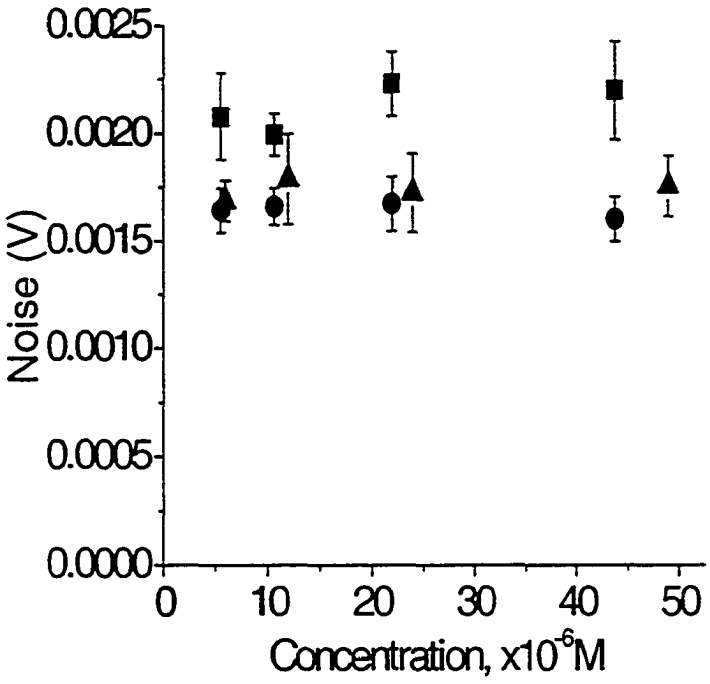

Figure 2-17: The graph in this figure illustrates the change in noise of the background signal as a function of concentration of tryptophan solution, for different filter set combinations. ***Legend***: ■ is for XF 3000 filter only; ▲for the XF 3000 and UG 11 combination; ● is for the XF 3000 and UG 1 combination.

FILTER SET	DARK SIGNAL (V)	DARK NOISE (V)	BACKGROUND SIGNAL (V)	BACKGROUND NOISE(V)
DATA SET A				
XF 3000	0.033	0.0055	0.065	0.0022
XF 3000 &UG 11	0.039	0.0015	0.055	0.0019
XF 3000 & UG 1	0.034	0.0015	0.041	0.0015
DATA SET B				
XF 3000			0.065	0.0021
XF 3000 &UG 11			0.046	0.0017
XF 3000 & UG 1			0.043	0.0016

Table 2-4: This table presents the background signal and noise for the data set presented in Figures 2-17 to 2-19 (Data Set A). Data set B presents background measurements that were taken on another day for comparison.

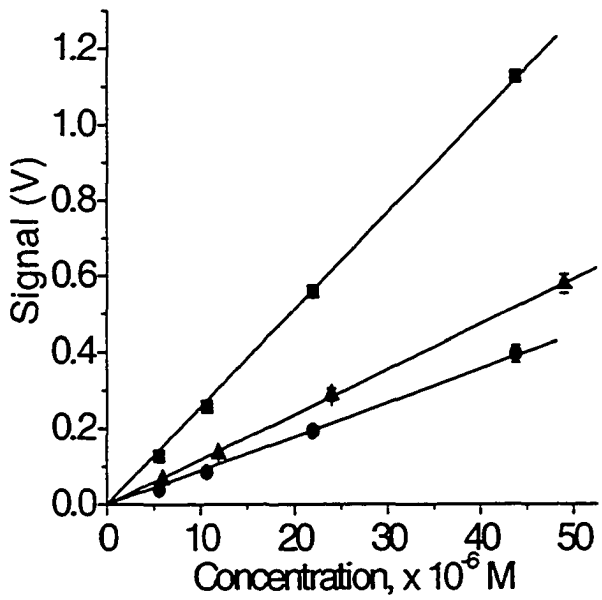

Figure 2-18: This figure shows the effect of the filter set combination on the intensity of the signal obtained for various concentrations of tryptophan solutions. Sample was electrokinetically injected for 2 s at 3 kV; Separation voltage = 3 kV; PMT voltage = 600 V
Legend: ■ is for XF 3000 filter only (R^2 = 0.9999); ▲for the XF 3000 and UG 11 combination (R^2 = 0.9997); ● is for the XF 3000 and UG 1 combination (R^2 = 0.9999). Error bars are s. d. for multiple injections and where not shown, are smaller than the points

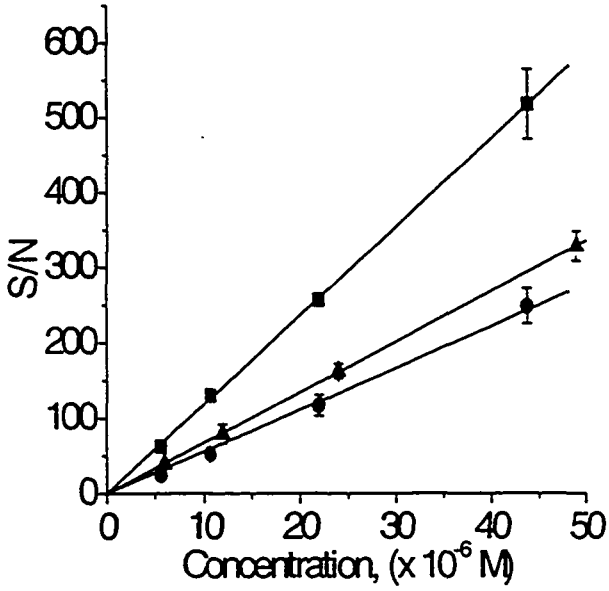

Figure: 2-19: Plot of S/N ratio as a function of W concentration. Sample was electrokinetically injected for 2 s at 3 kV; Separation voltage = 3 kV; PMT voltage = 600 V

Legend: Plot lines through points represented by, ■ (R^2 = 0.9998) only the XF 3000 filter, ▲ (R^2 = 0.9999) XF 3000 was cascaded with UG 11, ● (R^2 = 0.9998) XF 3000 and UG 1 combination.

2.4 CONCLUSION

In this chapter, we explored the application of a confocal epiluminiscent microscope [6] and a microfluidic platform for the development of a LINF detection scheme that can be employed for the detection of peptides and proteins. For applications involving microchip CE, LIF has been the dominant detection method utilised, due to the exceptional sensitivity that is achievable with it. However, its use requires the species of interest to be naturally fluorescent, or otherwise derivatized with a fluorogenic agent. The latter has been the case for most applications, particularly because of the prevalence of fluorescent dyes that fluoresce at the common available laser wavelengths. While this method of operation has its advantages, it is not always the first choice for many applications; it can be very cumbersome and problematic. Thus, the development of a detection method that does not rely on labelling, but still exploits the advantages of LIF was quite appealing.

This chapter exploited the intrinsic fluorescence of tryptophan with the aim of developing a label free detection method for peptides and proteins. An LOD of ~230 nM was achieved for tryptophan, higher than expected when compared with the 2 nM achieved by Issaq and co-workers [22] when applied to fused silica capillaries. Experiments

carried out to interrogate the factors limiting the sensitivity of the detection method revealed that background luminescence from the quartz glass was the most dominant factor in our system. The background luminescence was in the spectral range of tryptophan fluorescence. Changing the electronic filtering and amplification system did little to alter the signal obtained, thus eliminating the possibility of significantly improving signal intensity with the use of other electronic filter and amplifiers available in the laboratory. Cascading optical filters to reduce elastic scattering from the laser light did not yield any improvement, thus negating this as a dominant limiting factor. Signal intensity was reduced comparable to the optical density of the filters being applied. The use of a higher numerical aperture objective lens did not result in an increase in light collection efficiency as would have been expected. However, since this objective was not a typical lens, light collection has not been eliminated conclusively as being a limiting factor.

Despite the shortcomings of the present detector, it does present the first application of native detection on a CE microfluidic platform. Further, such a system eliminates the labelling steps that are always necessary for microchip CE experiments involving peptides and proteins. Finally, better optical filtering with a narrower bandpass and a deeper channel with increased optical path length may lead to a significant improvement in S/N ratio.

2.4 REFERENCES

(1) Swaile, D. F.; Sepaniak, M. J. *Journal of Liquid Chromatography* **1991**, *14*, 869-893.
(2) Lee, T. T.; Yeung, E. S. *Journal of Chromatography* **1992**, *595*, 319-325.
(3) Timperman, A. T.; Oldenburg, K. T.; Sweedler, J. V. *Anal. Chem.* **1995**, *67*, 3421-3426.
(4) Tseng, W.-L.; Chang, H.-T. *Anal. Chem.* **2000**, *72*, 4805-4811.
(5) Chan, K. C.; Muschik, G. M.; Issaq, H. J. *Electrophoresis* **2000**, *21*, 2062-2066.
(6) Ocvirk, G.; Tang, T.; Harrison, D. J. *The Analyst* **1998**, *123*, 1429-1434.
(7) Fan, Z. H.; Harrison, D. J. *Anal. Chem.* **1994**, *66*, 177-184.
(8) Fluri, K.; Fitzpatrick, G.; Chiem, N.; Harrison, D. J. *Anal. Chem.* **1996**, *68*, 4285-4290.
(9) Chiem, N.; Shultz-Lockyear, L. L.; Andersson, P.; Skinner, C.; Harrison, D. J. *Sensors and Actuators B* **2000**, *63*, 147-152.
(10) Sobek, D.; Young, A. M.; Gray, M. L.; Senturia, S. D. *Proceedings of the IEEE Micro-Electrochemical Systems Workshop*, Fort, Lauderdale, FL, Feb 7-10 1993; 219-224.
(11) Schmidt, M. A. *Hilton Head Sensor and Actuator Workshop - Technical Digest*, June 13-16 1994; 127-131.
(12) Effenhauser, C. S.; Manz, A.; Widmer, H. M. *Anal. Chem.* **1993**, *65*, 2637-2642.
(13) Koutny, L. B.; Schmalzing, D.; Taylor, T. A.; Fuchs, M. *Anal. Chem.* **1996**, *68*, 18-22.
(14) Chiem, N.; Harrison, D. J. *Anal. Chem.* **1997**, *69*, 373-378.
(15) Seiler, K.; Harrison, D. J.; Manz, A. *Anal. Chem.* **1993**, *65*, 1481-1488.
(16) Nakanishi, H.; Nishimoto, T.; Arai , A.; Abe, H.; Fujiyama, Y.; Yoshida, T. *Electrophoresis* **2001**, *22*, 230-234.
(17) Ericson, C.; Holm, J.; Ericson, T.; Hjerten, S. *Anal. Chem.* **2000**, *72*, 81-87.
(18) Jacobson, S. C.; Moore, A. W.; Ramsey, J. M. *Anal. Chem.* **1995**, *67*, 2059-2063.
(19) Jiang, G.; Attiya, S.; Ocvirk, G.; Lee, W. E.; Harrison, D. J. *Biosensors and Bioelectronics* **2000**, *14*, 861-869.
(20) Shultz-Lockyear, L. L.; Colyer, C. L.; Fan, Z. H.; Roy, K. I.; Harrison, D. J. *Electrophoresis* **1999**, *20*, 529-538.
(21) Ingle, J. D.; Crouch, S. R. *Spectrochemical Analysis*; Prentice Hall: New Jersey, 1988.
(22) Chan, K. C.; Janini, G. M.; Muschik, G. M.; Issaq, H. J. *Journal of Liquid Chromatography* **1993**, *16*, 1877-1890.

CHAPTER 3: SEPARATION OF PEPTIDES AND PROTEINS WITH NATIVE FLUORESCENCE DETECTION

3.1 INTRODUCTION

The growing effort to learn more about the composition and idiosyncratic functions of proteins within cells and other living bodies has resulted in CE becoming one of the premier tools in protein analysis. As a consequence, the technique of microchip capillary electrophoresis with its inherent advantages has also risen in prominence. Bearing this in mind, it is thought that the development of a label free CE microchip device for protein detection will be quite beneficial. In this chapter, we explore the use of the detector developed in Chapter 2 for peptide and protein detection after CE separation. Mixtures of four model peptides (α_1 mating factor fragment, luteinizing hormone releasing hormone, α_1 mating factor, and bombesin) were separated and detected on chip. Off chip digestion of horse heart cytochrome C (cyt C) subsequently followed by microchip CE was also explored to demonstrate the versatility of the system in dealing with real digests. Separation of a model protein mixture (carbonic anhydrase I and II, α–lactalbumin and β–lactoglobulin B) was explored under different pH conditions. A mixture of six model proteins was separated and detected to further demonstrate the capability of the system.

3.1 EXPERIMENTAL

3.1.1 SOLUTIONS AND REAGENTS

All experiments involving standard peptide samples were performed in 25 mM borate buffer (BDH Inc.), adjusted to pH = 9.0 by titration with 1 M NaOH. The digestion experiment (off chip) involving cytochrome C was done in 0.1 M NH_4HCO_3 digestion buffer, pH 8.0, in a siliconized vial (Rose Scientific Ltd, Edmonton). On-chip separation of the digested sample was done using 25 mM sodium phosphate buffer, pH 10.3, with 0.01% Tween-20 (Aldrich) added to reduce protein adsorption that may arise as a result of any undigested protein. Experiments with protein samples were done in 25 mM phosphate buffer, pH 7.5, 10.3, and 11.22, adjusted by titration with 0.1 M NaOH, with 0.01 % Tween-20 added. Samples were prepared in water and diluted to the required

concentration in the appropriate running buffer. Cytochrome C used in the digestion experiments was prepared in the digestion buffer. All solutions were prepared in ultra pure water (Millipore Canada) that was degassed by boiling. Buffer solutions were filtered through a 0.2 μm pore size Nylon filter (Chromatographic Specialities, Inc). Final peptide sample solutions were not filtered. However, the peptide digest and final protein samples were filtered using a 0.2 μm Millipore filter (Millipore Corporation, Bradford, MA, USA) before introduction into the chip. All protein solutions were prepared in siliconized vials.

Chemicals were acquired from the following suppliers: Ammonium bicarbonate (Sigma-Aldrich), sodium hydroxide (BDH Inc.), sodium phosphate (BDH Inc.), immobilised TPCK trypsin for protein digestion (Product # 20230, Pierce, Rockford, IL) α_1 mating factor fragment, luteinizing hormone releasing hormone, α_1 mating factor, and bombesin, carbonic anhydrase I and II (bovine erythrocytes), α–lactalbumin (Bovine milk), β–lactoglobulin A (bovine milk),), β–lactoglobulin A (bovine milk), Ovalbumin (chicken egg white) and horse heart cytochrome C were all obtained from Sigma-Aldrich (USA).

3.1.2 DEVICES AND CHIP OPERATION; PROCEDURE

The instrumental set up utilised for these experiments was detailed in Chapter 2, Section 2.3.3. The POCRE chip [1] device fabricated in a quartz substrate was also used and the device is described in Section 2.3.2.2. The conditioning and optimisation process elaborated in Sections 2.3.2.2 and 2.3.4, respectively, were followed.

The injection and separation events were electrokinetically governed as described previously [2-4]. No pinching or push back voltages were used in these experiments; during sample injection, the buffer and buffer waste ports were floating and during separation, the injection reservoirs were floating. For capillary zone electrophoresis of peptides and proteins, an injection time of 2 s was used. For peptides, the injection and separation voltage was 3 kV (350 V/cm). In the case of proteins, an injection voltage of 500 V was used followed by separation at 4 kV (466 V/cm), unless stated otherwise. The injector to detector distance was 3.1 cm. For the LOD studies of peptides and proteins, sample and buffer were alternated in order of increasing sample concentrations. In all experiments, in

between samples, the reservoirs were rinsed three times and channels flushed by pumping buffer electrokinetically through them for several minutes.

As was the case in Chapter 2, data collected was analysed using Origin 7.0. For the cases where calibration curves were plotted, the S/N calculations, and graphing were done as was described in Section 2.3.4. The LOD was determined by extrapolation to S/N = 3.

3.1.3 PROTEIN DIGESTION

Protein digestion followed the procedure recommended by the manufacturer (Pierce) of the TPCK Trypsin beads used. A 0.1 M digestion buffer was prepared using NH_4HCO_3 buffer salts. A stock solution of the protein sample was then prepared in the digestion buffer and a final concentration of 1 mg protein/0.5 ml of digestion buffer was prepared by dilution of the stock solution.

The immobilized TPCK Trypsin beads/gel is in the form of a slurry; 250 µl of the slurry containing the beads was washed with 500 µl of the digestion buffer. The gel was separated from the buffer by centrifugation. This washing process was repeated three times and finally, the gel was resuspended in 200 µl of the digestion buffer. This slurry was then added to the protein sample and the reaction mixture was incubated overnight at 37 °C. After digestion, the beads were separated from the digest by centrifugation. All protein solutions were prepared in siliconized vials.

3.2 RESULTS AND DISCUSSION

3.2.1 PEPTIDES

3.3.1.1 Separation and Detection

In the previous chapter, the detection limit of the native fluorescence detection system for microfluidic applications was determined to be in the several hundred nanomolar range for tryptophan. Figure 3-1 presents an electropherogram showing the separation of an equimolar concentration of tryptophan and peptide A (α_1 mating factor fragment). The two peaks were baseline resolved and were identified by running each sample independently and noting the migration times. The peak for tryptophan and peptide A corresponds to 5400 (0.17 million plates/m) and 6100 (0.2 million plates/m)

plates respectively, quite good separation efficiencies. Catai et al. [5] investigated the effect of using bilayer coated capillaries (50 μm ID, 60 cm total length, buffer: 5 mM sodium phosphate buffer with 25 mM sodium chloride) for peptide analysis that yielded efficiencies in the order of 0.25 million plates/m for des-Tyr-Met-enkephalin and 0.16 million plates/m for gonadorelin, separation performance that is quite comparable to that achieved in our experiments. Timperman et al. [6] reported an efficiency of ~ 0.5 million plates/m for a 10 s hydrodynamic injection of tryptophan in a 50 μm capillary with a 30 kV separation voltage.

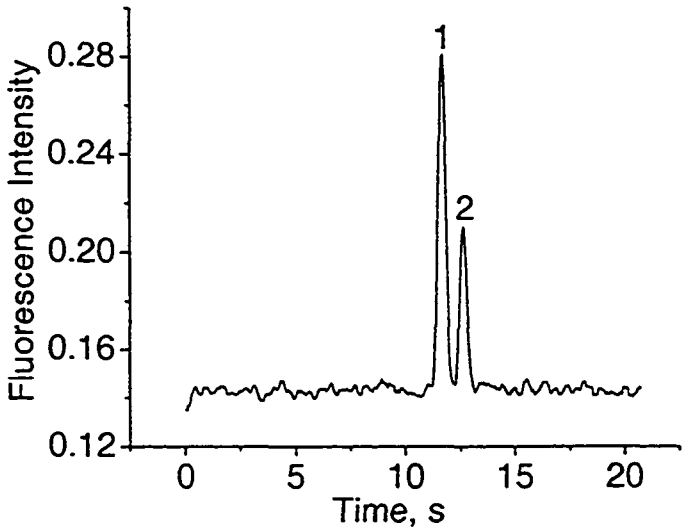

Figure 3-1: Electropherogram for the separation of 15 μM sample solution containing W (1) and peptide A (2) in a quartz microchip. Buffer = 25 mM borate, pH 9.0. Injector to detector distance = 3.1 cm. V_{inj} = 3 kV, t = 2 s; V_{sep} = 3 kV; PMT V = 600 V

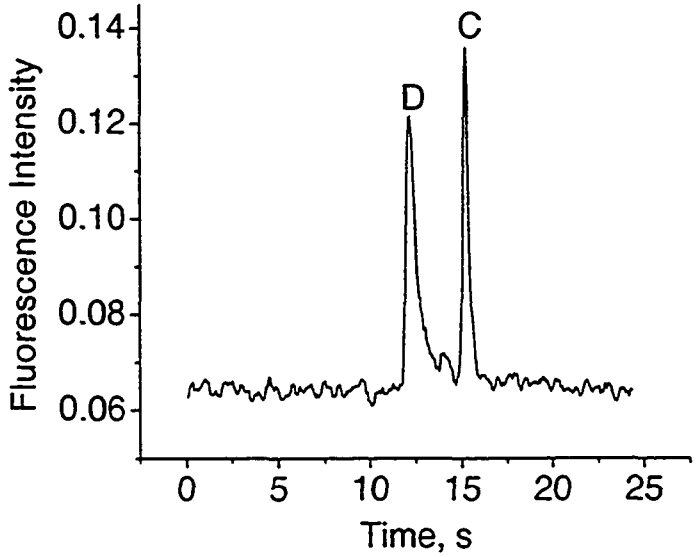

Figure 3-2: Electrophoretic separation of an equimolar mixture (15 μM) of peptides C (luteinizing hormone releasing hormone) and D ($(\alpha_1$- mating factor) in 25 mM borate buffer, pH 9.0. Injector to detector distance = 3.1 cm. V_{inj} = 3 kV, t = 2 s; V_{sep} = 3 kV; PMT V = 600 V

Figure 3-2 is the electropherogram obtained for the separation of an equimolar concentration (15 μM) of peptides C (luteinizing hormone releasing hormone) and D (α_1 mating factor). The peaks were fully resolved and a separation efficiency of ~ 0.64 million plates/m was achieved for peptide C. The utility of CE is dependent on its unparalleled separation efficiency and that obtained here on the microchip is quite comparable [5-8].

It is interesting to note that while peptide C has one W residue as compared with two in peptide D, the intensity of peptide C is higher. Hence, the fluorescence of these species is not always proportional to the number of W residues present in the molecules. This was also seen in later electropherograms. Differences in fluorescence quantum yields may be responsible for the differences in fluorescence obtained for these molecules [9]. A study of the fluorescence of peptides containing tryptophan or tyrosine by Cowgill showed that a peptide containing two tryptophan residues had a lower quantum efficiency as compared with one that was composed of tryptophan and tyrosine [10]. Both peptide C and D possess one tyrosine residue, which may also contribute to the emission signal. The data trace in Figure 3-3 is for the separation of 10 μM W and 15 μM peptides A and B (Bombesin). Peptide A has two W groups whilst peptide B has one. In this case, the intensity of the peak corresponding to A is quite large compared with B. This may be as a result of the number of W residues present, but the microenvironment and intrinsic properties of the species may be the dominant factor controlling fluorescence [11]. In addition, injection effects may also be playing a part in

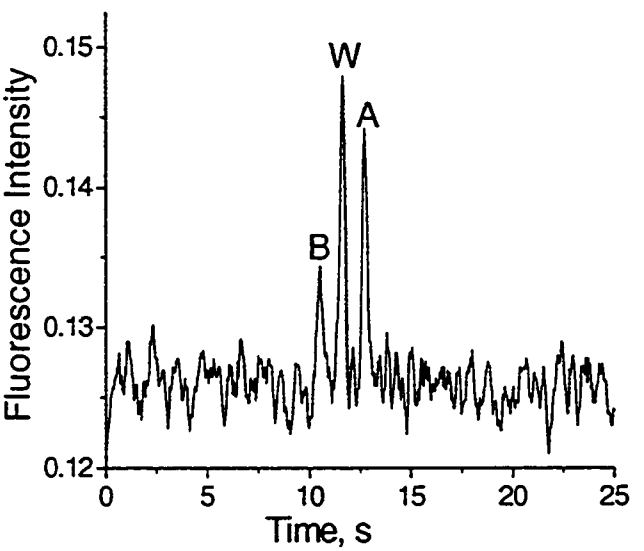

Figure 3-3: Electropherogram for microchip CE separation of W (10 μM), peptide A (α_1- mating factor fragment, 15 μM) and peptide B (bombesin, 15 μM) in 25 mM borate buffer, pH 9.0. Injector to detector distance = 3.1 cm. V_{inj} = 3 kV, t = 2 s; V_{sep} = 3 kV; PMT V = 600 V

the observed signal intensity. Electroosmotic and electrophoretic forces control the flow of solvent and ions within an electrokinetically controlled device. Ideally, the injection time, being long enough, will allow for the sample plug to be representative of the sample matrix, the plug being defined by the geometry of the injector. However, leakage effects at the intersection and differences in diffusion coefficients or electrophoretic mobilities could lead to some injection bias [12].

Figures 3-4 and 3-5 are electropherograms obtained for the separation of a 15 μM mixture of four peptides (peptides A, B, C, and D). These separations were carried out using 25 mM borate buffer, pH 9.0 with no added surfactant. After continuous use of the chip over several days, the length of time taken for elution of the separated species increased, likely due to adsorption changing the EOF. Figure 3-4 shows results on a used chip, while Figure 3-5 shows the electropherogram obtained after cleaning with 0.1 M NaOH for 40 min. The separation efficiencies observed, expressed as N, were very good for these separations. Peak C in Figure 3-4 gave 7300 plates (0.2 million plates/m), whilst for Peak C in Figure 3-5, the separation efficiency observed was in the order of 19000 plates (0.6 million plates/m). These observations implied that our buffer system used was quite effective for separation, and the high efficiencies observed make it comparable to that which is observed in conventional CE systems [6-8]. Contrasting plates/E also indicates that our efficiency obtained is competitive. Ye [7] reported values of N on the order of 0.36 and 0.45 million plates/m, with an electric field of 300 V/cm, for CE separation of proteins. This corresponds to 60 and 75 plates/E, as compared with 55 plates/E for peptide C in Figure 3-5.

Apart from using labelling to reduce detection limits, UV absorbance is the detection method of choice for CE because it preserves the sample for further analysis and does not suffer from the complications associated with labelling for LIF. The label free optical method based on LINF described here also preserves the sample for future studies. Further, a gain in simplicity and speed of analysis coupled with a vast reduction in sample consumption and waste generation are comparable CE advantages that are accrued with this system.

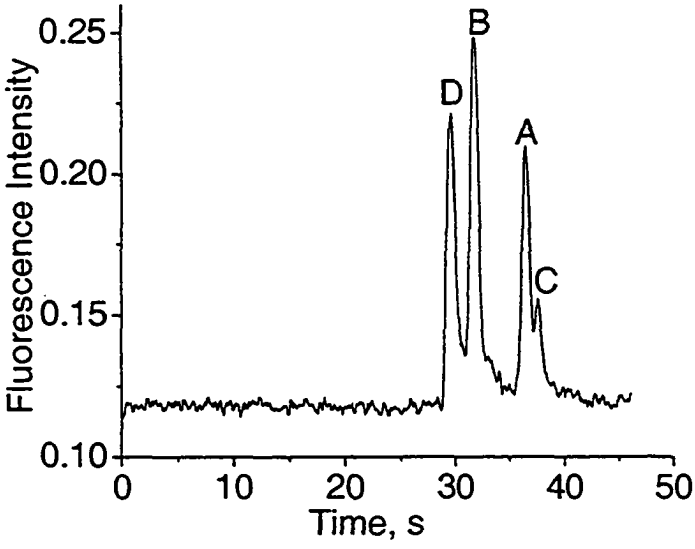

Figure 3-4: Microchip CE separation of four peptides (15 μM each) in 25 mM borate buffer, pH 9.0. Injector to detector distance = 3.1 cm. V_{inj} = 3 kV, t = 2 s; V_{sep} = 3 kV; PMT V = 600 V
Peaks: D, α_1- mating factor; B, bombesin; A, (α_1- mating factor fragment; C, luteinizing hormone releasing hormone

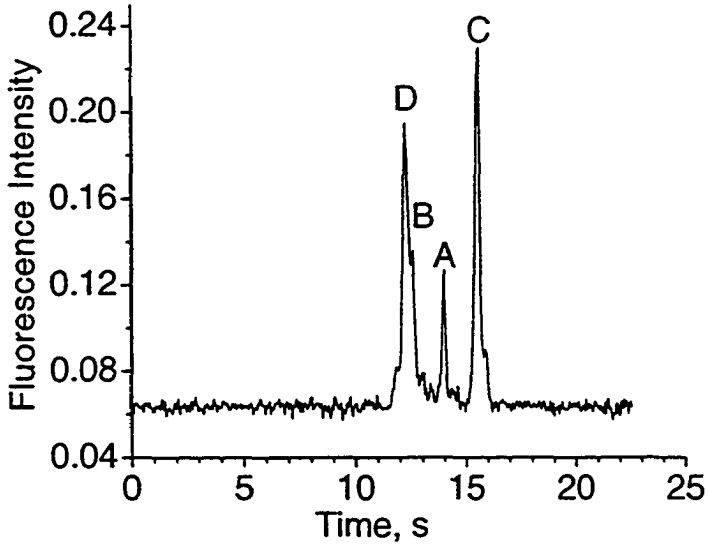

Figure 3-5: Microchip CE separation of four peptides (15 μM each) in 25 mM borate buffer, pH 9.0. Conditions same as in legend for Figure 3-4.
Peaks: D, α_1- mating factor; B, bombesin; A, (α_1- mating factor fragment; C, luteinizing hormone releasing hormone

3.3.1.2 Limit of Detection Studies for Peptides

The excellent LOD that is achievable with the use of LIF makes it quite apt for use in microfluidic applications, where the small sample volumes and short optical path lengths demand a sensitive detection method [13]. The limit of detection for LINF on chip was in the range of 300 - 400 nM for peptide A. The LOD was determined by extrapolating the linear part of the graph to S/N = 3. The S/N calibration graphs are presented in Figures 3-6 and 3-7 for peptides A and C respectively, for measurements

made between 5 - 80 μM. In both instances, there is a deviation from linearity at higher concentrations. The noise was independent of concentration, so the signal was not linear in concentration. This could be as a result of fluorescence quenching. However, the non-linearity could also be as a result of decreasing peak efficiency at higher concentrations, due to peak broadening. A trend of a slight decrease in N with increasing concentration was observed.

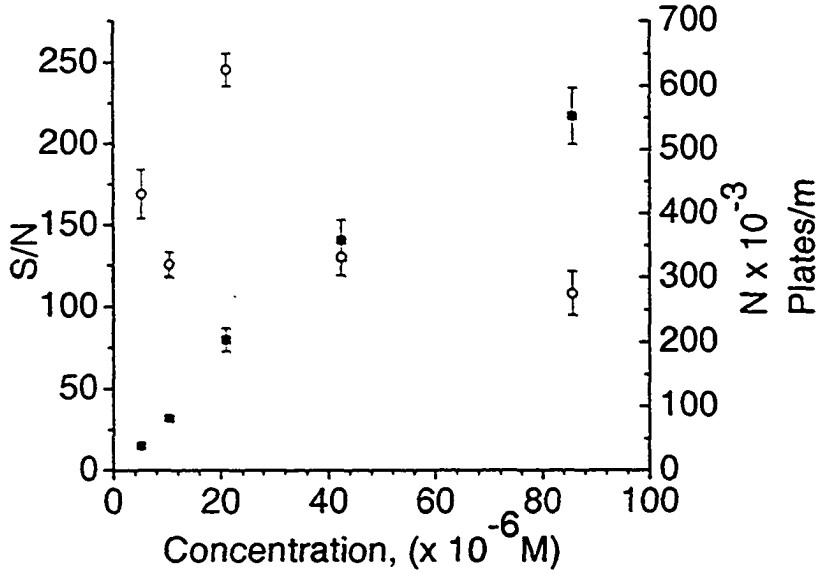

Figure 3-6: Plot of S/N ratio, ■ and efficiency, N, ○ (plates /m) as a function of peptide A concentration. Samples were electrokinetically injected for 2 s with a voltage of 3 kV. Separation voltage = 3 kV; PMT voltage = 600 V. Error bars are s.d. for nine multiple injections, and are smaller than the point where not shown.

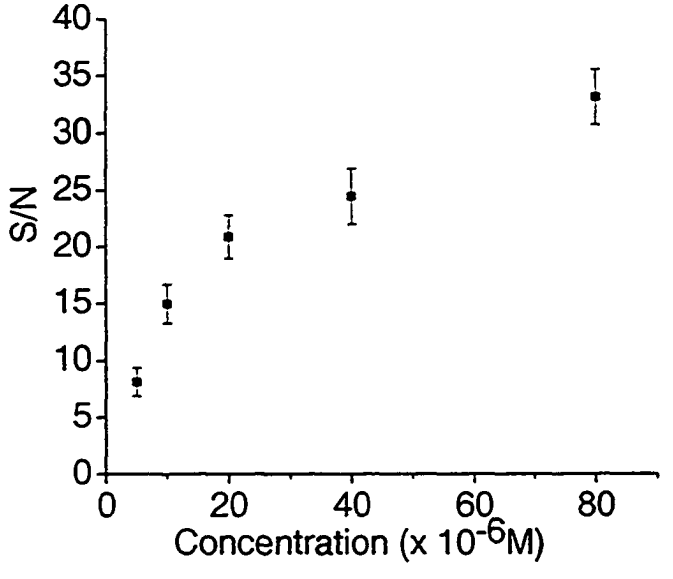

Figure 3-7: Plot of S/N ratio as a function of peptide C concentration. Samples were electrokinetically injected for 2 s with a voltage of 3 kV. Separation voltage = 3 kV; PMT voltage = 600 V. Error bars are s.d. for nine multiple injections.

Chan et al. [14] reported a LOD of 4.3 nM (S/N = 2) for SIP peptide (Trp-Ala-Gly-Gly-Asp-Ala-Ser-Gly-Glu) based on three repeat injections of a 100 ng/ml concentration, for a CE system (50 μm ID) utilising a similar laser. This is on the order of 100 times better sensitivity than that obtained for our system. The same researchers conducted a comparison study where they labelled a series of peptides with fluorescamine and detected them after separation using a solid state UV laser operating at 355 nM. The reported LOD of 3.2 and 2.6 nM for Angiotensin II and Ala-Ala-Ala peptides, respectively, were comparable to that achieved with the native detection method.

3.4.1.3 Off chip Digestion and On chip Separation and Detection

To demonstrate the capability of the system being developed, we analysed a digest of a model protein. Horse heart cytochrome C (cyt c) was digested as outlined in the experimental section and separated on a Beckman CE instrument, using a UV absorbance detection method. As is evident in the electropherogram shown in Figure 3-8, there was some undigested protein remaining. This undigested protein is responsible for the last peak in the electropherogram. For the chip studies with laser induced fluorescence, 50 μl of the 2 mg/ml protein digest was made up tol ml in 25 mM sodium phosphate buffer, pH 10.3, with 0.01% Tween 20.

The electropherogram in Figure 3-9 shows the trace obtained from on chip studies. Cyt C is a 104 amino acid protein with a molecular weight of 11,702 Da. It contains a single tryptophan residue at position 59, in addition to two haem groups covalently attached to Cys-14 and Cys-17. In the native conformation of the protein, the iodole side chain of the tryptophan residue is hydrogen bonded to the haem group. As a result of their close proximity, the fluorescence of the tryptophan residue is quenched. This occurs due to the resonance transfer of energy to the haem group [15]. As a result, as is expected, when a sample of cyt C was pumped electrokinetically through the fluidic channel, no fluorescence was observed. However, when the digested sample was injected and separated, two peaks can be identified in the electropherogram shown in Figure 3-9. The background is somewhat noisy, but the peaks are clearly discernable from the background. The small peak is as a result of missed cleavages during digestion.

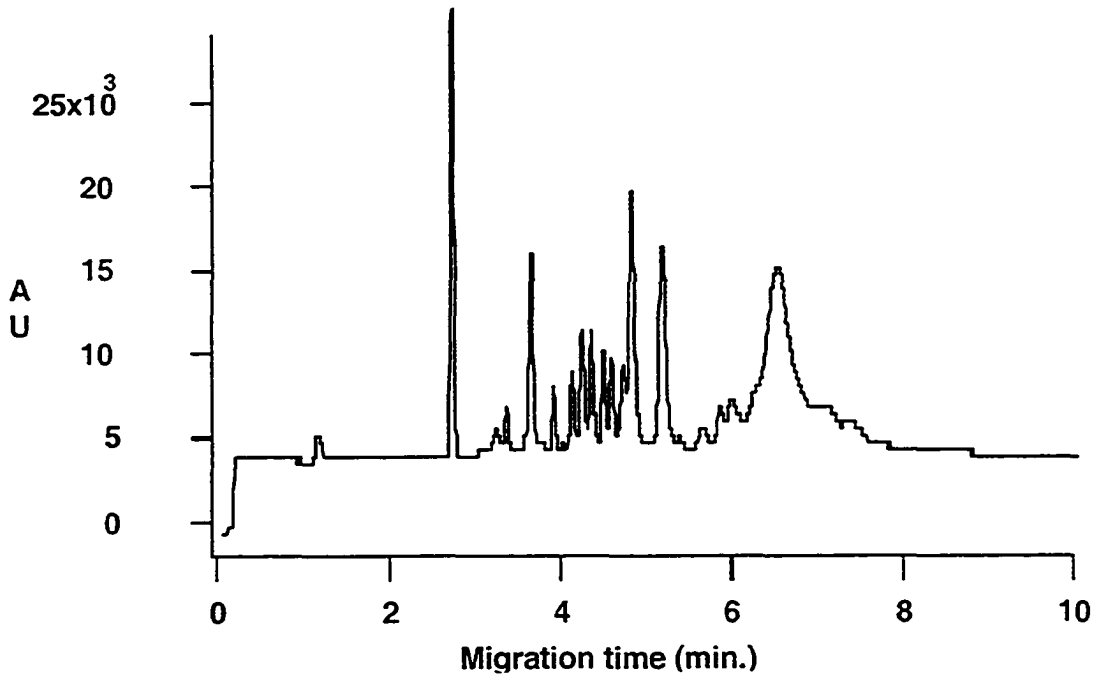

Figure 3-8: Electropherogram for horse heart cytochrome C protein digest obtained after CE separation on a Beckman instrument. Buffer, 10 mM ammonium bicarbonate + formic acid, pH 2.5; Capillary: 27 cm length; 50 μm ID; coated column (supplied by AIMS); V_{inj} = 5 kV, t = 5s; V_{sep} = 15 kV; λ = 214 nm
Separation conducted by G. Jiang

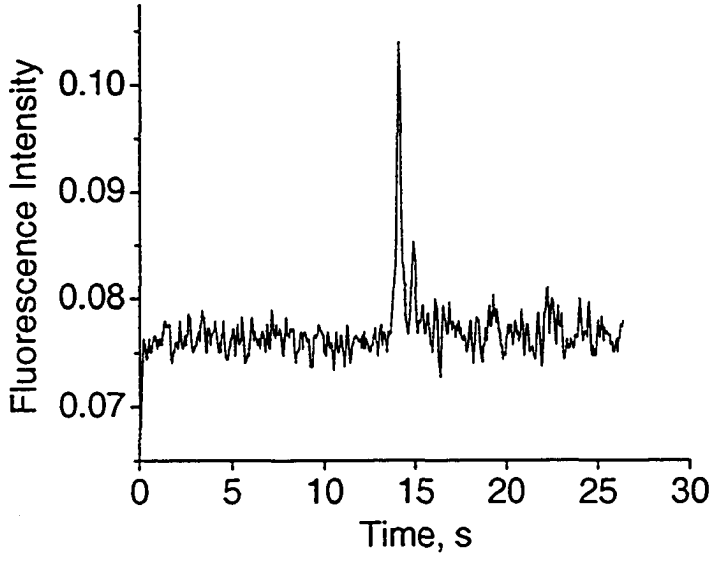

Figure 3-9: Electrophoretic separation of cyt C digest on chip in 25 mM sodium phosphate buffer, pH 10.3, with 0.01% Tween 20. Injector to detector distance = 3.1 cm. V_{inj} = 3 kV, t = 2 s; V_{sep} = 3 kV; PMT V = 600 V

3.2.2 PROTEINS

3.3.2.1 Separation and Detection

Figure 3-10 is the electropherogram for the detection of four model proteins after CE separation on microchip. Separation was achieved in less than 25 s with an applied field strength of 466 V/cm (4 kV) and this was further improved to less than 15 s when the applied field strength was 699 V/cm (6 kV). The graphs in Figure 3-11 show the separation of the four protein mixture at different applied field strengths. All proteins were negatively charged since the working pH was higher than the estimated pI value of the individual proteins.

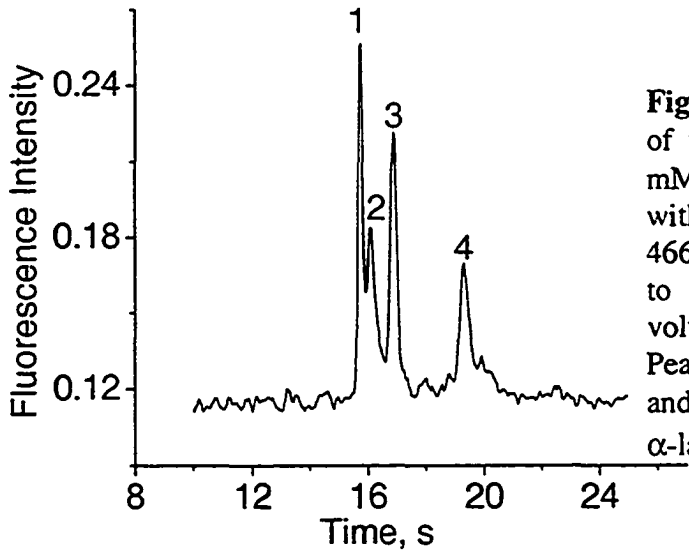

Figure 3-10: Electrophoretic separation of four model proteins (5 μM) in 25 mM sodium phosphate buffer, pH 10.3, with 0.01 % Tween 20. Field strength = 466 V/cm; V_{inj}= 500 V, t = 2 s; Injector to detector distance = 3.1 cm; PMT voltage = 600 V
Peaks: 1 and 2 = Carbonic anhydrase I and II, 3 = β-lactoglobulin B, and 4 = α-lactalbumin.

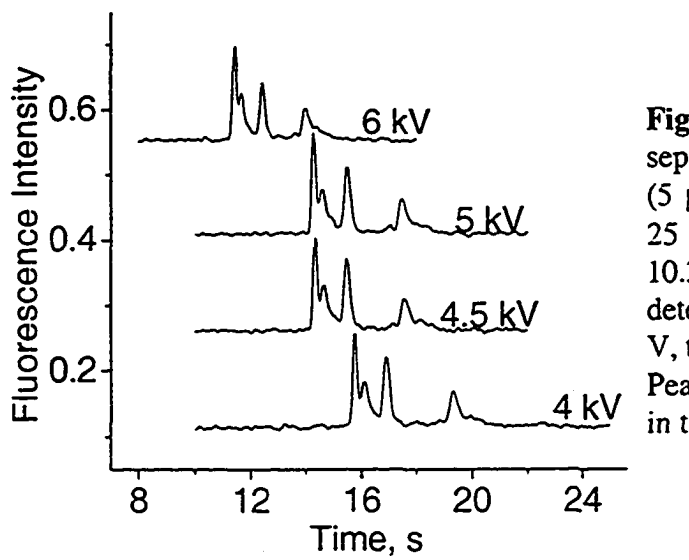

Figure 3-11: Electropherograms for the separation of the four protein mixture (5 μM) under various electric fields in 25 mM sodium phosphate buffer, pH 10.3, with 0.01 % Tween 20. Injector to detector distance = 3.1 cm. V_{inj} = 500 V, t = 2 s; PMT V = 600 V
Peak identification is same as described in the legend for Figure 3-10

Carbonic anhydrase I (pI = 6.6) eluted first, while α– lactalbumin (pI = 5.4) had the longest migration time. The peaks in the electropherogram were identified by either running individual samples and noting the retention times or by spiking the mixtures with additional reagent. Figure 3-12 shows the electropherogram obtained for six consecutive injections and separations. The relative standard deviations for migration times and peak areas were less than 0.3% and 4% respectively for six consecutive analyses. The protein peak height variation was less than 5% for peaks 3 and 4 and less than 3% for peaks 1 and 2. The reproducibility of peak heights may be attributed to the effect of the high ionic strength buffer used, as it helps to prevent protein adsorption onto the walls of the fluidic channels.

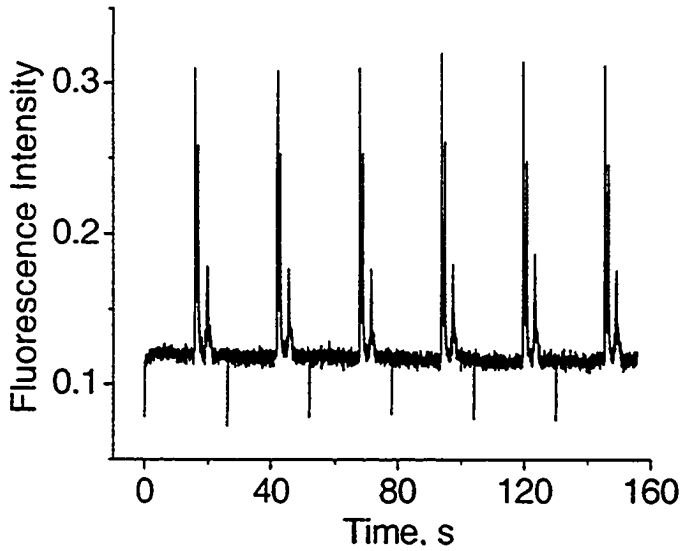

Figure 3-12: Six consecutive analyses of a 4 protein mixture (5 μM) in 25 mM sodium phosphate buffer, pH 10.3, with 0.01 % Tween 20. Injection was for 2 s at 500 V, followed by a 26 s separation time for each analysis, with an applied field strength of 466 V/cm (4 kV). Injector to detector distance = 3.1 cm; PMT voltage = 600 V Peak identification is same in Figure 3-10.

Peak 1 in Figure 3-10, which corresponds to carbonic anhydrase I, gave an efficiency, expressed as number of plates, N, of 51,000 (1.6 million plates/m). This high separation efficiency further indicates that the buffer system used was effective in reducing adsorption. These results also show that the optical detection system was not inducing significant band broadening, as this efficiency is close to the maximum that can be expected for such a device [16]. This high separation efficiency can be compared with that reported by Ye et al. [7] for a series of proteins. The maximum efficiency reported was in the order of 450,000 plates/m for myoglobin, post-column labelled. Figure 3-13 shows the effect of applied electric field on the number of theoretical plates for the CE analysis of β-lactoglobulin in 25 mM sodium phosphate buffer, pH 10.3. The efficiency increased rapidly as the applied electric field was increased from 349 V/cm to 699 V/cm, while the

analysis time decreased to less than half its initial value (26 s vs. 12 s). Ramsey and co-workers [17] reported a maximum efficiency of 180,000 plates for microchip CE of tetramethylrhodamine isothiocynate (TRITC) labelled α-lactalbumin.

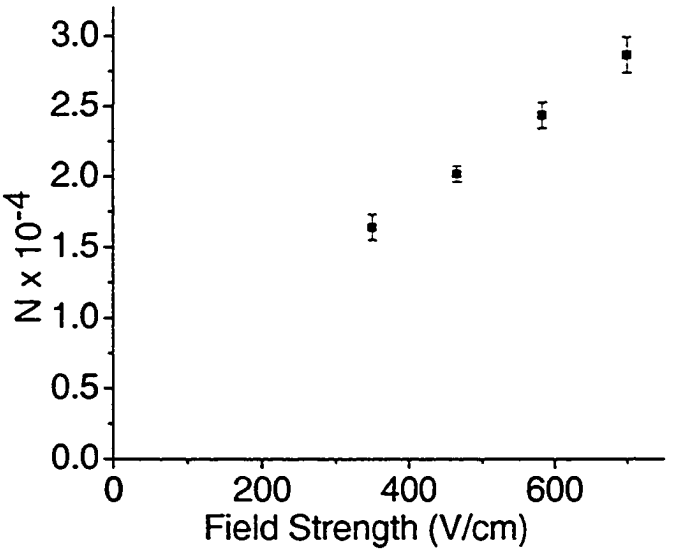

Figure 3-13: Graphs shows the effect of applied field strength on plate number, N, for microchip CE of 5 μM α-lactalbumin in 25 mM sodium phosphate buffer, pH 10.3, with 0.01% Tween 20. Error bars are s. d. calculated for nine consecutive analyses at each field strength. Injector to detector distance = 3.1 cm. V_{inj} = 500 V, t = 2 s; PMT V = 600 V

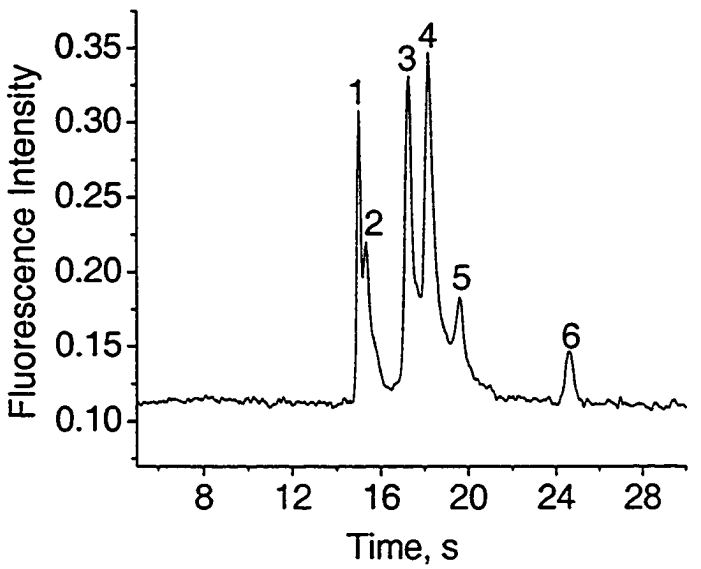

Figure 3-14: Electrophoretic separation of six model proteins (5 μM) in 25 mM sodium phosphate buffer, pH 10.3, with 0.01 % Tween 20. Field strength = 466 V/cm (4 kV); V_{inj}= 500 V, t = 2 s; PMT voltage = 600 V

Peaks: 1, carbonic anhydrase I; 2, carbonic anhydrase II; 3, β-lactoglobulin B; 4, β-lactalbumin A; 5, α-lactalbumin; 6, ovalbumin

A model protein mixture containing six species was also experimented with under the same conditions as above. All six species were nicely separated within a matter of 26 s, with an applied electric field of 466 V/cm (4 kV) and the electropherogram is shown in Figure 3-14. The separation time was further reduced to approximately 18 s with an applied field strength of 699 V/cm, (6 kV), with N = 682,000 plates/m for β-lactoglobulin B. For β-lactoglobulin B, Ye [7] reported an N value of 360,000 plates/m, thus indicating that our system is quite competitive in terms of efficiency. Figure 3-15 shows the electropherogram obtained. β-lactoglobulin B which has a pI of 5.23 and β-lactoglobulin A which has a pI of 5.13 were resolved, even though they have very similar molecular weights and the difference in pI values is only 0.1. The resolution value, R, was calculated to be ~ 1.

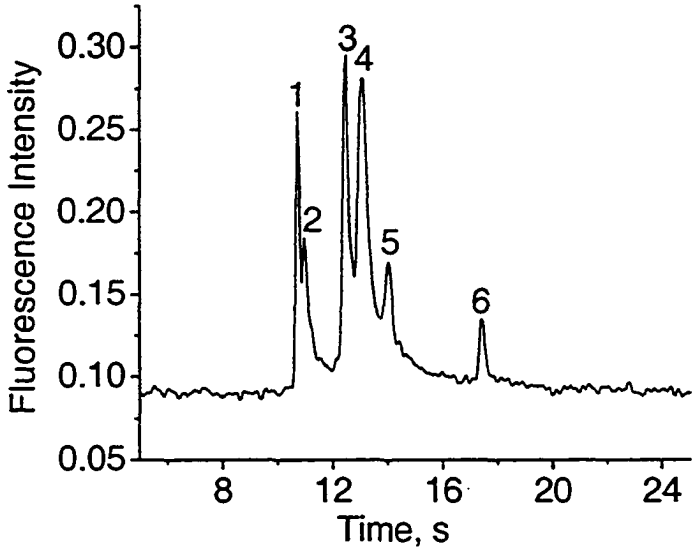

Figure 3-15: Electrophoretic separation of six model proteins (5 μM) in 25 mM sodium phosphate buffer, pH 10.3, with 0.01 % Tween 20. Field strength = 699 V/cm; V_{inj}= 500 V, t = 2 s; PMT voltage = 600 V
Peak identification same as in Figure 3-14

3.3.2.2 Effect of pH on Separation

The native fluorescence detection method (LINF) was further evaluated for the separation of the model protein mixture at various pH values. Figure 3-16 shows the separations. Separations at all pH values seem to be satisfactory, as most peaks were nicely resolved. However, carbonic anhydrase resolution at pH 7.5 was not as good as at pH 10.3 and 11.2. Charge differences between proteins are generally larger when the pH of the buffer is close to the average pI. As a result, better separations are normally obtained under these conditions [17, 18]. However, this was not observed here for the

carbonic anhydrase proteins. In addition, the separation of β-lactoglobulin B and carbonic anhydrase is poorer at pH 7.5. The effect of changing pH did not have a significant impact on the peak intensities of the proteins in the mixture separated. Any variation between the electropherograms obtained may be attributed to sample preparation and system optimization, rather than the difference in pH, as the experiments were conducted on different days. However, it is noted that there is a shift towards longer migration times as the pH increased from 7.5 to 11.2. This can be attributed to change in the electrophoretic mobility of the proteins. As all the proteins are negatively charged (pH greater than pI) they will be migrating towards then anode, while electroosmotoic flow is toward the cathode. As the pH increases, this negative charge becomes more pronounced and as a consequence, the protein species are more strongly attracted towards the anode. However, as pH increases, the EOF also increases which would result in shorter migration times. Nevertheless, the observed longer migration times indicate that the dominant parameter was the increased charge which resulted in a change of the electrophoretic mobility of the species.

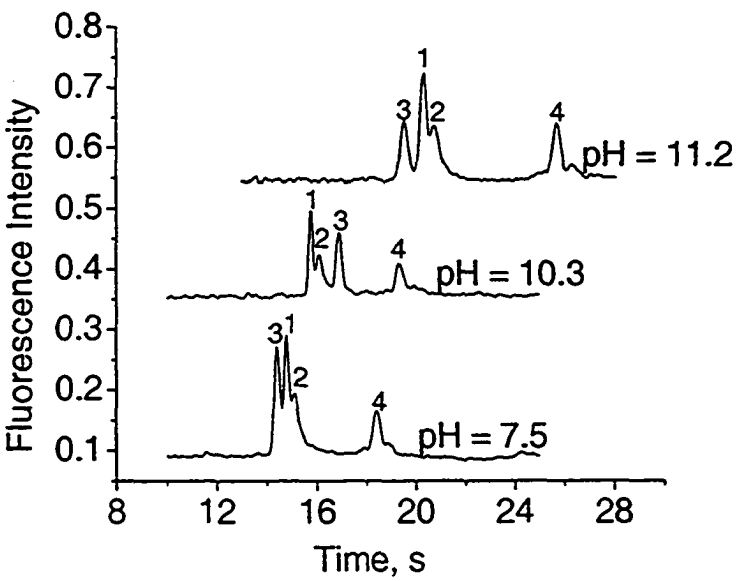

Figure 3-16: Electrophoretic separation of a mixture of four model proteins (5 μM) in 25 mM sodium phosphate buffer, with 0.01 % Tween 20 at pH 7.5, 10.3, and 11.2. Field strength = 466 V/cm; V_{inj}= 500 V, t = 2 s; PMT voltage = 600 V
Peak identification same as in the legend for Figure 3-10

3.3.2.3 Limit of Detection Studies

The detection limit may be determined for each species by extrapolating a plot of S/N vs. concentration to a value of 3. This was the method used for LOD determinations reported in this thesis. In the case of proteins, this was done for α-lactalbumin and the calibration curve is presented in Figure 3-17. The results are based on measurements between 2.5 - 20 μM. The LOD was ascertained to be ~ 500 nM. However, another way of determining LOD, when using a single concentration observation, is by assuming a linear calibration sensitivity and extrapolating to S/N = 3. This method was used in determining the LOD for the other species in the model protein mixture in the electropherogram of Figure 3-10. The S/N ratio for carbonic anhydrase I and β-lactoglobulin was calculated to be 53 and 35 respectively, and assuming linear calibration sensitivity, these correspond to detection limits of ~286 nM for carbonic anhydrase I and 430 nM for β-lactoglobulin B. Comparing the LOD for the three proteins, β-lactoglobulin B which has two tryptophan residues has roughly the same LOD as α-lactalbumin which has four. In comparison, carbonic anhydrase, which possess 7 tryptophan moieties, has an LOD of ~ 290 nM. From this it can be noted that the observed signal is not linearly related to the number of tryptophan moieties contained in the protein molecule. This observation was previously reported by both Lee [19] and Issaq [20].

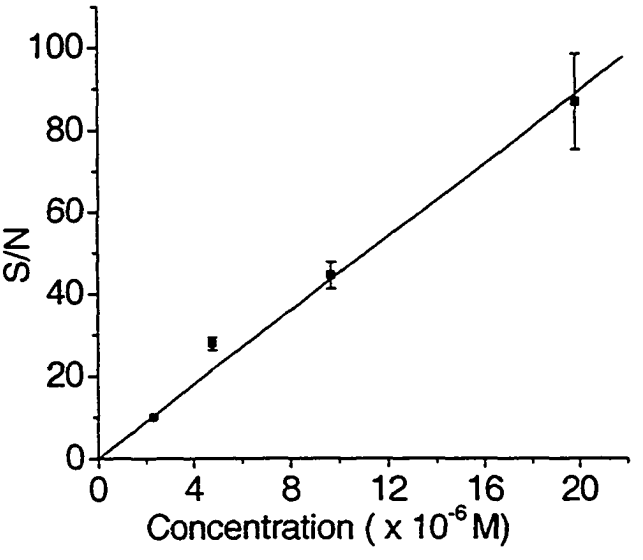

Figure 3-17: Plot of S/N as a function of α-lactalbumin concentration. Field strength = 466 V/cm; V_{inj}= 500 V, t = 2 s; PMT voltage = 600 V. Error bars are for s. d. for 7 multiple injections and are smaller than the point, where not visible. Data points were fit with a linear function and forced through origin, $R^2 = 0.9959$

The non-linearity in detection sensitivity with respect to the number of tryptophan residues in proteins may be due to several factors. The number of exposed tryptophan residues and the microenvironment, whether hydrophobic or hydrophilic will have an effect on the fluorescence yield [11]. It has been reported that the quantum yield of fluorescence of tryptophan residues in a hydrophobic microenvironment is about three times smaller than for residues present in a hydrophilic microenvironment [9, 19]. In addition, peptide bonds and protonated amine groups are also known to cause quenching of tryptophan fluorescence in proteins [10]. Finally, the quantum efficiency of fluorescence per tryptophan or tyrosyl residue is not the same for all proteins and neither is it the same for different residues in the same protein [21, 22].

3.4 EVALUATING THE DETECTION METHOD

It is important that the detection system being presented in this thesis be evaluated and contrasted with similar and dissimilar detection methodologies already in use. This will enable us to gauge the contribution and potential advantages that may be accrued with this optical detection method. The sensitivity or LOD of the method is an important parameter that is normally used in evaluating the system. This is the metric that will be used in the discussion that follow, for our analysis.

3.4.1 Overview/Discussion

Under optimised conditions, we reported concentration LOD (S/N = 3) for W, peptides and proteins in the several hundred nanomolar range. While W LOD was 230 nM, that for peptides was calculated to be in the range of 300-400 nM, and proteins, in the range from 200-500 nM. In addition to concentration LOD, the mass limit of detection is another important figure of merit for fluorescence detection. Our observed concentration LOD's correspond to 5.5 amol of injected molecules for tryptophan, and 4 – 12 amol for peptides and proteins, as presented in Table 3-1. An injection volume of 24 pL (the geometric injector size) was assumed for these calculations.

The LOD in our study can be compared to a variety of reports in the literature employing a variety of lasers, with labelling or native schemes for detection [6, 7, 14, 19, 20, 23-29]. Table 3-1A shows that the best detection for tryptophan obtained with LINF was 0.2

nm, corresponding to 0.8 amol of injected molecules. In this study, a Kr laser operating at 284 nM and a sheath flow cuvette, which minimizes scattering, was used. Pulsed Nd:YAG lasers yielded an LOD for tryptophan around 2 – 3 nM, and between 6 – 26 nM for various proteins. Path lengths were either 50 or 75 μm, in contrast to the 10 μm path length in our μ - CE device. Injected mass detection limits were not available for most reports but, Chan et al. [14] used about 10 amol of injected molecules. Comparison of our results to Chan's, who used a very similar laser, requires the definition of LOD as occurring at S/N = 2, instead of 3, as shown in Table 3-1A. It can be seen that the microchip has about an 80 times worse LOD that Chan observed with a 5 times longer path length. However, the mass detection limit is about 2.5 times better. The relationship between fluorescence intensity and path length is presented in the following equation:

$$F = 2.3K'\varepsilon bcP_o \qquad 3\text{-}1$$

where K'is the quantum yield, ε is the molar absorptivity, b is the optical path length, c is the concentration of the sample and P_o power of the incident light. As can be observed from Equation 3-1, a longer path length does translate to higher fluorescence intensity. This contributes to the better concentration detection limits obtained with the longer path length systems.

The performance of LINF on chip may also be compared with protein labelling methods used on chip. Table 3-1A compares several different labelling methods. It can be seen that the best limits are in the range of 15 – 30 nM. Electrochemical detectors on chip offer an intriguing alternative to fluorescence methods, and Galloway [30] et al. showed a 8 nM LOD for alanine. However, the detection limits for proteins were inferior to fluorescence methods, as illustrated in Table 3-1. It can be seen that staining gives about 10 times lower LOD than the LINF approach, but both are preferred to the conductivity method.

Ref #	Detection	Species	S / N	CLOD (nM)*	Moles injected at CLOD (amol)	Path Length μm
Current Study	LINF 266 nm Nd: YAG (7 kHz)	Tryptophan	3	230	5.52	10
		Tryptophan	2	170	4.08	10
		CA[a] I	3	286	6.86	10
		α-lactalbumin	3	500	12	10
		β- lactoglobulin B	3	430	10.3	10
Capillary - LINF						
Chan (2000) *Ref 14*	266 nm Nd: YAG (> 8 kHz)	Tryptophan	2	2.1	10	50
		Conalbumin	2	5.9	30	50
		BSA[b]	2	8.0	40	50
Chan (1993) *Ref 20*	248 nm UV laser (2 kHz)	Tryptophan	2	3.3		75
		Conalbumin	2	1.3		75
		BSA[b]	2	4.0		75
Timperman *Ref 6*	Kr 284 nm CW; (sheath flow)	Tryptophan	3	0.2	0.8	50
		Tyrosine	3	20	80	50
Yeung *Ref 23*	275 nm Ar ion	Tryptophan	2	0.7		50
Tseng *Ref 24*	266 nm Nd: YAG (3 kHz)	CA[a]	3	26		75
Chip - LIF						
Liu *Ref 25*	488 nm Ar ion / NanoOrange	α-lactalbumin	3	85	32	10
		β- lactoglobulin A and B	3	70	24	10
Giordano *Ref 26*	488 nm Ar ion / NanoOrange	BSA[b]	3	15		
Bousse *Ref 27*	650 nm laser Agilent dye	CA[a]	3	30		13
Chip - Conductivity						
Galloway *Ref 30*		Alanine	3	8	3.4	85
		CA[a]		1700[d]		
Zuborova		Protein Mixure		100[d] mg/ml		200

Table 3-1A: Comparing LOD for different protein detection methods

a: CA, carbonic anhydrase; b: BSA, bovine serum albumin; c: HSA, human serum albumin; d: Concentration of sample investigated; e: NDA, naphthalene-2,3-dicarboxaldehyde; f: 2,6 – TNS, 2-(p-toluidino)naphthalene-6-sulfonic acid

Ref #	Detection	Species	S / N	CLOD (nM)*	Moles injected at CLOD (amol)	Path Length μm
Capillary - LIF						
Harvery *Ref 28*	488 nm Ar ion / NanoOrange	HSA[c]	6	3.2		50
Ye *Ref 8*	488 nm Ar ion / NDA[e]	α-lactalbumin	3	26	112	50
		β- lactoglobulin B	3	30	117	50
Benito *Ref 29*	325 He – Cd 2,6 - TNS[f] Dye	α-lactalbumin	3	3000		75
		β- lactoglobulin A and B	3	300		75
		BSA[b]		60		75

Table 3-1B: Comparing LOD for different protein detection methods
a: CA, carbonic anhydrase; b: BSA, bovine serum albumin; c: HSA, human serum albumin; d: Concentration of sample investigated; e: NDA, naphthalene-2,3-dicarboxaldehyde; f: 2,6 – TNS, 2-(p-toluidino)naphthalene-6-sulfonic acid

Label-based fluorescence detection of proteins has been explored extensively in CE, and some representative results are provided for comparison in Table 3-1B. The NanoOrange dye gives similar results for chips and capillaries, and is amongst the best seen. The other dyes such as the covalently binding NDA gave an LOD of ~ 20 – 30 nM with a mass injected of ~ 110 amol. It can be seen that in capillaries, both LINF and labelling can give similar performance. Since LINF avoids labelling challenges, it is thus an attractive approach and should be interesting for μ - CE, if the quartz emission problem can be resolved.

3.4.2 Summary/Evaluation

The above discussion presented the case for our detection method in terms of performance using the metric of LOD as the evaluation tool. It was noted that while the concentration detection limit was not as low as those reported in the literature for LINF-CE, the amount of injected material in most cases was comparable, or even lower in some cases. For systems using labelled analytes, whether on chip or with conventional CE applications, the concentration limit of detection, was in most case in the 3 – 100

nanomolar range. However, these LOD for labelled analytes are not always a true representation of the assay sensitivity as the labelling process usually starts from protein solutions prepared at high concentrations and then diluted [31]. Thus, while our LOD is not as low as we would like it to be, the performance is not orders of magnitude worse, in terms of mass detection limits, when compared with our systems. In addition, in our approach, the labelling steps are eliminated.

3.5 CONCLUSION

The application of the detector based on tryptophan fluorescence for the detection of peptides and proteins was investigated in this chapter. Unlike the applications of μ-CE that demanded a labelling step, this detection methodology exploited the intrinsic fluorescence of the bio molecules for their detection. Peptides and proteins were separated, the influence of pH on the separation of proteins was explored and the LOD of these species evaluated. Further, a model protein sample was digested off chip and then separated on chip with LINF detection to demonstrate the capability of the system. Finally a candid analysis of the performance of our detection system was done.

An important metric by which the value of a detection method will be judged is the LOD achievable by that method. From the comparison and evaluation in the preceeding section, it can be concluded that the concentration LOD achieved in our LINF detection scheme for proteins on microchip is higher compared with other LINF-CE, LIF-CE and μ-CE systems. However, even though it may not be realistic to strictly compare the systems as equals, the mass sensitivity obtained by the microchip system was acceptable. The amount of injected sample in our system is more often comparable and sometimes even lower than the systems yielding lower concentration limits of detection. This means that if the fluorescence background problem from the quartz can be reduced, it will certainly be possible to improve concentration LOD. The efficiency obtained for the on chip separations are comparable to those obtained in conventional CE analysis. We briefly discussed possible issues limiting our sensitivity in Chapter 2 and we believe that it is possible to exploit this system to yield improved performance. Thus, the system does have the potential to be more competitive, if optimised further, as outlined in Chapter 4. In addition, though protein analysis has been done on chip, to our knowledge,

this work presented the first attempt to exploit the intrinsic fluorophores for protein detection on chip eliminating all the problematic issues associated with labelling, while potentially preserving the sample for further analysis.

3.6 REFERENCES

(1) Fluri, K.; Fitzpatrick, G.; Chiem, N.; Harrison, D. J. *Anal. Chem.* **1996**, *68*, 4285-4290.
(2) Chiem, N.; Harrison, D. J. *Anal. Chem.* **1997**, *69*, 373-378.
(3) Fan, Z. H.; Harrison, D. J. *Analytical Chemistry* **1994**, *66*, 177-184.
(4) Seiler, K.; Harrison, D. J.; Manz, A. *Anal. Chem.* **1993**, *65*, 1481-1488.
(5) Catai, J. R.; Somsen, G. W.; de Jong, G. J. *Electrophoresis* **2004**, *25*, 817-824.
(6) Timperman, A. T.; Oldengurg, K. E.; Sweedler, J. V. *Anal. Chem.* **1995**, *67*, 3421-3426.
(7) Ye, M.; Hu, S.; Quigley, W. C.; Dovichi, N. J. *Journal of Chromatography A* **2004**, *1022*, 201-206.
(8) Ye, M.; Hu, S.; Schoenherr, R. M.; Dovichi, N. J. *Electrophoresis* **2004**, *25*, 1319-1326.
(9) Konev, S. V. *Fluorescence and Phosphorescence of Proteins and Nucleic Acids*; Plenum Press: New York, 1967.
(10) Cowgill, R. W. *Biochim. Biophys. Acta* **1963**, *75*, 272-273.
(11) Longworth, J. W. In *Excited States of Proteins and Nucleic Acids*; Steiner, F. R., Weinryb, I., Eds.; Plenum Press: New York, 1971, pp Chapter 6.
(12) Shultz-Lockyear, L. L.; Colyer, C. L.; Fan, Z. H.; Roy, K. I.; Harrison, D. J. *Electrophoresis* **1999**, *20*, 529-538.
(13) Uchiyama, K.; Nakajima, H.; Hobo, T. *Anal. Bioanal. Chem.* **2004**, *379*, 375-382.
(14) Chan, K. C.; Muschik, G. M.; Issaq, H. J. *Electrophoresis* **2000**, *21*, 2062-2066.
(15) Parks, J. H.; Rodriguez - Cruz, S. E.; Khoury, J. T.; http://www.rowland.org/labs/iontraps/images/ASMS_2000.pdf: Cambridge.
(16) Harrison, D. J.; Fluri, K.; Seiler, K.; Fan, Z. H.; Effenhauser, C. S.; Manz, A. *Science* **1993**, *261*, 895-897.
(17) Liu, Y.; Foote, R. S.; Culbertson, C. T.; Jacobson, S. C.; Ramsey, R. S.; Ramsey, J. M. *J. Microcolumn Separations* **2000**, *12*, 407-411.
(18) Schmalzing, D. K.; Pigee, C. A.; Foret, F.; Carrilho, E.; Karger, B. L. *Journal of Chromatography A* **1993**, *652*, 149-159.
(19) Lee, T. T.; Yeung, E. S. *Journal of Chromatography* **1992**, *595*, 319-325.
(20) Chan, K. C.; Janini, G. M.; Muschik, G. M.; Issaq, H. J. *Journal of Liquid Chromatography* **1993**, *16*, 1877-1890.
(21) Cowgill, R. W. *Archives of Biochemistry and Biophysics* **1963**, *100*, 36-44.
(22) Teale, F. W. J. *Biochemical Journal* **1960**, *76*, 381-388.
(23) Chang, H.-T.; Yeung, E. S. *Anal. Chem.* **1995**, *67*, 1079-1083.
(24) Tseng, W.-L.; Chang, H.-T. *Anal. Chem.* **2000**, *72*, 4805-4811.
(25) Liu, Y.; Foote, R. S.; Jacobson, S. C.; Ramsey, R. S.; Ramsey, J. M. *Anal. Chem.* **2000**, *72*, 4608-4613.

(26) Giordano, B. C.; Jin, L. J.; Couch, A. J.; Ferrance, J. P.; Landers, J. P. *Anal. Chem.* **2004**, *76*, 4705-4714.
(27) Bousse, L.; Mouradian, S.; Minalla, A.; Yee, H.; Williams, K.; Dubrow, R. *Anal. Chem.* **2001**, *73*, 1207-1212.
(28) Harvey, M. D.; Bablekis, V.; Banks, P. R.; Skinner, C. D. *Journal of Chromatography B* **2001**, *754*, 345-356.
(29) Benito, I.; Marina, M. L.; Sza, J. M.; Diez-Masa, J. C. *Journal of Chromatography A* **1999**, *841*, 105-114.
(30) Galloway , M.; Stryjewski, W.; Henry, A.; Ford, S. M.; Llopis, S.; McCarley, R. L.; Soper, S. A. *Anal. Chem.* **2002**, *74*, 2407-2415.
(31) Pinto, D. M.; Arriaga, E. A.; Craig, D.; Angelove, J.; Sharma, N.; Ahmadzadeh, H.; Dovichi, N. J. *Anal. Chem.* **1997**, *69*, 3015-3021.

CHAPTER 4: SUMMARY

4.1 CONCLUSION AND SUGGESTIONS FOR FUTURE RESEARCH

This chapter summarises the results and discussion presented in the preceding chapters, and advances suggestions that may lead to an improvement of the current system. The thesis presented the development of the LINF detector and its subsequent applications. As such, this section follows suit; the discussion will follow the order of the chapters.

Chapter 2 explored the application of a confocal epiluminiscent microscope, developed by Ocvirk [1] and co-workers, towards the realization of an optical detection method that exploits the intrinsic fluorescence for tryptophan. Ocvirk reported concentration detection limits in the high femtomole (fM) range for continuous flow detection and in the low picomole (pM) for capillary electrophoresis of fluorescein. Jiang [2] explored the application of this system to the development of a red diode laser detection system and reported figures of merit in the low pM range for Cy-5 dye. In the current study, we obtain detection limits for tryptophan in the mid-hundred nM range for capillary electrophoresis measurements. This LOD was a factor of ~ 100 times poorer than that reported by Chan and co-workers [3]. The mass detection limit in our study was half that of theirs. However, in their case, the optical path length was 50 μm as compared with 10 μm in the present study. This leads to the suggestion that improvement in concentration LOD be attempted increasing the optical path through using deeper channels. This will result in an increase in the number of molecules detected. Signal collection can also be enhanced with the use of a higher numerical aperture objective. In our study, this was attempted with the use of a 36x mirror – based objective, though we could not eliminate light collection as a limiting factor in our analysis, since this was not a typical objective. It may also be beneficial to conduct an investigation into the effect of the pinhole size on the S/N ratio. This may result in an increase in the sectioning power of the microscope in order to reduce background, discriminating against the quartz emission by the use of smaller pinholes.

Quartz luminescence was observed on exposure of the chip to the 266 nm laser. This was subsequently investigated for pristine quartz using a spectrophotometer to

measure its luminescence at 266 nm. The emission spectrum revealed two bands in the following ranges: ~290 – 340 nm and 350 – 390 nm. This falls within the spectral bandwidth of tryptophan emission, which is ~300 – 425 nm, with maxima at around 350 nm. We believe that a more prudent selection of optical filter that will eliminate most of the luminescence from the quartz substrate, but still capturing most of tryptophan emission may lead to an improvement in S/N. A filter with an optical band with between 325 – 350 nm would be suitable. Recently, such a filter has been obtained commercially. S/N may also be improved with the use of a time gated detection (boxcar averager) approach. Since the laser is pulsed at 7 kHz, with an on time of 0.5 ns, and lifetimes are a few nanoseconds, such a system will integrate signal essentially only when it is being generated, thus eliminating noise arising when the signal is not being generated.

In Chapter 3, we presented the first application for the fluorescent detection of peptides and proteins on chip without the need for labels. Because μ-CE offers advantages such as short analysis times and the capability of developing high-throughput systems, it has been receiving a great deal of attention. However, all of the current applications on – chip involve a labelling step, which has its inherent disadvantages. Even though at times labelling may be necessary, efforts must be made to utilise native fluorophores when possible. The commercial availability of UV lasers that are relatively inexpensive, compact and have adequate power output now makes this approach attractive. Should the approaches suggested above yield an improvement in the concentration limit of detection, this system will be uniquely poised to offer an alternative to cumbersome labelling reactions. In most applications, proteins are often digested before being subject to MS for identification. The use of labels further complicates this, thus, LINF is ideally suited for such applications. It preserves the sample integrity for further analysis, if required. In the past, efforts have been made to apply the use of microfluidic chips towards enhancing isoelectric focusing for proteins separation. A LINF detection scheme could be employed for detection with subsequent collection of the separated proteins for mass spectrometry or other forms of analyses

With an increase in the detection capability of the method, real samples can be analysed for the mapping of protein composition of individual cells. This approach might then ultimately be coupled with the MS for identification.

4.2 REFERENCES

(1) Ocvirk, G.; Tang, T.; Harrison, D. J. *The Analyst* **1998**, *123*, 1429-1434.

(2) Jiang, G.; Attiya, S.; Ocvirk, G.; Lee, W. E.; Harrison, D. J. *Biosensors and Bioelectronics* **2000**, *14*, 861-869.

(3) Chan, K. C.; Muschik, G. M.; Issaq, H. J. *Electrophoresis* **2000**, *21*, 2062-2066.